Estimation of Plant and Soil Evaporation from Cropped Lands

W H Van Zyl and J M De Jager

WRC Report No.507/1/97

ESTIMATION OF

PLANT AND SOIL EVAPORATION

FROM CROPPED LANDS

By

W.H. VAN ZYL AND J.M. DE JAGER

DEPARTMENT OF AGROMETEOROLOGY

UNIVERSITY OF THE ORANGE FREE STATE

Report to the Water Research Commission on the Project

"Improved estimation of plant and soil evaporation from cropped lands"

Project Leader : Professor J.M. de Jager

WRC Report No.: 507/1/97
ISBN : 1 86845 364 2

TABLE OF CONTENTS

EXECUTIVE SUMMARY

1. RATIONALE

Total evaporation from cropped lands comprises components for evaporation from the vegetation and the bare soil surface. Any analysis of crop total evaporation, whether it be for purposes of either simulation, or problem solving, must consider both components separately. This applies to both rainfed and irrigated situations.

Any water evaporated through the soil surface is wasted because it does not contribute to producing crop biomass. Hence, for the management of scarce water resources, an accurate mathematical simulation of plant and soil evaporation is required.

In the past, experimental difficulties have been encountered with the measurement of soil evaporation separately. This has hindered the simulation of soil and plant evaporation. hence the present project sought to develop a new method of executing such measurements as well as to develop a new model for simulation of these variables.

In pursuit of these goals, the main objective of the study was the measurement of sunlit and shaded foliage and sunlit and shaded soil surface temperatures and evaporation from the vegetation and soil components of crops. Various new methods of observation were investigated. For evaporation, these included micro-meteorological techniques and the utilization of lysimeters. Data for the different weather elements were measured routinely by an automatic weather station because the eventual practical application of any new model developed would depend on the continuous provision of such input data.

The maize and wheat crops were studied and modelling of vegetation and soil surface temperatures and evaporation attempted using the latest scientific theories.

2. OBJECTIVES

While the overall objective of the study was to produce an accurate model for estimating plant and soil evaporation from cropped lands, the specific objectives addressed in this study were:

- develop and test the accuracy of an iterative model for simulating foliage and soil surface temperatures;
- measure or estimate various values needed for the complete characterisation of evaporation from cropped lands (reference crop evaporation; crop total evaporation and its two components, plant and soil evaporation) using various lysimetric techniques as well as data

collected by means of automatic weather stations and micrometeorological instrumentation; and

- refine two models (Shuttleworth and Gurney; PUTU) for simulation of plant and soil evaporation.

3. METHODOLOGY

3.1 Measuring evaporation rates

Crop total evaporation was measured using two 2 m x 2 m x 1 m drainage lysimeters, while crop plant evaporation was measured by covering the soil surface of a large (3 m x 3 m x 2 m) weighing lysimeter with a plastic sheet to suppress soil evaporation. Soil evaporation was then simply obtained from the difference between measured crop total and plant evaporation. The weighing lysimeter has a resolution of 0,04 mm of water. Two additional drainage lysimeters were also used to measure plant evaporation, soil evaporation again being prevented with a plastic-sheet cover. The plastic sheet was in turn covered by a shallow (10 mm) layer of soil which ensured that plant micro-climate (soil and air) remained representative of surrounding field conditions.

Numerous micro-lysimeters (10 cm diameter x 20 cm deep) were also used in an attempt to measure soil evaporation directly, both from a bare soil surface and from between crop rows.

Micro-meteorological techniques of estimating crop total evaporation in this study included:

- direct measurement using the eddy correlation method,
- derivation from surface energy budget measurements and eddy correlation measurements of sensible heat flux density, and
- determination from energy budget and Bowen ratio measurements.

3.2 Mathematical simulation

The reliability of two mathematical models for estimating plant and soil evaporation separately was tested with a view to developing an improved simulation procedure.

The one, here termed the SG-iteration model, is based upon a model developed by Shuttleworth & Gurney (1990). It requires surface temperature as an input. Originally Shuttleworth and Gurney suggested that foliage temperature might be measured by infra-red thermometry. This was not permissible here in view of the objective of the project, which was to produce a technique for simulating plant evaporation solely from routine data provided by an automatic weather station. Hence, the development of a computerised numerical iteration procedure for achieving reliable estimates of soil and leaf temperatures was the first matter studied. The values so obtained were then substituted in appropriate equations in order to obtain estimates of plant and soil evaporation.

The second mathematical approach entailed re-investigation of the existing PUTU-model, which utilizes the products of evaporation coefficients (one of each for plant and soil evaporation) and reference crop (short grass) evaporation.

Refinements for accommodating the so-called second phase evaporation by means of evaporation coefficients were examined. Second phase evaporation from the soil surface commences approximately six days following a wetting event.

4. RESULTS

Major results of the research included:

Micro-meteorological methods of determining crop total evaporation were found to underestimate plant evaporation as measured in the large weighing lysimeter. This could have been a real effect caused by the altered surface energy balance due to suppression of soil evaporation. In effect it meant that soil evaporation could not be determined satisfactorily by a difference method.

- micro-lysimeter determinations of soil evaporation overestimated weighing lysimeter values for bare soil conditions by a factor of nearly 3. This could have been due to restricted drainage from the micro-lysimeters which caused excessively wet conditions to persist.
- Agreement between drainage and weighing lysimeter values of plant evaporation was sometimes good, but not consistently so.
- For a bare soil surface, evaporation values from the drainage lysimeter overestimated weighing lysimeter values by a factor of 1,5.
- The dry-down model of the soil evaporation coefficient as used in the PUTU-model reliably estimated soil evaporation measured on bare soil. A reliable mathematical adjustment for second phase evaporation was developed.
- Foliage temperature obtained from an iteration technique in a modified SG-model compared fairly well with the mean of sunlit and shaded leaf temperatures as measured by infra-red thermometer.
- A good relationship was evident between sunlit and shaded soil surface temperatures, both measured using the infra-red thermometer.
- Plant evaporation simulated by both the PUTU and SG-models compared well with the weighing lysimeter values on both hourly and daily basis.
- PUTU and SG-model daytime values of soil evaporation compared reasonably well with weighing lysimeter values of soil evaporation.
- Possibly due to the drainage procedures adopted, the values of bare soil evaporation, as measured by the micro-lysimeters, greatly overestimated soil evaporation computed by both models.

- Suggested improvements to existing albedo (i.e. surface reflectivity to solar radiation) functions and formulae for estimating net radiation appear to offer minimal benefit at this stage.

5. DEGREE OF ACHIEVEMENT OF OBJECTIVES

The plastic covered, large lysimeter measured plant evaporation accurately in cases of a dry soil surface and a closed canopy. This made possible successful, practicable improvements to the sub-models for estimating plant evaporation. In respect of plant evaporation then, the objectives of this project have been achieved for both maize and potato crops. The PUTU- and SG-models as here modified may be recommended for use in the future.

Because of the rapid dry-down of wet soil surfaces and the fact that crop canopies shield the soil surface from incoming solar radiation, growing season soil surface evaporation in cropped lands is less than plant evaporation. Errors in the estimation of soil evaporation thus have smaller practical significance than do errors in plant evaporation estimates. For this reason the overall objectives of this research have, to a large extent been achieved.

The measurement and modelling of soil temperature and soil evaporation, however proved unsuccessful in this study. This was possibly due to the inherent problems experienced with the particular experimental techniques employing eddy correlation measurements, drainage lysimeters and micro-lysimeters.

6. FUTURE RESEARCH

The results obtained, show that the models as developed here have probably reached a level of sophistication and refinement which is sufficient for practical irrigation scheduling, mathematical modelling, or other problem solving. Limited further development is thus foreseen at this point in time.

The measurement and modelling of soil evaporation from a partially vegetated surface is difficult and was not satisfactorily solved by this study. Future work could pursue the improvement of techniques to achieve this goal. Such work includes application of the empirical relationship here developed for estimating shaded soil surface temperatures in terms of sunlit soil surface temperatures.

SYMBOL DEFINITION

a	:	Absorbtivity
AED	:	Atmospheric evaporative demand (mm)
C_p	:	Specific heat of air (J kg^{-1} $°C^{-1}$)
D	:	Number of days elapsed since the latest soil surface wetting event (usually exceeding 10 mm)
e'	:	Instantaneous turbulent fluctuation from the mean water vapour pressure (°C)
e	:	Water vapour pressure (kPa)
e(T)	:	Saturated water vapour pressure at temperature T (kPa)
E	:	Crop total evaporation (mm)
E_o	:	Reference (0,15 m short-grass) evaporation (mm)
E_s	:	Soil surface evaporation (mm)
E_v	:	Plant evaporation (mm)
E_{ss}	:	Sunlit soil surface evaporation (mm)
E_{sd}	:	Shaded soil surface evaporation (mm)
E_{vs}	:	Sunlit leaf evaporation (mm)
E_{vd}	:	Shaded leaf evaporation (mm)
F_g	:	Dry-down factor equal to the ratio of soil evaporation from a partially dry soil surface to reference evaporation
F_g-adj	:	Soil evaporation dry-down factor adjusted for second phase evaporation
FI	:	Fractional radiation interception (0 - 1)
F_v	:	Crop growth factor regulated by plant water status
G	:	Soil heat flux density (W m^{-2})
H	:	Sensible heat flux density (W m^{-2})
h	:	crop height (m)
k	:	Von Karman's constant (0,4) in the logarithmic wind profile or, with appropriate subscript (v or s), the evaporation coefficient
K_h	:	The eddy diffusion coefficient at the top of the canopy (m^2 s^{-1})
LE	:	Latent heat flux density (W m^{-2})
L	:	Latent heat of evaporation at constant temperature (J kg^{-1})
r_a	:	Aerodynamic resistance (s m^{-1})
r	:	Surface resistance (s m^{-1})
R_{ld}	:	Long-wave downward radiation (W m^{-2})
R_{lu}	:	Long-wave upward radiation (W m^{-2})
R_n	:	Net radiation (W m^{-2})
R_s	:	Incoming global solar radiation (W m^{-2})
T'	:	Instantaneous turbulent fluctuation from the mean air temperature (°C)

T : Temperature (°C)
T_a : Air temperature (°C)
T_{ss} : Sunlit soil surface temperature (°C)
T_{sd} : Shaded soil surface temperature (°C)
T_{vs} : Temperature of sunlit vegetation (°C)
T_{vd} : Temperature of shaded vegetation (°C)
T_{vm} : Mean temperature of sunlit and shaded foliage (C°)
w' : Instantaneous turbulent fluctuation from the mean wind speed (m s^{-1})
ρ : Density of air (kg m^{-3})
γ : Psychrometric constant (kPa $°C^{-1}$)
α : Albedo
ß : The Bowen Ratio (H/LE)
θ : sun elevation angle (degrees)
η : Climate adjustment factor for crop evaporation coefficients
Subscript f : Foliage
Subscript l : leaf
Subscript m : mean value
Subscript o : Maximum, or water non-stressed, or effective surface for energy exchange of vegetation
Subscript p : A potential value corresponding to a given set of conditions
Subscript r : Reference height
Subscript s : Soil surface
Subscript sd : Soil surface shaded (dark)
Subscript ss : Soil surface sunlit
Subscript v : Vegetation
Subscript vd : Shaded vegetation (dark)
Subscript vs : Sunlit vegetation
Subscript w : wet bulb
Subscript a : air or dry bulb

SYMBOL DEFINITION FOR THE RESISTANCES IN THE SHUTTLEWORTH & GURNEY (1991) MODEL

r_{aa} : Aerodynamic resistance between canopy source height and the reference level
r_{sv} : Bulk equivalent of the stomatal resistance of the canopy, or canopy resistance to water vapour transfer.
r_{av} : Bulk boundary layer resistance.

r_{as} : Aerodynamic resistance between soil surface and mean canopy source position (sub-canopy)

r_{ss} : Soil surface resistance to water vapour flow. The subscript s for sunlit and d for shaded can be applied to all the variables eg r_{svs}.

ACRONYM DEFINITION

AWS : Automatic weather station

AWSO; Automatic weather station observations

CAL : Calculated values

DL : Drainage lysimeter

GL : Grass lysimeter

M : Measured values

ML : Micro-lysimeter

MMO : Micro-meteorological observations

PME : Penman-Monteith equation

PUTU : A numerical crop growth simulation model

SG : The Shuttleworth and Gurney model for evaporation from a sparsely vegetated surface

WL : Weighing lysimeter

CHAPTER 1

INTRODUCTION

1.1 RATIONALE

Evaporation through the soil surface, E_s, is water wasted because it is not used in the crop production process. This soil evaporation component is most significant, accounting in many cases, for almost 100% of that portion of water lost from vegetated soil which is not used in biomass production. This is true in varying degrees of both dryland and irrigated conditions. Because of this, the measurement and modelling of E_s and E_v have become indispensible to decision taking for the purpose of saving water in practical crop production.

Previous research approaches (Boast & Robertson, 1982; Matthias, Salehi & Warrick, 1986 and Steiner, 1989) have included measuring E_s using micro-lysimeters and then finding E_v by difference from measured crop total evaporation, E. Soil evaporation values which exceed plant evaporation by almost 125% have been reported (Unger & Phillips, 1973 and Hattingh, 1991) when using this approach. Such high values, if correct, cause concern, because they could imply the need for fundamental changes in field crop cultivation practice, which would affect the delimitation of good and marginal crop production areas. Furthermore, a revision of the present theory for soil surface evaporation, which in general does not predict such high values, would bring about considerable modification in modern water management. This report will describe and evaluate direct measurements of plant evaporation, E_v. The measurement of E_s by micro-lysimeter will also be re-evaluated.

Crop foliage and soil surface temperatures play an important role in determining the energy budget and water lost from a cropped surface. Hence, an attempt will be made to produce models for the accurate simulation of the surface temperatures, T_{vs}, T_{vd}, T_{ss} and T_{sd} in terms of micro-meteorological (MMO) and automatic weather station (AWSO) observations. These modelled values of T_{vs}, T_{vd}, T_{ss} and T_{sd} will then be used in an energy balance equation to estimate E_v and E_s. Existing models and energy balance equations (De Jager & Van Zyl, 1989; Shuttleworth & Gurney 1990; Shuttleworth 1991; Nichols 1992) for E_v and E_s will be used, but modified to meet the objectives of this project.

The theory developed needs to be directly applicable to planning cultivation strategies. In addition, the mathematical expressions for plant and soil evaporation coefficients are intended to improve irrigation scheduling efficiency.

Plant and soil evaporation subroutines constitute most important components in most crop growth models. In the RSA, such models have long been integral parts of hydrological research (Schulze, 1984), the determination of climatic risk in crop production (Singels & De Jager, 1991) and drought assessment (Fouché, 1992). Attempts will be made to improve the reliability of such models, particularly for RSA conditions.

1.2 AIMS

The original overall objective of this study was to develop sound mathematical models for the evaporation of water from the soil and foliage components of the maize and potato crops in terms of the natural physical environment variables. The ability of these models to predict water use accurately by a developing crop experiencing different degrees of soil surface wetness would be evaluated and suitable software procedures for incorporation into the crop growth simulation systems such as PUTU, developed.

Specific objectives were to model:

(a) sunlit and shaded leaf temperatures and sunlit and shaded soil surface temperatures from micro-meteorological and automatic weather station data, and

(b) plant and soil evaporation from the sunlit and shaded temperatures mentioned under (a) from micro-meteorological and AWS data.

CHAPTER 2

THEORY

Unless otherwise indicated, evaporation from leaf (the plant), or soil surfaces will be referred to as plant (E_v) or soil (E_s) evaporation, respectively.

2.1 MICRO-METEOROLOGICAL TECHNIQUES FOR DETERMINING PLANT AND SOIL EVAPORATION

The subscript convention here adopted, prescribes that the first subscript denotes either vegetation (v), or soil (s) and the second subscript denotes either direct sunlight (s), or shade (d).

By definition, total evaporation, E, from a vegetative crop is given by

$$E = E_v + E_s \qquad 2.1$$

where

$$E_v = E_{vs} + E_{vd} \qquad 2.2$$

and

$$E_s = E_{ss} + E_{sd} \qquad 2.3$$

Where, in equations 2.1, 2.2 and 2.3

E_v = plant evaporation (mm)

E_s = soil evaporation (mm)

E_{vs} = evaporation from sunlit leaves (mm)

E_{vd} = evaporation from shaded leaves (mm)

E_{ss} = evaporation from sunlit soil surface (mm)

E_{sd} = evaporation from shaded soil surface (mm)

The upper limit of crop water consumption is known as the atmospheric evaporative demand and was defined by De Jager & Van Zyl, (1989) as:

$$AED = E_{vo} + E_s \qquad 2.4$$

$$E_{vo} = E_{vos} + E_{vod} \qquad 2.5$$

Where,

AED = atmospheric evaporative demand (mm)

E_{vo} = water non-stressed plant evaporation (mm)

E_s = soil evaporation (mm)

E_{vos} = water non-stressed evaporation from sunlit leaves (mm)

E_{vod} = water non-stressed evaporation from shaded dark leaves (mm)

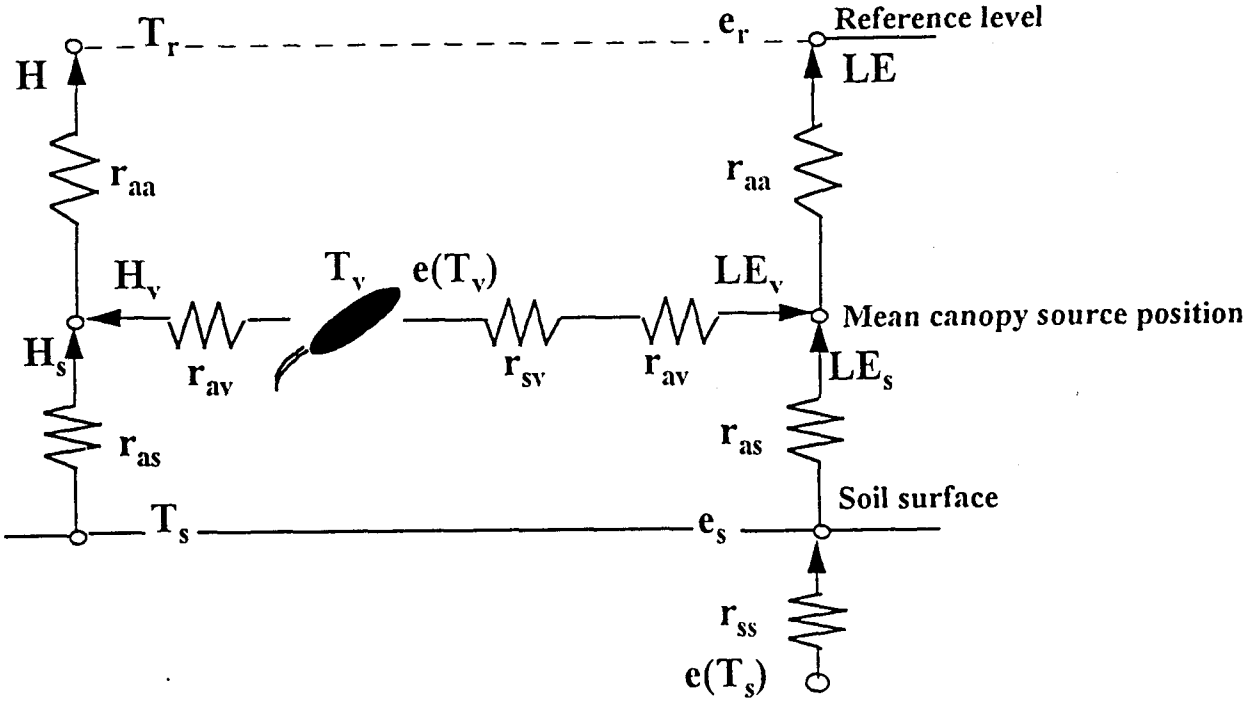

Fig. 2.1 **Schematic diagram of the one-dimensional model of crop energy partition which is the framework of the theory of evaporation from a cropped surface with partial vegetative cover**

Shuttleworth (1990), depicted the surface energy balance of a cropped surface with partial vegetative cover as in Fig. 2.1. The symbols in Fig. 2.1 are defined according to the definitions on pages I to III. The resistances are defined as follows:

r_{aa} : Aerodynamic resistance between canopy source height and the reference level

r_{sv} : Bulk equivalent of the stomatal resistance of the canopy, or canopy resistance to water vapour transfer.

r_{av} : Bulk boundary layer resistance.

r_{as} : Aerodynamic resistance between soil surface and mean canopy source position (sub-canopy)

r_{ss} : Soil surface resistance to water vapour flow.

The subscript s for sunlit and d for shaded can be applied to all the variables.

Later, in this report, a single bulk boundary layer resistance, r_v, was used,

where $r_v = r_{svs} + r_{av} + r_{svd} + r_{av}$ (with $r_v = 30_s\ m^{-1}$ or $70_s\ m^{-1}$)

A cropped surface may be analysed in terms of sunlit and shaded components. Thus, the energy budget for the sunlit leaf surfaces, for instance, is given by

$$R_{nvs} + G_{vs} + H_{vs} + LE_{vs} = 0 \qquad 2.6$$

where,

R_n = net radiation (W m^{-2})

G = soil heat flux density (W m^{-2})

H = sensible heat flux density (W m^{-2})

LE = latent heat flux density (W m^{-2})

Here the convention was adopted where energy flow away from the surface is considered to be +ve and vice versa.

The subscript (vs) here refers to vegetation surface (the v) exposed to direct sunlight (the second subscript, s).

According to the Ohm's analogue (see Fig. 2.1) sensible heat flux from the sunlit vegetation, H_{vs}, in Equ. 2.6 is given by

$$H_{vs} = \frac{\rho C_p (T_{vs} - T_o)}{r_{avs}} \qquad 2.7$$

and

$$LE_{vs} = \frac{\rho C_p (e(T_{vs}) - e_o)}{\gamma (r_{avs} + r_{vs})} \qquad 2.8$$

where,

L	=	latent heat of evaporation at constant temperature (J kg^{-1})
ρ	=	air density (kg m^{-3})
C_p	=	specific heat of air (J kg^{-1} $°C^{-1}$)
r_{avs}	=	aerodynamic resistance between the sunlit leaf surfaces and effective canopy source height (s m^{-1})
T_{vs}	=	temperature of the sunlit leaf surface (°C)
T_o	=	air temperature at effective canopy source height (°C)
$e(T_{vs})$	=	saturated vapour pressure at T_{vs} (kPa)
e_o	=	vapour pressure at effective canopy source height (kPa)
γ	=	psychrometric constant (kPa $°C^{-1}$)
r_{vs}	=	surface resistance of the sunlit leaf surfaces, (s m^{-1})

The various aerodynamic and surface resistances can be calculated using the methods described by Shuttleworth & Gurney (1990), Shuttleworth (1991) and Nichols (1992).

The saturated vapour pressure $e(T_{vs})$ in Equ. 2.7 was calculated from the integrated form of the Clausius Clapeyron equation which for sunlit leaves with temperature T_{vs} reads

$$e(T_{vs}) = 6.11 (\exp (5347{,}61 (1/273{,}16 - 1/(273{,}16 + T_{vs}))))^{0{,}1} \qquad 2.9$$

Eqs. 2.6, 2.7 and 2.8 with appropriate subscripts, are also valid for shaded leaves and sunlit and shaded soil surfaces.

2.1.1 The model of Shuttleworth and Gurney (SG)

Shuttleworth & Gurney (1990) employed numerous relationships to obtain the mathematical expressions required to solve for E_v and E_s. These will now be described

(i) Canopy-aerodynamic resistance, r_{av}

$$r_{av} = r_l/2\,LAI \qquad 2.10$$

where, by definition, the equivalent stomatal resistance is given by

$$r_l = \frac{100}{n'}\left[\frac{(W/u_h)^{1/2}}{[1-\exp(-n'/2)]}\right] \qquad 2.11$$

W = leaf width (mm)

u_h = wind speed just above canopy height (m s^{-1})

n' = a dimensionless attenuation coefficient for eddy diffusivity = 0,6 (Nichols, 1992)

(ii) Sunlit surface-air resistance, r_{svs}

$$r_{svs} = \frac{(\rho Cp/\gamma)[e(T_{vs}) - e_o]}{(R_n - R_{ns}) - \rho Cp\,(T_{vs}-T_o)/r_{avs}} - r_{avs} \qquad 2.12$$

where

r_{svs} = bulk stomatal resistance of the sunlit canopy (s m^{-1})

R_n = net radiation measured over the canopy (W m^{-2})

T_o = temperature measured at the effective source height (m)

R_{ns} = the net radiation at the soil surface = $R_n \exp(-a\,LAI)$ (W m^{-2}) 2.13

where

$$a = 0{,}5 \operatorname{cosec} \theta \qquad 2.14$$

θ = sun elevation angle (degrees)

LAI = leaf area index

(iii) Aerodynamic resistance above the soil surface, r_{as}

$$r_{as} = \frac{h \exp(n)}{n K_h} [\exp(-n z'_o/h) - \exp(-n z/h)] \qquad 2.15$$

having

h = crop height (m)

n = eddy diffusivity decay constant of the canopy = 2,5 (dimensionless)

$$z_o = z_o' + 0{,}3\, h\, (0{,}07LAI)^{0,5} \qquad \text{for LAI} < 2{,}85 \qquad 2.16$$

where

z_o' = roughness parameter of the substrate (soil surfaces) (m)

z_o' is also a function of LAI and, for high LAI

$$z_o = 0{,}3h\,(1 - d/h) \qquad \text{for LAI}>2{,}85 \qquad 2.17$$

Where, the zero plane displacement level, d, is given by

$$d = (1.1h)\ln\{1 + (0{,}07\, LAI)^{0,25}\} \qquad 2.18$$

In addition, where LAI $\geq$ 4 it is preferred to use values for z_o and d, to evaluate the source/sink interchange level, given by:

$$z = z_o + d$$

where,

z = height of the effective surface for energy exchange (m)

z_o = 0,13h 2.19

d = 0,63h 2.20

K_h = k u*(h - d) 2.21

where

K_h = the eddy diffusion coefficient at the top of the canopy ($m^2\ s^{-1}$)

k = von Karman's constant

u_* = friction velocity ($m\ s^{-1}$) given by

$$u_* = \frac{k\,u}{\ln\{(z_r - d/z_o)\}} \qquad 2.22$$

where

z_r = reference height of 1,0 m above the effective surface for energy exchange (m), and

u_z = windspeed above effective surface for energy exchange ($m\ s^{-1}$)

In our experiments z was usually equal to Z_r = 1,0 m.

(iv) Sunlit soil-air surface resistance r_{ss}

$$r_{ss} = \frac{(\rho Cp/\gamma)[e(T_{ss}) - e_o]}{(R_{ns}) - \rho Cp\,(T_{ss}-T_o)/r_{as}} - r_{as} \qquad 2.23$$

2.1.2 The PUTU-model

An evaporation coefficient (k) is defined as the ratio of evaporation from a crop component (vegetation or soil) to reference crop evaporation (E_o).

In the PUTU-model (De Jager, 1992) the subroutine used to calculate crop total evaporation, E, is based upon evaporation coefficient theory expressed mathematically as follows:

$$E = E_v + E_s \quad 2.24$$

$$= (k_v + k_s)\, E_o \quad 2.25$$

where

E_o = Reference crop evaporation from a 0,15 m tall grass surface (mm).

The vegetation evaporation coefficient

$$k_v = k_{vo}\, FI\, F_v \quad 2.26$$

and the soil evaporation coefficient

$$k_s = k_{so}\, F_g\, (1 - FI) \quad 2.27$$

Here, FI is the radiation fractional interception and F_v is a crop growth factor (0-1) controlled by crop water status.

Fg is a dry-down factor quantifying the fraction of potential soil evaporation permitted by the degree of dryness of the soil surface.

Also, k_{vo} and k_{so} are maximum evaporation coefficients for vegetation and soil respectively.

For a crop not short of water $F_v = 1$, while under water stressed conditions $F_v < 1$ is computed by an iteration technique as described in De Jager (1992).

It was shown by Van Zyl & De Jager (1994) that k_{vo} = 1,13 for potato evaporation and 1.09 for maize. It was furthermore assumed that $k_{so} = 1$.

It was thus possible from Equ. 2.25, 2.26, and 2.27 to write:

$$E_v = 1{,}13\ FI\ F_v\ E_o \text{ for a potato crop} \quad 2.28$$

and $$E_v = 1{,}09\ FI\ F_v\ E_o \text{ for a maize crop} \quad 2.29$$

with,

$$E_s = F_g\ (1 - FI)\ E_o \text{ for both crops} \quad 2.30$$

The fractional radiation interception can be computed from FI = 1 - exp (-0.7 LAI) (Ritchie, 1983) and F_g = exp(-0,4D) (De Jager, Van Zyl, Bristow & Van Rooyen, 1982). Here, D denotes the number of days elapsed since the last wetting event exceeding 10 mm. Reference crop evaporation can be calculated from AWS-data and the Penman-Monteith equation (PME) (Van Zyl & De Jager, 1987).

In the latest version of PUTU the values 1,13 for potato and 1,09 for maize are compensated for varying climate according to (see Van Zyl & De Jager (1994) and Van Zyl & De Jager, 1992) a climate adjustment factor, η, which for potato, is written as:

$$\eta = 1{,}13\ (a + bR_s + cT + de + fu) \quad 2.31$$

where,

R_s = total global radiation (W m^{-2})

T = air temperature at 1,5 m above ground level (°C)

e = water vapour pressure (kPa)

u = wind speed at 3 m above ground level (m s^{-1})

a, b, c, d, and f are regression constants and for the maize crop the initial term takes the value 1,09 instead of the 1,13 for potato.

2.1.3 General

It is evident from the above that LE_{vs} may now be calculated from Equ. 2.8 through Equ. 2.12, or alternatively Equ. 2.24 through 2.31.

Soil evaporation LE_{ss}, and the shade components, LE_{vd} and LE_{vd} can be obtained using equations similar in form to Equ. 2.8 through 2.31, but modified with appropriate subscripts.

2.2 MICRO-METEOROLOGICAL TECHNIQUES FOR DETERMINING EVAPORATION

2.2.1 Direct eddy correlation technique (EC)

For a horizontal surface with an upwind fetch adequate to ensure measurements representative of the surface, the vertical transport of water vapour can be determined from

$$LE = L\overline{w'e'} \qquad 2.32$$

where w' (measured in m s^{-1}) and e' (measured in kg m^{-3}) are instantaneous departures from the mean vertical wind speed and mean water vapour pressure respectively.

2.2.2 Energy budget/eddy correlation technique (EBC)

Following Equ. 2.6 and assuming negligible advection (see Lang, 1973) total evaporation, E, from the energy budget at a surface is given by

$$LE = -(R_n + G + H) \qquad 2.33$$

Sensible heat flux density, H, may be obtained from eddy correlation measurements by

$$H = \rho Cp\ \overline{w'T'} \qquad 2.34$$

where T' is the instantaneous deviation from the mean vertical air temperature.

Substitution of Equ. 2.34 into Equ. 2.33 yields the energy budget/eddy correlation (EBC) formula for determining evaporation, viz.

$$LE = -(R_n + G + \rho Cp\ w'T') \qquad 2.35$$

2.2.3 Energy budget/Bowen ratio technique (EBBR)

Total evaporation, LE, can be obtained from the energy budget in terms of the Bowen ratio assuming that advection is zero (see Lang, 1973). Thus,

$$LE = -(R_n + G)/(\beta + 1) \quad 2.36$$

In Eq. 2.35 $\beta = H/LE$ and hence 2.37

$$\beta = \frac{\rho Cp\,(T_{a1} - T_{a2})}{L(e_1 - e_2)} \text{ (Campbell, 1977)} \quad 2.38$$

$$= \frac{\gamma\,(T_{a1} - T_{a2})}{(e_1 - e_2)} \quad 2.39$$

where $\gamma = \rho Cp/L$ 2.40

and applying the assumption that the resistance to water vapour transfer (measured in s m^{-1}) equals the resistance to heat transfer (measured in s m^{-1}), and measurements of atmospheric temperature (T_{a1}, T_{a2}) and vapour pressure (e_1, e_2) are made at two heights denoted 1 and 2 respectively.

CHAPTER 3

EQUIPMENT, METHODOLOGY AND MEASUREMENT OF EVAPORATION

This chapter describes the meteorological observations, the installation of all the instruments, as well as the design, specifications and operation of the large weighing lysimeter, four drainage lysimeters and 24 micro-lysimeters which were used in the study. All observations and experiments were carried out at the Agrometeorology Field Laboratory on the West Campus of the University of the Orange Free State.

Prior to experimentation, all the instruments, with the exception of the Bowen ratio and eddy correlation systems, were calibrated against either standard, or similar instruments. This was done on the grass site (80 m x 80 m) adjacent to the potato field (described in Van Zyl & De Jager, 1994). Calibration procedures and some results are given in Appendix I.

3.1 MICRO-METEOROLOGICAL EQUIPMENT

The following hourly micro-meteorological observations, here denoted (MMO), were made in and above the potato and maize crops:

- Net radiation 1,5 m above the potato crop and maize crops.
- Soil heat flux density with sensors, embedded 50 mm below soil surface and placed as follows:

(i) one within the row,

(ii) one at a position 0,25 times row width, and

(iii) two at a position 0,50 times row width.

- Soil temperature using copper-constantan thermocouples, located at depths of 10, 50 and 150 mm below soil surface adjacent to the two soil heat flux sensors, positioned at 0,50 times row width.
- Soil surface temperature (sunlit and shaded) and leaf temperature (sunlit and shaded) using copper-constantan thermocouples. These temperatures were measured just below soil surface while leaf temperatures were measured by inserting a thermocouple into the leaf in such a manner that it is not exposed to direct solar radiation.
- Soil surface (sunlit and shaded) and leaf (sunlit and shaded) temperature using an infra-red thermometer.
- Windspeed 0,5 and 1,0 m above canopy height.

- Latent heat flux density and sensible heat flux density using eddy correlation techniques. Two identical systems were installed 1,5 m above canopy surface. Copper-constantan thermo-couples, sonic anemometers and a Krypton hygrometer supplied by Campbell Scientific, Logan, USA, were utilized.
- Water vapour pressure and temperature just above the crop and at 1,0 m above canopy height.

Micro-meteorological measurements were recorded on a CR7 and two 21X data loggers both from Campbell Scientific, Logan, USA.

3.2 AUTOMATIC WEATHER STATION MEASUREMENTS

An automatic weather station installed on the grass next to the experimental site was used to record global radiation, R_s, air temperature, T_a, and wet bulb temperature, T_w, at 1,5 m height above grass level and windspeed, u, at 3 m height above grass level. All sensors were calibrated in the standard manner.

3.3 LYSIMETERS

3.3.1 Weighing lysimeter

A large weighing lysimeter covered with a thin plastic sheet was used to measure plant evaporation, E_v. The plastic sheet restricted water loss from the lysimeter to only plant evaporation. The plastic sheet was covered with a layer of soil approximately 5 mm thick to minimize disturbance of the micro-environment. The layer of soil was made as thin as possible so as virtually to eliminate water storage in the layer which would eventually evaporate and be erroneously recorded as plant evaporation. The thin plastic cover became completely embedded in the soil without any air spaces between its upper and under sides. The plastic has a low thermal capacity and good heat conductivity. This ensured normal heat transfer downwards from the soil surface. The minimal disturbance of soil temperature is illustrated in Fig. 3.3. Furthermore a 30 cm x 30 cm grid of perforated 10 mm diameter tubing with open ends exposed to the atmosphere was positioned immediately below the plastic cover to permit gaseous exchange. The area, effective soil depth, resolution and accuracy at moderate windspeeds of the lysimeter system were 9,73 m^2, 2,5 m, 0,07 mm and 0,02 mm respectively. The construction and performance of the lysimeter is fully described in De Jager, Van Zyl, Kelbe & Singels (1987). Gravitational drainage through the 2,6 m soil profile was ensured by a Biddim layer on top of 10 mm stone chips.

The high resolution of the lysimeter enabled hourly measurement of evaporation. Conversion of mass of water evaporated to mm of water evaporated was obtained by dividing the change in mass of water by the product of the density of water and cross sectional area of the lysimeter.

3.3.2 Drainage lysimeters

Four identical steel drainage lysimeters with area 3,35 m^2 and effective depth of 0,87 m were installed next to the weighing lysimeter. These lysimeters were furthermore equipped with drain pipes covered by 10 mm grade stone chips to a thickness of 50 mm. The stones were covered by 5 mm Biddim material, which acted as a porous membrane. The lysimeters were filled with red Bainsvlei soil to a density of 1,6 Mg m^{-3}. The latter figure corresponds to the soil density in the weighing lysimeter.

The soil surface in two of the metal drainage lysimeters like that of the weighing lysimeter was covered with a plastic sheet so as to permit measurement of E_v alone, while the other two were left uncovered in order to measure total evaporation, E. So as to ensure no water stress, the soil water potential was held at approximately -10 kPa using the following procedure. At approximately 17:00 on the first day of a 7 day cycle, the large weighing lysimeter and four drainage lysimeters were saturated with water. The next two days were used to extract free water from the profile of the drainage lysimeters at a suction of approximately 25 kPa. Suction was maintained during this period and the water was extracted from the drainage lysimeters utilizing a three phase 1 kW pump. As explained in Section 3.3.1 drainage by gravity took place in the weighing lysimeter. The lysimeters were then allowed to evaporate freely from the second day till 17:00 of the seventh day, whereafter the entire cycle was repeated.

3.3.3 Micro-lysimeters

A total of twenty-four 88 mm outer diameter micro-lysimeters, filled with the same Bainsvlei soil to a density of 1,6 Mg m^{-3} were installed next to the weighing and drainage lysimeters. The micro-lysimeters fitted snugly into holes drilled into the soil at the selected points within and between crop rows. The micro-lysimeters, made from PVC-pipe, were bottomless to permit free drainage. The area and height of the lysimeters was 0,00238 m^2 and 300 mm respectively.

Each measuring cycle the lysimeters were initially saturated with water and then allowed to drain freely for a period of approximately 48 hours inside a closed container. Drainage was not carried out on a sand bed which would have been preferable for ensuring adequate drainage. Eight of the micro-lysimeters were installed at 0,5 times row width, eight at 0,25 times row width and eight centrally within the crop rows. The lysimeters were weighed early every morning during the week with the exception of Saturdays and Sundays. Temporary bottoms were fitted during the wetting process. These were removed just prior to installation in the soil. Apparently the drainage during the initial

stages of exposure in the soil was inadequate and representative values of soil evaporation only occurred after five days (see Fig. 8.2 and Fig. 8.4). The entire technique is described by Bennie (1994) and an analysis of its problems given by Evett, Warrick & Matthias (1995).

During rainfall or irrigation lysimeters were left in position in the field.

Mass of water weighed was converted to mm of water by dividing the former by the product of the density of the water and the cross sectional area of the micro-lysimeters.

3.4 CROP MORPHOLOGY MEASUREMENTS

The following measurements of crop development were made at weekly intervals:

- crop height
- leaf area index, and
- leaf width.

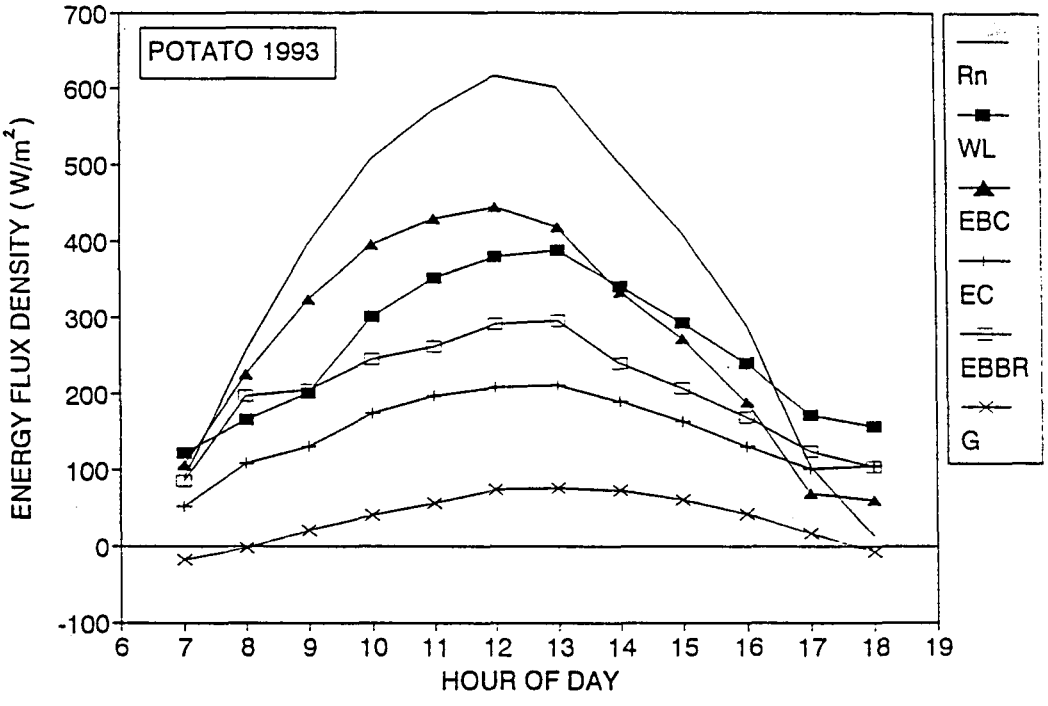

Fig. 3.1 **Diurnal variation of mean hourly flux densities for the different energy forms in the potato crop**

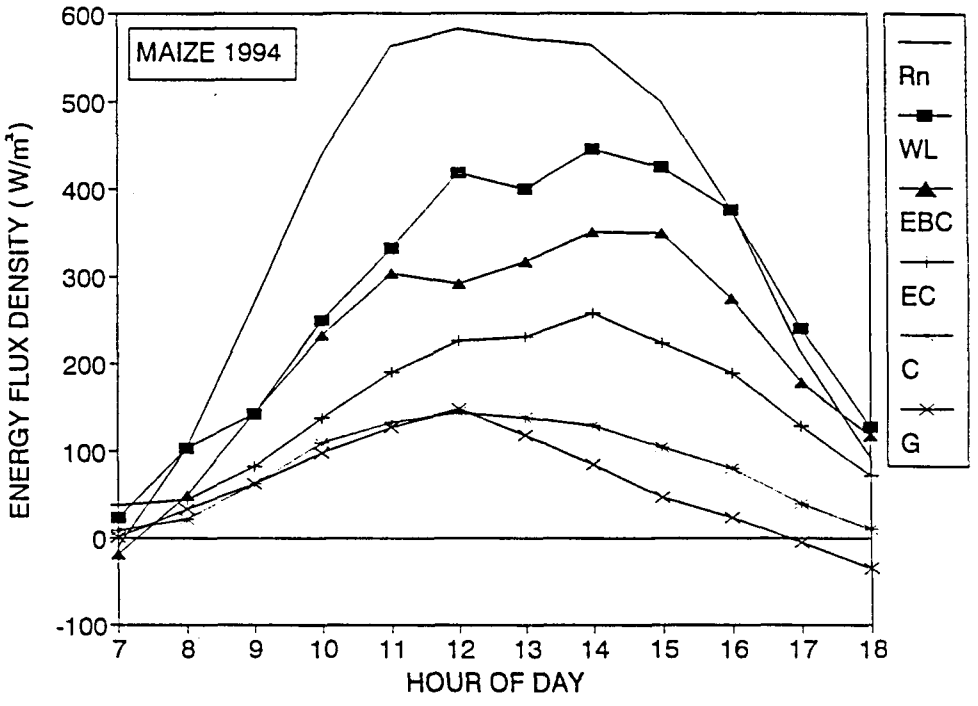

Fig. 3.2 **Diurnal variation of mean hourly flux densities for the different energy forms in the maize crop**

3.5 RESULTS AND DISCUSSION

3.5.1 Diurnal variation of energy flux densities for potato and maize

Diurnal variation in the different mean hourly energy flux densities for the potato and maize crop are shown in Figs. 3.1 and 3.2.

Plant evaporation (E_v) values from the potato crop measured by the large weighing lysimeter (WL) were lower than eddy correlation/energy budget values EBC up to 14:00 which is to be expected (see Fig. 3.1). However, from 14:00 onward and for virtually the whole of the day in the case of maize (see Fig. 3.2), plant evaporation E_v exceeded the E as determined by EBC. This anomaly is either attributable to the fact that EBC underestimated E, or that the plastic sheet covering the large weighing lysimeter somehow influenced E_v. In an attempt to explain this phenomenon, soil temperatures at a depth of 0,01 m were measured underneath the plastic sheet and in an adjacent uncovered soil (see Fig. 3.3). It was found that the temperature under plastic was about 2°C lower than in uncovered soil, indicating that a small insulational effect was introduced by the plastic cover. This relatively small temperature difference should have had negligible influence on E_v(WL) and implies that EBC, and EC and EBBR, underestimated E, possibly for different reasons.

It was reasoned that changes in the energy balance due to the plastic covering eliminating evaporation were nulified by entrainment of air from the surrounding canopy. Furthermore, the high thermal

conductivity and capacity of the moist sub-soil should cause cool soil conditions which would also tend to compensate any increase in surface temperature due to lack of evaporation.

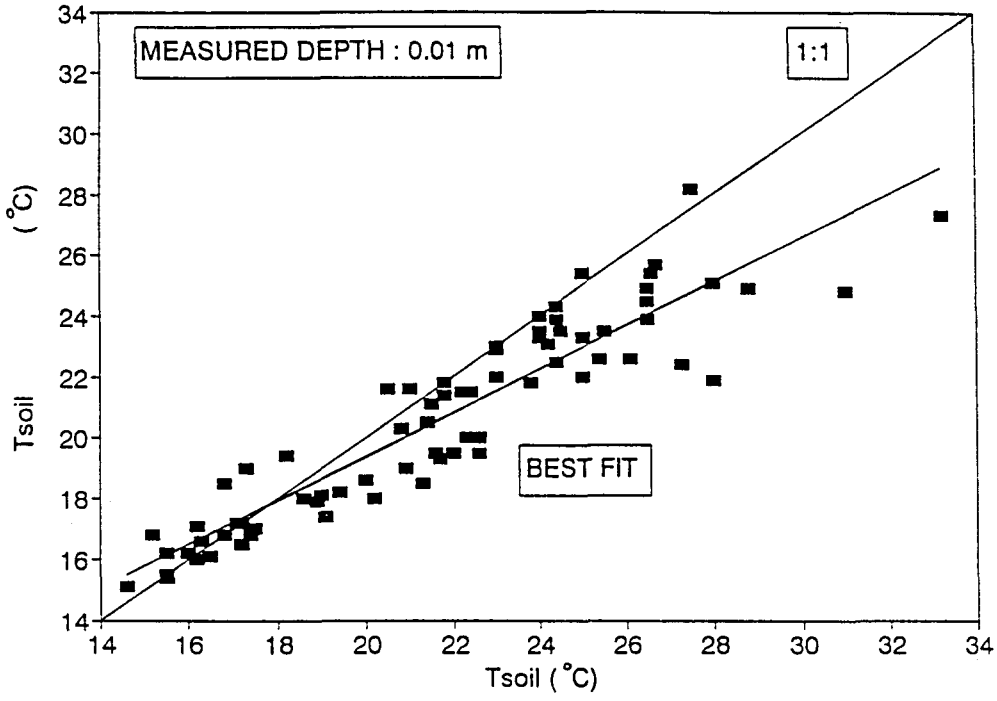

Fig. 3.3 **Relationships between temperature 0,01 m beneath plastic covered lysimeter soil surface and uncovered adjacent soil**

3.5.2 Lysimeter results

Tables 3.1 and 3.2 summarize measurements of E, E_v, and E_s made on both crops with the large weighing lysimeter, the drainage lysimeters and the micro-lysimeters. Also tabulated in Tables 3.1 and 3.2 are values of soil evaporation, E_s, derived by subtracting values in Column 5 from corresponding values in Column 8.

From Table 3.1 it is apparent that E_v(DL) for potato agree to within 10% with E_v(WL) in some instances (see columns 2 and 5, rows 1, 3 and 5), 20% (row 6) and poorly in the other other (remaining 2 rows in columns 2 and 5). Rows 3 and 5 agreed to within 5%.

Table 3.2 shows that measurements of E_v for maize follow a similar pattern. Agreement within 10% is apparent between E_v(DL) and E_v(WL) (see Column 2 and 5, Row 1, 3, 4 and 6). For rows 3 and 4 agreement was better than 5%. The rest of the rows in Column 2 and 5 correspond poorly.

On two occasions, Row 4 and 6, good correspondence was obtained for E_s(ML) measured and E_s(DL) calculated from Column 8 - Column 5 for the potato crop (Table 3.1). For maize, significant

overestimation of soil evaporation by micro-lysimeter E_s(ML), was observed on all occasions when compared to E_s(ML) obtained from Column 8 - Column 5 in Table 3.2. In most cases on both crops the drainage lysimeters seemed to have malfunctioned (negative values for E).

3.6 SUMMARY AND CONCLUSIONS

Detailed results of the calibrations carried out on instruments are given in Appendix I. It may be assumed that all instruments used in the study were adequately calibrated. Several anomalies however, deserve mention. These include:

- Total evaporation values, E, obtained from micro-meteorological measurements underestimated the E_v measured by the large weighing lysimeter, thereby suggesting that the micro-meteorological measurements underestimated E. The micro-meteorological measurements were thus accorded little attention in ensuing studies.
- Comparison between the large lysimeter and drainage lysimeters used to measure E_v were of acceptable accuracy for part of the time, but poor at others. The large lysimeter values were used in most of the subsequent analyses.
- E_s measured by micro-lysimeters tended to overestimate E_s calculated from (E-drainage lysimeter - E_v-drainage lysimeter). A discussion of this follows in Chapter 8.

The results of the more important calibrations carried out, are reported in the figures and tables in Appendix I.

From these it may be concluded that excellent agreement was obtained between:

- radiometers used in the study and a standard instrument,
- different SHF-sensors,
- IRT and manufacturer's calibration radiation source in the range 0 -50°C,
- output from the large weighing lysimeter and applied weights and
- two eddy correlation systems for determining sensible heat flux density, H.

Good agreement was obtained between

- three three-cup anemometers and a wind-run meter. An appropriate regression equation was used to correct field observations, and
- the two eddy correlation systems used to measure latent heat flux density, LE.

Table 3.1 Evaporation measured with different lysimeters for the potato crop over different time interval periods

Row	Column 1 PERIOD DOY	Column 2 E_V(WL) mm	Column 3 E_V1(DL) mm	Column 4 E_V2(DL) mm	Column 5 E_V(Mean DL) mm	Column 6 E1(DL) mm	Column 7 E2(DL) mm	Column 8 E(Mean DL) mm	Column 9 E_S(DL) mm	Column 10 E_S(ML) mm
1	256-264	19,0	16,7	17,2	17,0	17,1	19,6	18,3	+1,3	xxxx
2	267-271	21,1	15,1	17,4	16,2	15,6	18,9	17,2	-1,0	xxxx
3	298-305	52,7	50,4	50,5	50,5	xxxx	xxxx	xxxx	xxxx	13,8
4	306-313	34,5	20,1	28,9	24,5	48,0	49,0	48,5	24,0	21,4
5	314-320	39,3	36,6	39,5	38,0	47,5	47,7	47,6	9,6	21,5
6	321-328	45,8	32,9	39,7	36,3	48,9	51,9	50,4	14,1	16,2
7	329-334	53,5	22,1	27,9	25,0	53,8	48,0	50,9	25,9	xxxx

WL - Weighing lysimeter [Cross sectional area: 9,73 m^2]
DL - Drainage lysimeter [Cross sectional area: 3,35 m^2]
ML - Micro-lysimeter [Cross sectional area: 0,002827 m^2]
xxxx - Missing data
The number 1 and 2 identify the drainage lysimeter.

Table 3.2 Evaporation measured with different lysimeters for the maize crop over different time interval periods

Row	Column 1 PERIOD DOY	Column 2 E_V(WL) mm	Column 3 E_V1(DL) mm	Column 4 E_V2(DL) mm	Column 5 E_V(Mean DL) mm	Column 6 E1(DL) mm	Column 7 E2(DL) mm	Column 8 E(Mean DL) mm	Column 9 E_S(DL) mm	Column 10 E_S(ML) mm
1	55-61	31,0	32,2	37,1	34,7	27,5	39,7	33,6	-1,1	15,8
2	62-69	28,0	69,0	63,3	66,2	36,7	77,6	57,2	-9,0	14,0
3	70-75	34,0	32,9	33,1	33,0	40,5	40,6	40,6	7,5	23,4
4	76-83	44,0	38,5	37,9	38,2	33,9	46,7	40,3	2,1	11,8
5	84-88	29,0	39,7	36,4	38,1	32,5	29,4	31,0	-7,1	3,8
6	89-98	48,0	60,6	52,6	56,6	52,6	48,7	50,7	-5,9	21,6
7	99-105	33,0	21,8	23,9	22,9	8,7	13,4	11,1	-11,8	9,2

WL - Weighing lysimeter [Cross sectional area: 9,73 m^2]
DL - Drainage lysimeter [Cross sectional area: 3,35 m^2]
ML - Micro-lysimeter [Cross sectional area: 0,002827 m^2]
The numbers 1 and 2 identify the drainage lysimeter.

In general, poor agreement was obtained between the IRT and thermocouples used to measure surface temperatures.

While, Berliner, Oosterhuis & Green (1984) highlighted shortcomings with the IRT, both practical and logistical errors were encountered when using thermocouples. For instance, thermocouples became detached from leaves even under moderate wind conditions, or wind forces could cause shaded leaves to be exposed to the sun and vice versa.

CHAPTER 4

ESTIMATION OF NET RADIATION FROM GLOBAL RADIATION

Automatic weather stations measure incoming global radiation, R_s. The models in this study however require values of net radiation, R_n. The possibility of developing a reliable relationship for R_n based on R_s was investigated. Two different methods were considered.

4.1 AN EMPIRICAL RELATIONSHIP

First, a simple empirical relationship was developed between simultaneous hourly measurements of R_s and R_n. R_s was measured by the LICOR sensor on the AWS installed above short grass, adjacent to the experimental field, while R_n was measured by a net radiometer installed 1,5 m above the potato, or maize crop. Hourly mean observations were recorded on CR10 (for R_s) and CR7 (for R_n) data loggers. Measurements were undertaken for vegetative cover for which FI values exceeded 0,93 on both crops during maturity.

Hourly mean R_n was regressed on hourly mean R_s. The resulting empirical relationship between R_n and R_s for the potato crop, reads:

$$R_n = 0{,}66\ R_s - 57\ W\ m^{-2} \qquad 4.1$$

The coefficient of determination, r^2, for 160 observations was 0,90.

The regression equation obtained for maize, reads:

$$R_n = 0{,}66\ R_s - 10\ W\ m^{-2} \qquad 4.2$$

The coefficient of determination was $r^2 = 0{,}86$ for 106 observations.

These regression constants are within 18% of those (0,83 and
79 W m^{-2}) found by Van Zyl, & De Jager, (1987) for a short grass cover.

It was concluded that reliable estimation of R_n is possible using these equations and hence they may with confidence, be included in models for estimating E_v and E_s.

The difference between the equations for the two different crop types is minimal suggesting use of a single equation for both crops.

4.2 THE FAO MODEL

Jensen *et al.*, (1990), report an equation for estimating R_n from R_s which was further refined by Smith (1992) to become known as the FAO model. This equation is expressed

$$R_n = R_{ns} - R_{nl} \qquad 4.3$$

where,

R_n = Net radiation (MJ m^{-2} d^{-1})

R_{ns} = Net incoming short-wave radiation (MJ m^{-2} d-1)

R_{nl} = Net outgoing long-wave radiation (MJ m-2 d-1).

The first term on the right hand side of this equation is found from

$$R_{ns} = (1 - \alpha) R_s = 0{,}77 R_s \qquad 4.4$$

where

α = albedo, or canopy reflection coefficient, (0,23 overall average for grass).

R_s = incoming solar radiation (MJ m^{-2} d^{-1}).

R_{nl} was computed using the standard FAO method reported by Smith (1992).

Albedo

The role of albedo in the above equation is evident in equation 4.4, the equation for estimating R_{ns}. It was an objective of the project to determine the significance of albedo in the models. With this in mind, albedo was measured above red soil and black soil to evaluate any differences. A scenario of albedo over some seven days is presented in Fig. 4.1. From this it is evident that black soil in the middle of the day has an albedo of approximately 0,15. Red soil is much higher at approximately 0,2. This effect is sufficiently large to require consideration in models.

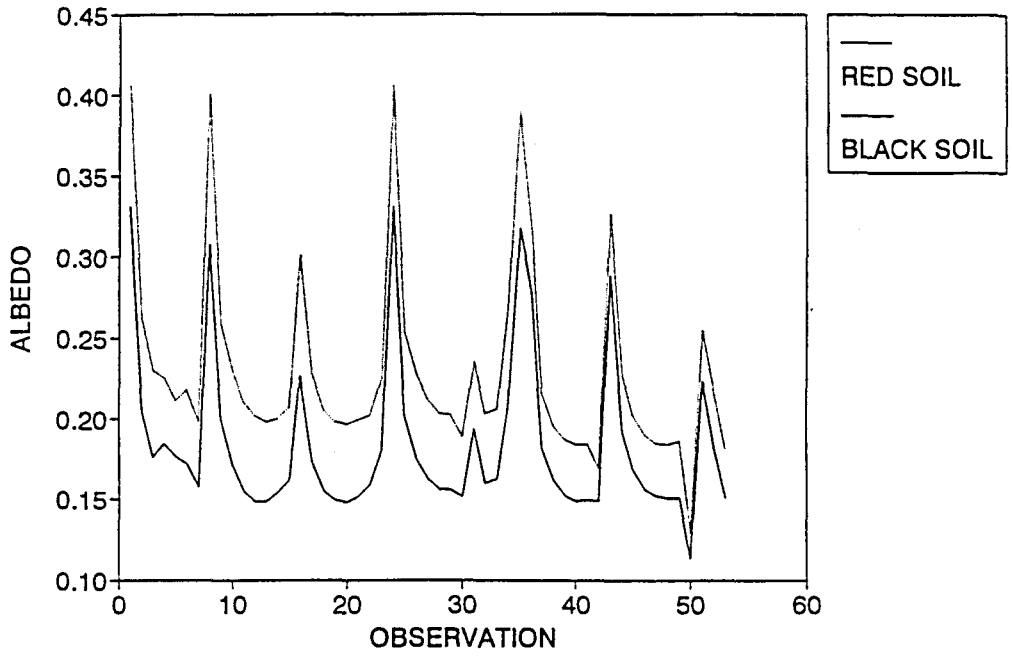

Fig. 4.1 Hourly mean albedo for red and black soil surfaces for six days

FAO calculation of R_n

Hourly mean net radiation was calculated, R_nCAL, using the FAO method. This was compared to measured values, R_nM. Results of the linear regression analysis for an albedo of 0,23 and 0,4 are given in Fig. 4.2 and 4.3. In Fig. 4.2 it is evident that using the prescribed albedo value of 0,23,

$$R_{ns} = 0{,}77\ R_s\text{AWS} \qquad 4.5$$

where,

R_sAWS is the global radiation measured by the automatic weather station,

leads to R_nCAL overestimating measured R_nM by approximately 150 W m^{-2} which is unacceptable. The regression was re-run with R_{ns} = 0,6 R_sAWS and the results are depicted in Fig. 4.3. Better agreement was obtained particularly for high R_n suggesting that an albedo of 0,4 would be a better value to use in the R_n-model. Results here reported, refer to full vegetative canopy cover. Hence a suggested linear function adjusting albedo between 0,20 and 0,4 for canopy radiation interception on red soil and 0,15 and 0,4 for black soil seems appropriate.

4.3 CONCLUSIONS

In view of the big difference between the suggested 0,6 and the prescribed 0,77 for albedo for grass cover and the empirical nature of this adjustment, it was decided that the simple linear regression found for the maize and the potato crops is a more reliable submodel. Ensuing work was carried out using the empirical relationship.

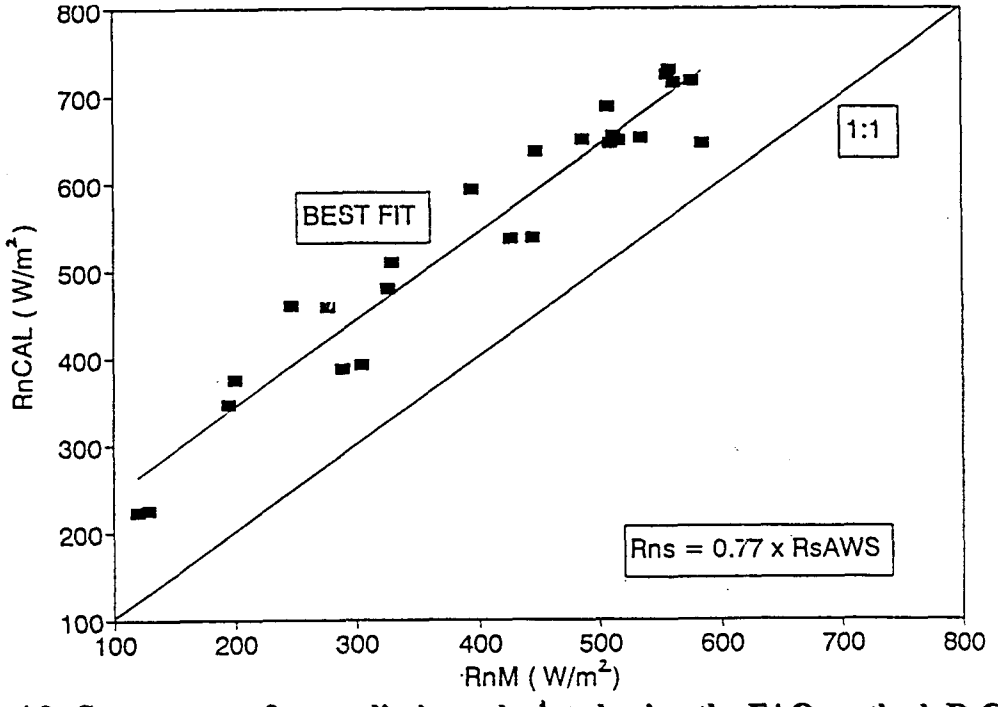

Fig. 4.2 Scattergram of net radiation calculated using the FAO-method, R_nCAL, compared to measured hourly mean values, R_nM for R_{ns} = 0,77 R_s AWS

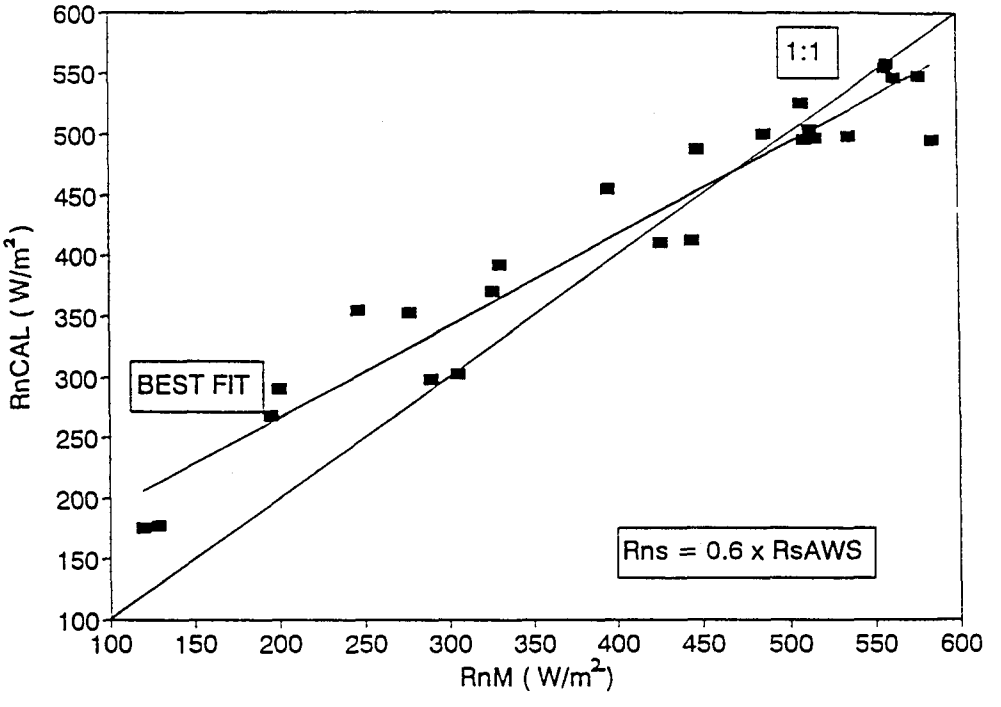

Fig. 4.3 Scattergram of net radiation calculated using the FAO-method, R_nCAL, compared to measured hourly mean values, R_nM for R_{ns} = 0,6 R_s AWS

CHAPTER 5

LEAF TEMPERATURE SIMULATION

Successful simulation of plant and soil evaporation rates using equations of the Shuttleworth and Gurney type (SG) require accurate simulation of leaf temperature. For widespread application this should proceed preferably using AWS data. This chapter investigated the accuracy of such approach. Fundamental to the SG approach, then, is the need to simulate leaf temperature from AWS data.

5.1 OBJECTIVES

Assess the accuracy of the simulation of leaf temperature using the routines from the SG-model together with an iterative technique developed in this project.

The specific objectives of this chapter were to:

- Compare values of T_{vs} with values of Tvd where both were measured by the IRT.
- Compare with each other T_{vs}, T_{vd} and T_{vm}, all measured by the IRT.
- Validate the SG-iteration technique for the potato and maize crops.

5.2 METHOD

Micro-meteorological observations and data from the automatic weather station were used and both the potato and maize crops were investigated.

For expediency, any procedure involving measurements made with instruments other than those found on the automatic weather station were termed micro-meteorological and such methods were denoted MMO. AWS observations were denoted AWSO. The major differences between MMO and AWSO observations were as follows:

In the case of MMO, measurements included:

- R_n, 1,5 m above the relevant crop,
- e, 10 cm above canopy height,
- u_z, 10 cm above canopy height,
- T_a, 10 cm above canopy height,

In the case of AWSO observations:

- R_s was measured at 2,5 m above grass level and R_n was calculated using the formula $R_n = a\ R_s + b$ where a and b are the empirical constants equal to 0,66 and -57 W m^{-2} respectively (see Chapter 4).
- Wet and dry-bulb temperatures, T_w and T_a whereby vapour pressure, e, and the saturated vapour pressures, $e(T_w)$ and $e(T_a)$ were derived, were measured 1,5 m above grass level, and
- the windspeed, u_z, was measured at a height of 3 m above grass level.

The equations needed for the modelling exercise were

Equ. 2.8, 2.9, 2.10. Furthermore, canopy resistance values of either $r_v = 33$ s m^{-1} or $r_v = 70$ s m^{-1} were examined using both micro-meteorological, MMO, and AWSO observations.

Initially, unknown leaf surface temperature was solved for either T_{vs}, or T_{vd}, or the mean of T_{vs} and T_{vd} denoted T_{vm}, by iteration by substituting a guessed (seed) value for one of them together with appropriate values of r_{av} and r_{vs} calculated from Equ. 2.10 and 2.12 respectively, into Equ. 2.8 and 2.9. The unknown was then iterated for to attain an energy balance in Equ. 2.6 of better than 1 W m^{-2} to obtain the appropriate required leaf temperature.

Unfortunately, due to the manner in which the defining equation Equ. 2.12, had been derived, such procedure produced automatic closure. Therefore an independent estimate of rvs is required to make the iteration work. Based upon present knowledge (Russell, 1980; Jensen, *et al.* 1990; Van Zyl, De Jager, Maree and Singels, 1988) a constant water non-stressed value for daytime lying between 70 s m^{-1}, or 33 s m^{-1} seems possible. Hence, these two values were tested. The iteration was made to proceed exactly as described above except that one of these constant values of rvs instead of the values computed from Equ. 2.12 were used in studying the third objective of this chapter.

Thus the closure criterion was derived from Equ. 2.6 assuming a starting value for sunlit vegetation, say, of $T_{vs} = 0$. The iteration process was terminated when,

$$|R_{nvs} + LE_{vs} + H_{vs}| < 1 \text{ W m}^{-2} \qquad 5.1$$

where,

$$R_{nvs} = R_n * (1 - EXP(-\alpha * LAI)) \qquad 5.2$$

R_n = net radiation measured above the potato, or maize crop,

$$H_{vs} = \rho Cp\ (T_{vs} - T_a)/r_v \qquad 5.3$$

and LE_v was computed from Equ. 2.9 using either 33 s m^{-1} or 70 sm^{-1} for r_v.

In this way T_{vs}, T_{dv} or their mean value, T_{vm} were determined.

5.3 RESULTS AND DISCUSSION

Graphical comparison of T_{vd} and T_{vs} both measured by the IRT appear in Fig. 5.1 . Scattergrams of simulated against measured values appear in Fig. 5.2 to 5.9. These relate T_v simulated using the SG-iteration model with either $r_v = 33$ s m^{-1}, or $r_v = 70$ s m^{-1} for both MMO and AWSO and appropriate vegetation temperatures measured using the IRT. The various statistical tests undertaken are summarized in Table 5.1 and 5.2.

Because of the small intercept of 0,9°C and nearly 1:1 correspondence between T_{vd} and T_{vs} (see Table 5.1 and Fig. 5.1) it was decided to report only results applicable to T_{vm}. They are tabulated in Table 5.2. Although the tests were carried out on T_{vs} and T_{vd} individually, little additional useful information was forthcoming for both crop types.

It is clear from Table 5.2 that better agreement between simulated and measured T_{vm} was achieved when AWSO were used. A slope approaching unity and high r^2 values by comparison with corresponding parameters obtained for MMO support this statement. While unexpected, this was an encouraging result because, in practice, it will indeed be AWS-data on which the model will be used.

While validation is characterized by high scatter, the $r^2 = 0,7$ for the AWS procedure demonstrated acceptable simulation. Apparently, here an $r_v = 70$ s m^{-1} is more reliable than a value of 33 s m^{-1}.

5.4 CONCLUSIONS

- A small difference of 0,9°C and a virtual 1:1 relationship was found between sunlit leaf surface temperatures and shaded leaf temperatures measured with the IRT. This meant that future computation need be undertaken on simply a mean foliage temperature (T_{vm}) and that sunlit and shaded leaves need not be considered separately.
- A virtual 1:1 relationship between T_{vm} measured by the IRT and simulated using the SG-iteration model was found for both potato and maize.

- While a relatively high degree of scatter was obtained (r^2 varied between 0,36 to 0,72 for the various cases), the slope lay between 0,80 and 1,03 in six out of the eight cases reported.
- The validation statistics suggest that the SG-iteration model offers an improved technique for estimating foliage temperature.

Table 5.1 Statistics quantifying the relationship between T_{vd} and T_{vs} for potato and maize crops respectively

Statistical parameter	Parameter value Potato	Maize
Intercept (°C)	-0,84	-0,90
* SEE (°C)	1,86	1,94
r^2	0,81	0,83
n	139	119
Slope	0.96	0.94

* SEE is the Std. Error of the y-Estimate. It is defined in Chapter 7

Table 5.2 Statistics quantifying the agreement between T_v simulated using the SG-model with either values of r_v = 33 s m^{-1} or r_v = 70 s m^{-1} and MMO or AWSO data and T_{vm} measured with the IRT for the potato and maize crops.

Statistical parameter	Parameter value							
	Potato				Maize			
	MMO		AWSO		MMO		AWSO	
	r_v=33 (s m^{-1})	r_v=70 (s m^{-1})	r_v=33 (s m^{-1})	r_v=70 (s m^{-1})	r_v=33 (s m^{-1})	r_v=70 (s m^{-1})	r_v=33 (s m^{-1})	r_v=70 (s m^{-1})
Intercept(°C)	7,3	6,1	0,0	0,0	5,7	2,9	0,0	0,0
SEE (°C)	2,7	2,8	2,3	2,4	2,3	2,7	1,6	1,8
r^2	0,45	0,53	0,46	0,58	0,36	0,40	0,66	0,72
n	139	139	144	144	102	102	125	125
Slope	0,61	0,75	0,87	0,96	0,80	0,99	0,96	1,03

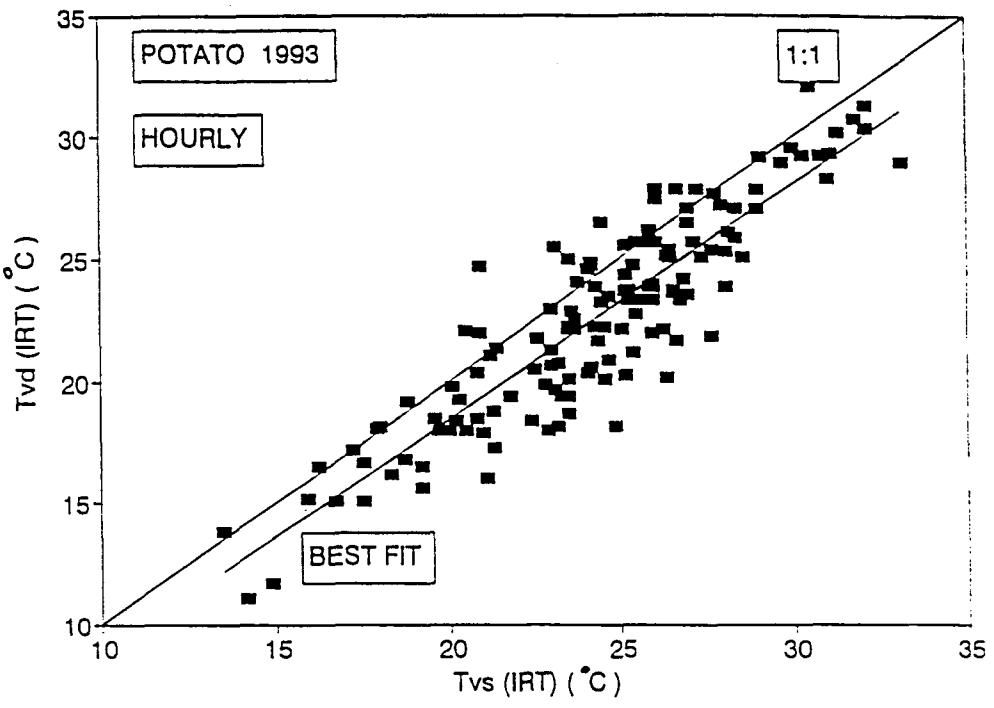

Fig. 5.1 **Scattergram of hourly mean T_{vd} and T_{vs} measured with the IRT**

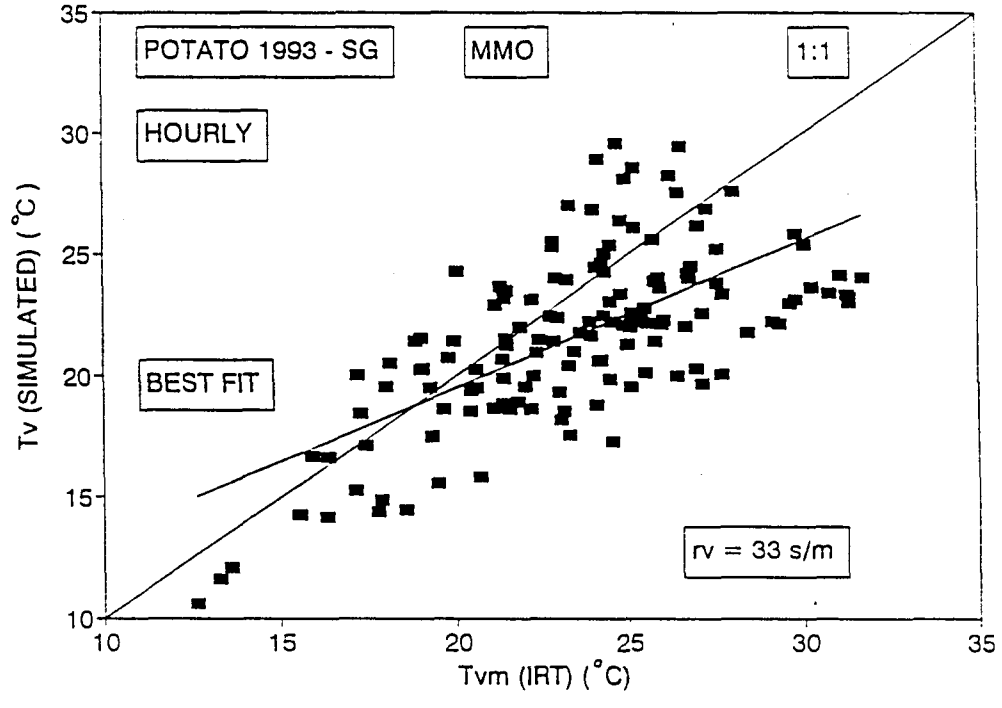

Fig. 5.2 **Scattergram of hourly mean T_v simulated using the SG-model on MMO for $r_v = 33$ s m^{-1} against leaf temperature measured by the IRT, T_{vm}, for the potato crop**

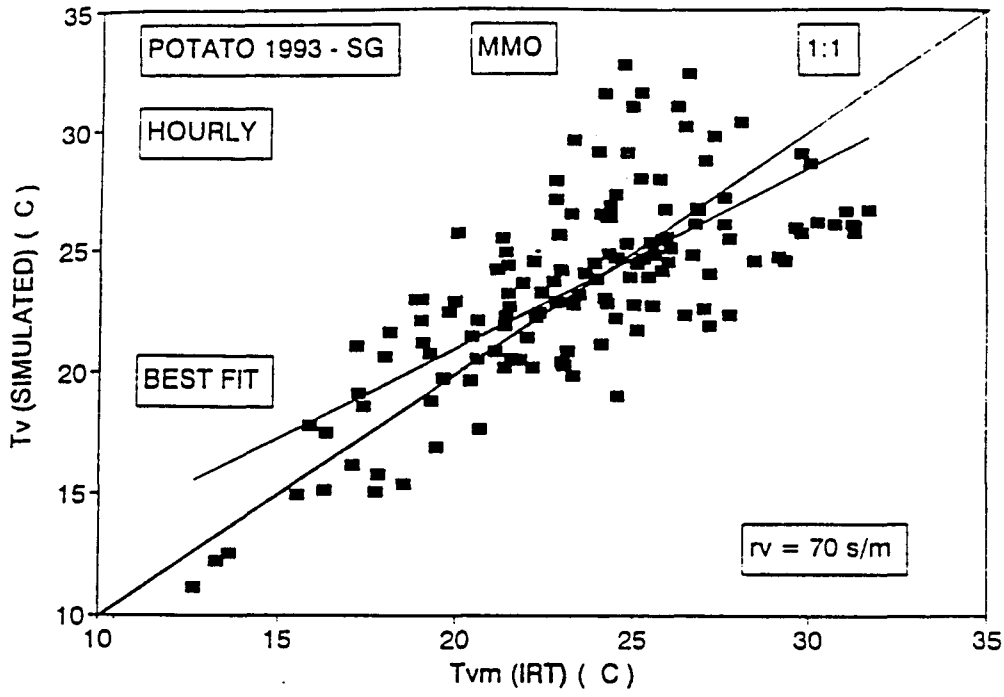

Fig. 5.3 **Scattergram of hourly mean foliage temperature, T_v, simulated using the SG-model and MMO for $r_v = 70$ s m^{-1} and leaf temperature measured by the IRT, T_{vm}, for the potato crop**

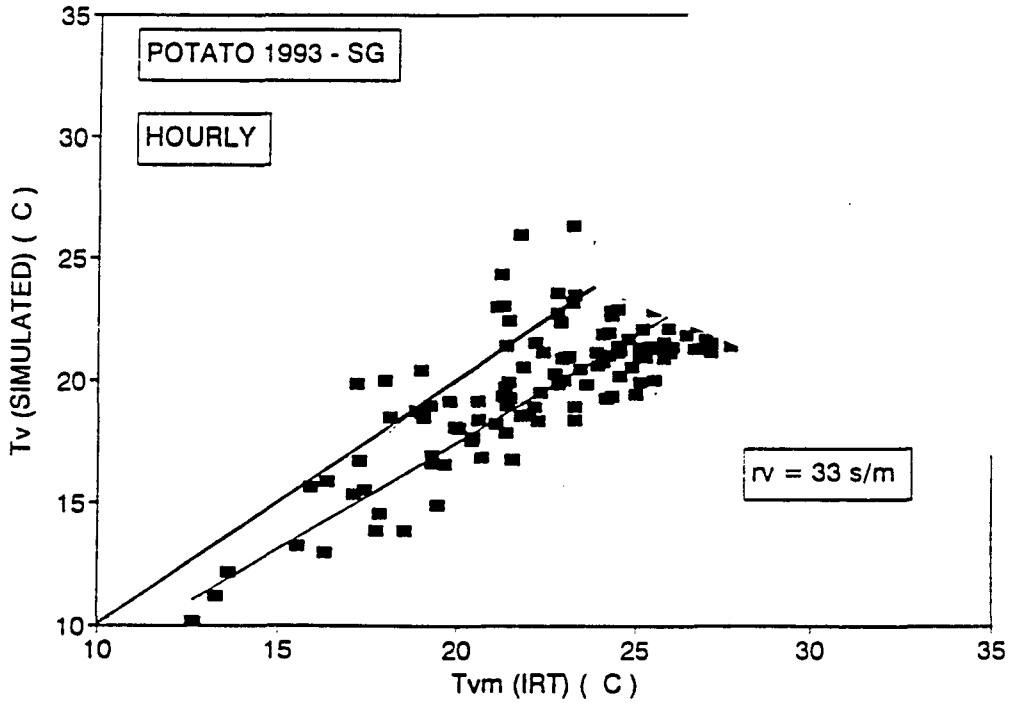

Fig. 5.4 **Scattergram of hourly mean foliage temperature T_v simulated using the SG-model and AWSO for $r_v = 33$ s m-1 and leaf temperature measured by the IRT, T_{vm}, for the potato crop**

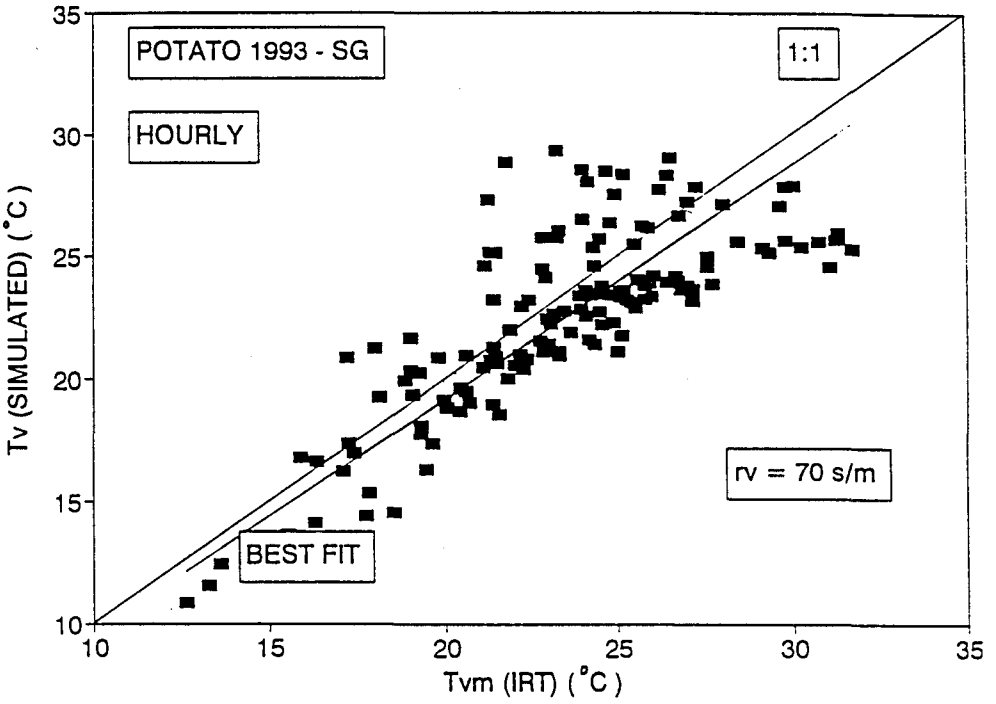

Fig. 5.5 **Scattergram of hourly mean foliage temperature, T_v, simulated using the SG-model and AWSO for r_v = 70 s m^{-1} and leaf temperature measured by the IRT, T_{vm}, for the potato crop**

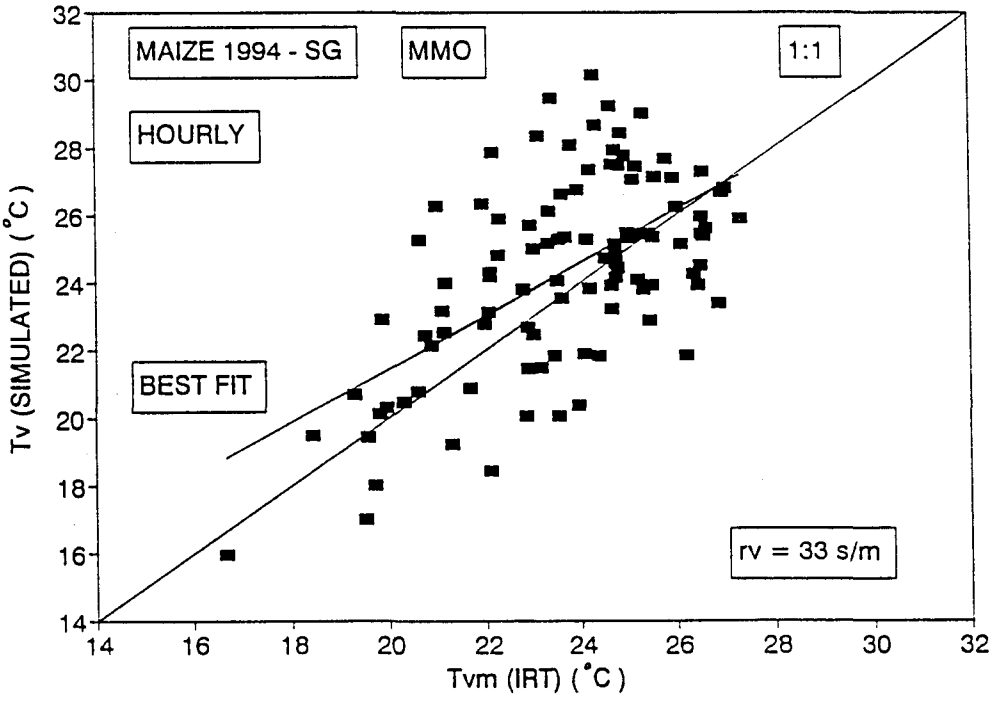

Fig. 5.6 **Scattergram of hourly mean foliage temperature T_v simulated using the SG-model and MMO for r_v = 33 s m^{-1} and leaf temperature measured by the IRT, T_{vm}, for the maize crop**

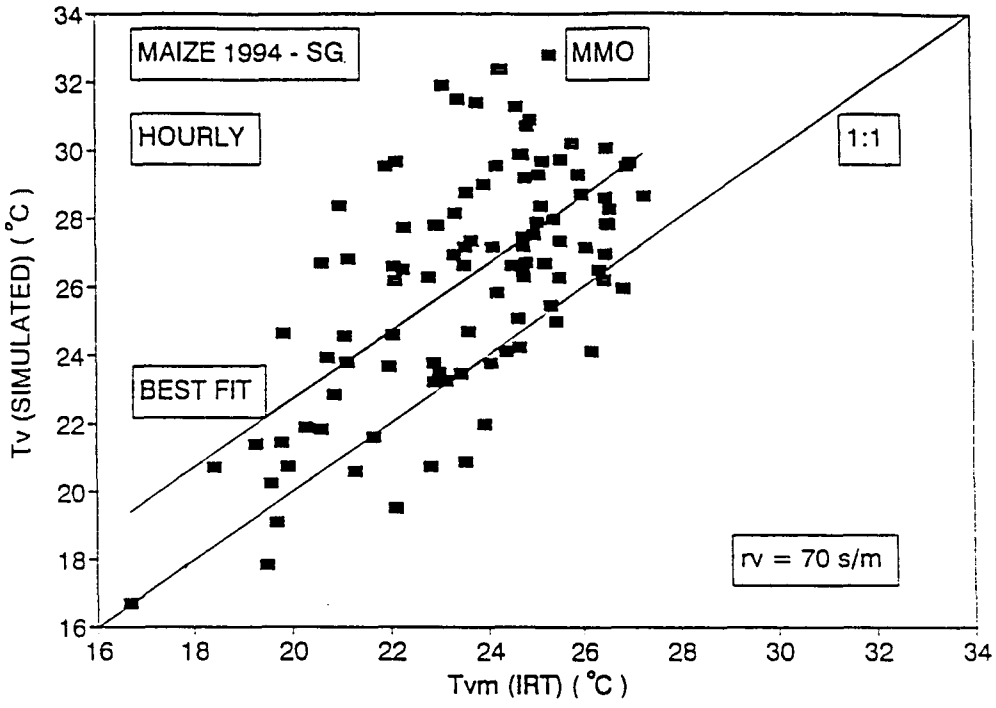

Fig. 5.7 **Scattergram of hourly mean foliage temperature, T_v, simulated using the SG-model and MMO for $r_v = 70$ s m^{-1} and leaf temperature measured by the IRT, T_{vm}, for the maize crop**

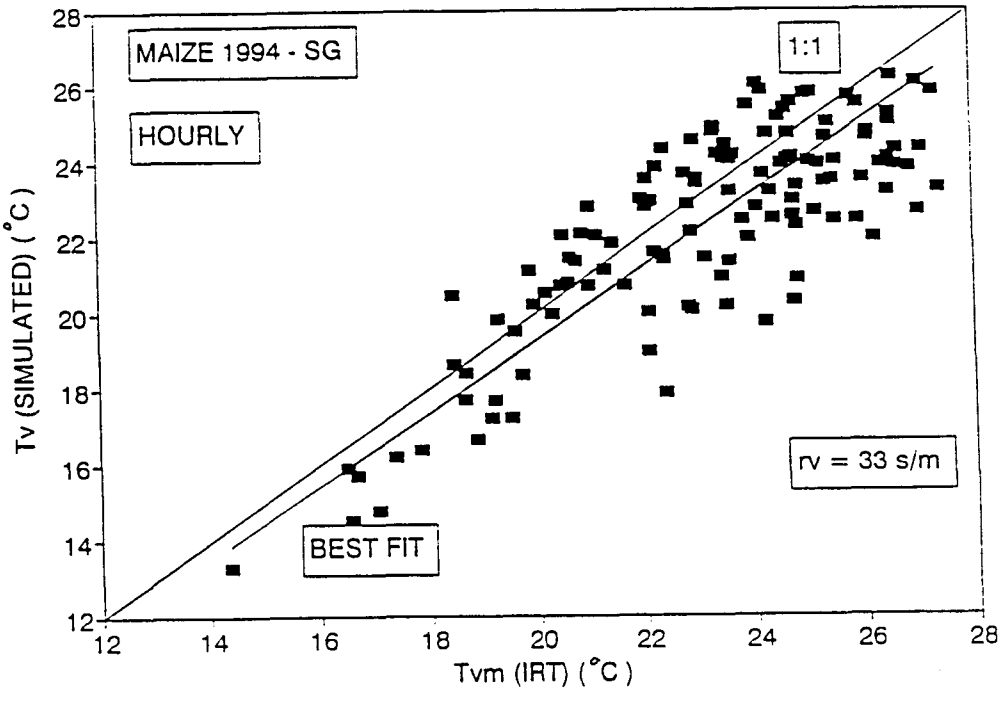

Fig. 5.8 **Scattergram of hourly mean foliage temperature, T_v, simulated using the SG-model and AWSO for $r_v = 33$ s m^{-1} and leaf temperature measured by the IRT, T_{vm}, for the maize crop**

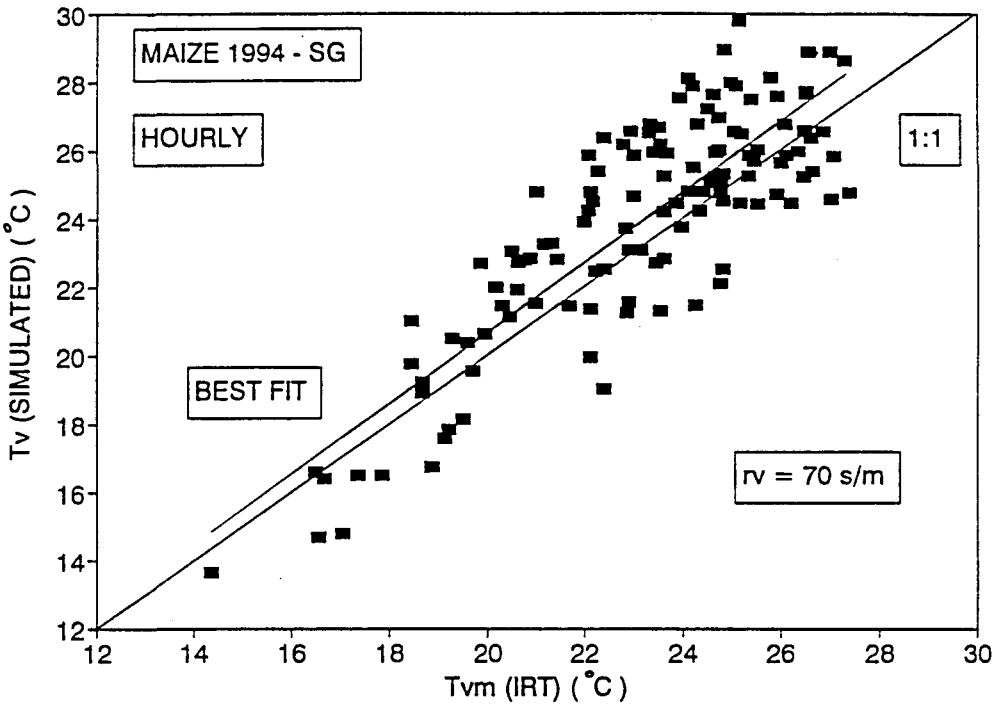

Fig. 5.9 **Scattergram of hourly mean foliage temperature, T_v, simulated using the SG-model and AWSO for r_v = 70 s m^{-1} and leaf temperature measured by the IRT, T_{vm}, for the maize crop**

CHAPTER 6

SOIL TEMPERATURE SIMULATION

With few exceptions, the same SG-iteration model, as developed in Chapter 5 for foliage temperature, was applied here in Chapter 6 to the simulation of soil temperature.

6.1 OBJECTIVES

The objectives in Chapter 6 were to:

- Compare with one another T_{sd} and T_{ss}, both as measured by the IRT, and
- Validate the soil temperature subroutines and iteration technique in the SG-iteration model for computation of T_{ss} and T_{sd}.

6.2 METHOD

The saturated vapour pressure at the soil surface was determined for the temperature measured at a depth of 10 mm below the soil surface. The integrated form of the Clausius Clapeyron equation (Equ. 2.9) was used.

Both T_{ss} and T_{sd} were measured by the IRT in the potato and maize crops. Measurements were compared with values obtained by iteration and the SG-model.

Similarly to Chapter 5 the equations involved were:

Equ. 2.8, 2.9 and 2.15 with appropriate subscripts inserted. The required resistance value to start the iteration was given by

$$r_{ss} = r_{so}/F_g \qquad 6.1$$

where, the soil surface dry-down factor as used in Equ. 2.30, Chapter 2 is given by

$$F_g = \exp(-0{,}4D) \quad 6.2$$

$$r_{so} = 33 \text{ s m}^{-1}$$

Analyses were carried out on both MMO and AWSO.

For the same reason given for foliage in Chapter 5 a value of r_{ss} calculated from Equ. 2.24 could not be used. Instead Equ. 6.1 and Equ. 6.2 were used to estimate a starting resistance, r_{ss}.

The criterion for closure used to terminate iteration for sunlit soil surface was the same as expressed by Equ. 5.1 in Chapter 5, but with appropriate subscripts for soil.

$$| R_{nss} + LE_{ss} + H_{ss} + G_{ss} | < 1 \text{ W m}^{-2}$$

A simple correction was applied to soil heat flux plate readings, because the Campbell temperature profile method was deemed more reliable (see Appendix II). Hence,

$$G_{ss} = 0{,}98 \text{ SHF}_p - 0{,}36 \text{ W m}^{-2} \quad 6.3$$

Where,

SHF_p = the soil heat flux measured by soil heat flux plate

and $H_{ss} = \rho Cp (T_{ss} - T_o)/r_{ss}$ 6.4

The entire procedure was repeated for the

- potato crop using AWSO
- maize crop using MMO, and
- maize crop using AWSO.

Regression analyses were used to validate the procedures. The results are reported in Table 6.2 and Table 6.3.

Because of the uncertainty in measured E_s evident from Chapter 3 (and especially later in Chapter 7) the E_s simulated, using the above model, could not meaningfully be compared against measured E_s in the micro-lysimeters.

The appropriateness of simulated soil temperatures could only be demonstrated by giving scenarios of simulated E_s. From Fig. 6.2 and Fig. 6.3 the simulations for potato and maize crops appear to be of the correct magnitude.

6.3 RESULTS AND DISCUSSION

In Fig. 6.1 and Table 6.2 measured sunlit and shaded soil surface temperatures are compared. As expected T_{ss} largely exceeded T_{sd} especially one to two days following a wetting event. However, a useful empirical relationship for estimating T_{sd} from T_{ss} was developed, viz.

$$T_{sd} = 0{,}31\ T_{ss} + 11{,}5 \qquad 6.5$$

While lack of time in this study prevented ascertaining whether the SG-iteration model together with Equ. 6.5 would produce improved simulation of T_{sd} and E_s this remains a decided possibility.

6.4 CONCLUSIONS

As expected, IRT measured T_{ss} exceeded measured T_{sd}, considerably. A simple linear empirical relationship exists between the two. It would be valuable to ascertain whether use of this expression will improve simulations of soil and plant evaporation.

- Extremely poor relationships between simulated T_{ss} and T_{sd}, using the SG-iteration model and T_{ss} and T_{sd} respectively measured with the IRT were obtained.
- A scenario of E_s simulated using a modified SG-model and MMO is demonstrated. The values appear to be reasonable.

From Table 6.2 and Table 6.3 it is evident that the SG-iteration technique produced poor agreement between measured and simulated soil surface temperatures (sunlit and shaded) in both crops. The SEE approximated 7°C, r^2 values were of the order of 0,1 and slopes ranged between 0,25 and 0,65. Notwithstanding these poor results, when soil surface temperatures simulated by the proposed technique are substituted in the modified SG-model, reasonable values of E_s are forthcoming (see Fig. 6.2 and Fig. 6.3).

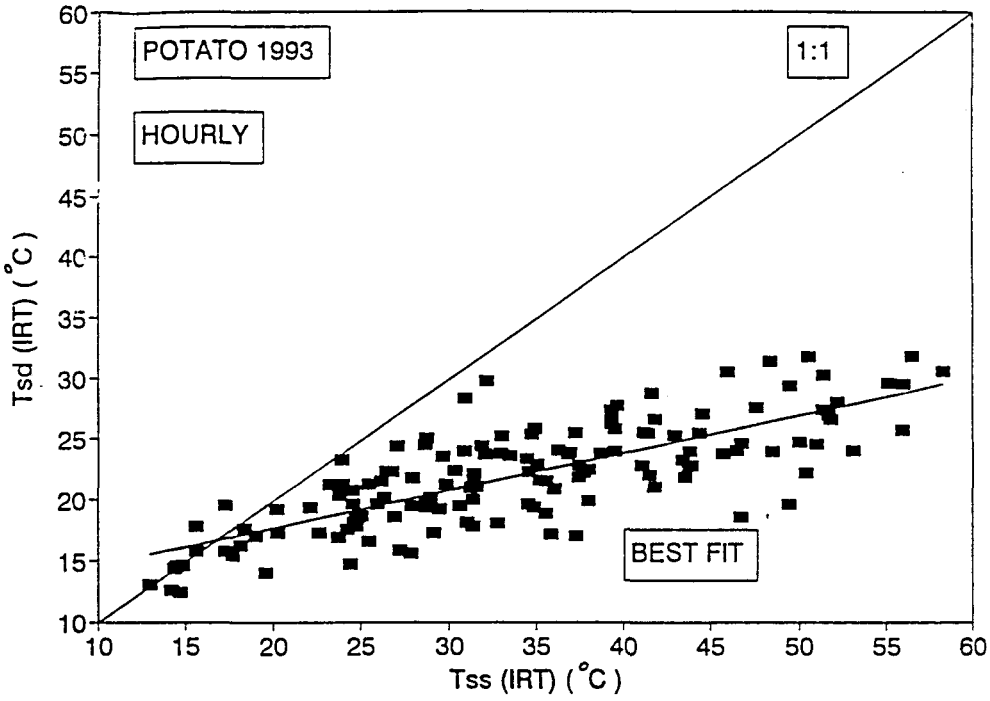

Fig. 6.1 **Scattergram of hourly mean shade and sunlit soil surface temperatures (T_{sd} and T_{ss}) measured with the IRT**

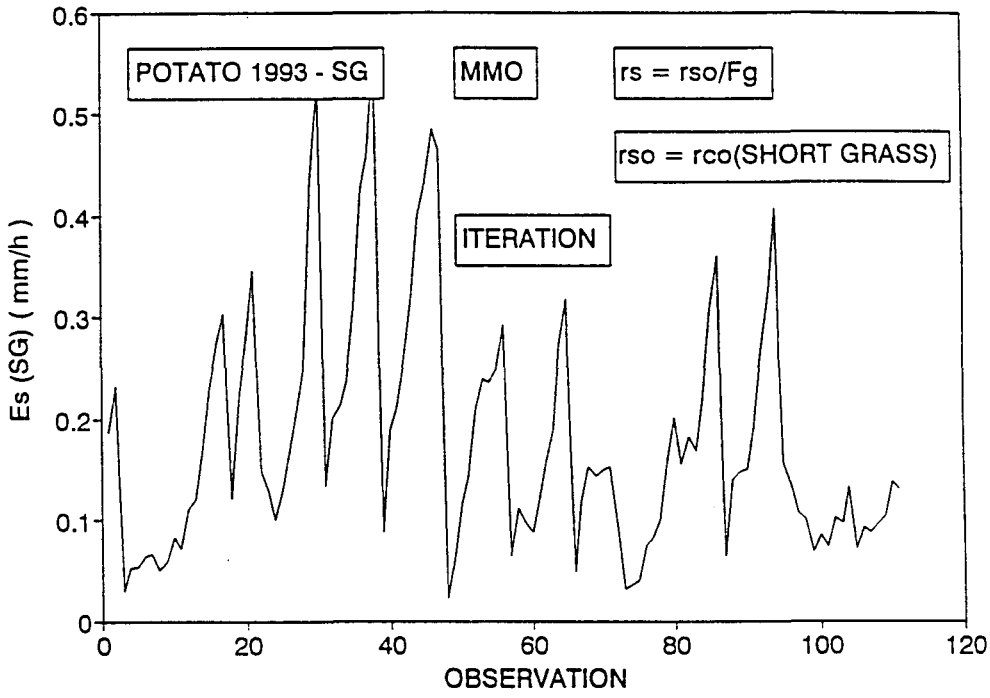

Fig. 6.2 **A sequence of E_s simulated using simulated soil surface temperatures in the modified SG-model and MMO for the potato crop**

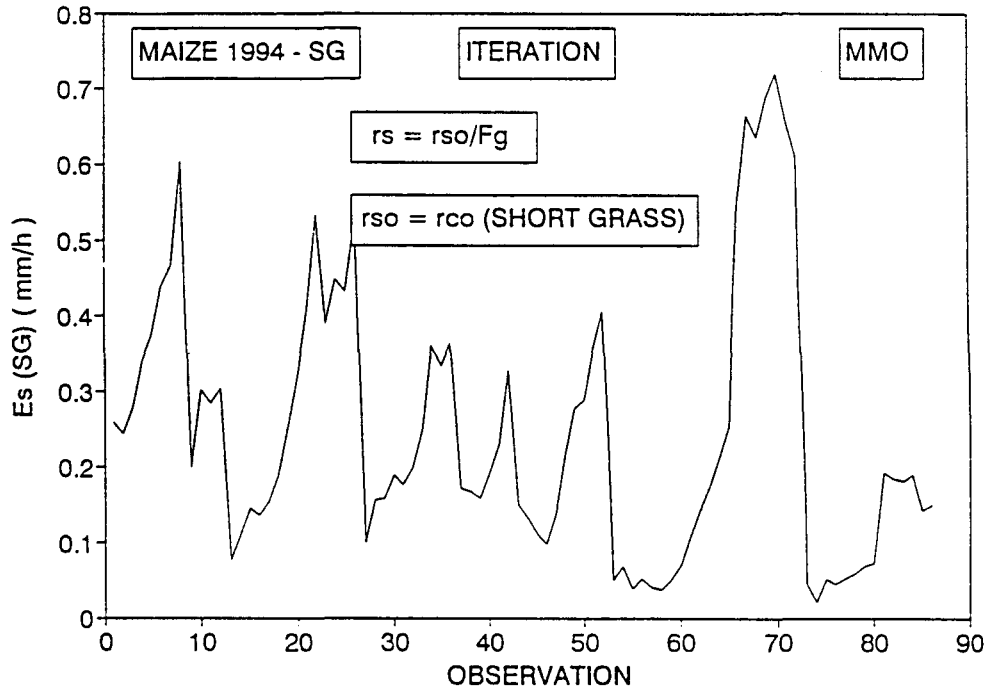

Fig. 6.3 **A sequence of E_s simulated using simulated soil surface temperature in the modified SG-model and MMO for the maize crop**

Table 6.1 **Statistics evaluating the relationship between T_{sd} and T_{ss} values measured with the IRT**

Statistical parameter	Parameter value
Intercept (°C)	11,5
SEE (°C)	2,7
r^2	0,61
n	144
Slope	0,31

Table 6.2 **Statistics describing the agreement between T_{sd} and T_{ss} using the modified model of SG with MMO measurements and the corresponding temperatures measured by IRT for potato and maize**

Statistical parameter	Parameter value			
	Potato		Maize	
	T_{ss}	T_{sd}	T_{ss}	T_{sd}
Intercept (°C)	0,0	0,0	0,0	0,0
SEE (°C)	8,3	8,0	6,1	6,0
r^2	0,03	0,10	0,02	0,05
n	111	111	86	86
Slope	0,41	0,65	0,44	0,58

Table 6.3 **Statistics describing the agreement between T_{sd} and T_{ss} using the modified model of SG for AWS and the corresponding temperatures measured by IRT for potato and maize**

Statistical parameter	Parameter value			
	Potato		Maize	
	T_{ss}	T_{sd}	T_{ss}	T_{sd}
Intercept (°C)	4,8	3,8	8,5	0,8
SEE (°C)	7,2	7,2	4,9	4,8
r^2	0,13	0,06	0,09	0,14
n	129	129	89	89
Slope	0,25	0,43	0,23	0,64

CHAPTER 7

VALIDATION OF THE PLANT EVAPORATION MODEL FOR THE POTATO AND MAIZE CROPS

7.1 OBJECTIVES

The objective in this chapter was to validate the SG-model, modified as described in Chapter 2 and Chapter 5. Its accuracy for simulating plant evaporation, E_v, for the potato and maize crops was tested.

7.2 METHOD

Symbol definitions for the variables used in the validation are:

E_v(SG) - plant evaporation simulated using the SG-iteration technique

E_v(PUTU) - plant evaporation computed using the existing PUTU-model from De Jager (1992)

E_v(WL) - plant evaporation measured in the large weighing lysimeter

The following validation procedures were followed:

First, for each data set the hourly mean leaf surface temperature was computed using the iterative technique developed in Chapter 2 and Chapter 5. Then hourly mean values of E_v were simulated using Equ. 2.8 with appropriate substitutions from Equ. 2.10 for r_{av} and 2.12 for r_{avs}. Saturated vapour pressure was calculated by Equ. 2.9 and the source vapour pressure, e_o, measured at estimated foliage source height. The accuracy of the entire technique for estimating E_v was then validated on data sets independent of those used in developing the submodels.

Data used in the validation of simulated versus measured plant evaporation included the following:

(i) Hourly mean E_v(SG) and E_v(WL) using either $r_v = 33$ s m^{-1}, or $r_v = 70$ s m^{-1}, including both MMO or AWSO and either iteration values for T_{vm} or IRT measured values. The criterion

for closure of the iteration process was the same as explained in Chapter 5 (see Equ. 5.1, and 6.2).

(ii) Mean daytime E_v(WL) and E_v(SG) for r_v = 33 s m^{-1} or 70 s m^{-1} including both AWSO and MMO and either T_{vm} iterated or measured by IRT.

(iii) Mean daytime E_v(WL) and E_v(PUTU) for r_v = 33 s m^{-1} using Equ. 2.23, FI = 1 - exp (-0,7* LAI) k_{vo} = 1,13 and k_{vo} = 1,09 for potato and maize respectively. In this case AWSO was used.

In all cases F_g = exp (-0,4D) + 0,06 exp (-0,0001D) 7.1

Development of this function for F_g will be described in Chapter 8.

7.3 RESULTS AND DISCUSSIONS

7.3.1 Validation criteria

Validation procedure was based upon the linear regression equation Y = ax + b, where a is the slope and b is the intercept both computed using the QUATTRO package. The criteria for acceptable accuracy chosen were slope = 1 ± 5%, coefficient of determination $r^2 > 0,7$ and standard error of Y estimate, SEE, of less than 0,2 mm/h or 0,6 mm/day.

All regressions were forced through zero as no empirical correction of the models was envisaged. The standard error of Y estimate, SEE, was computed using

$$SEE = \left[\Sigma_i (\hat{Y}_i - Y_i)^2 \right]^{0.5} / N$$

where,

N = number of observation pairs of X and Y in the data set used in deriving the linear regression, and

$\hat{Y}_i$ = ith value of the Y computed using the derived linear regression equation.

N = N - 1 when the regression line is not forced through 0.

Y_i = the corresponding observed value of Y.

7.3.2 Objectives

The experiments were designed with a view to ascertaining which alternatives of the submodels were the most reliable for simulating E_v in potato and maize crops. Investigations tried to determine which of:

1. Canopy resistances $r_v = 33$ s m^{-1} or $r_v = 70$ s m^{-1} provide the most reliable results in the SG-model.
2. SG-iteration or PUTU-model simulates hourly plant evaporation most accurately.

The method adopted to obtain the required hourly and daytime values of plant evaporation are described in Chapter 3. For modelling and validation purposes comparisons between simulated E_v from submodels were compared to plant evaporation measured in the large weighing lysimeter which had been suitably covered with plastic sheeting to eliminate soil evaporation.

A complete summary of the most relevant validation tests undertaken, is given in Table 7.1. Graphical representation of the various results are given in Fig. 7.1 to 7.14.

7.3.3 Hourly simulations

Values for r_v reported in the literature ranged between $r_v = 33$ s m^{-1} and $r_v = 70$ s m^{-1} (see Van Zyl, De Jager & Maree, 1988). Preliminary validations on the present data for potato and maize suggested that rv between these limits yielded acceptable results. Both extreme values were investigated.

From the comparisons of hourly values of E_v simulated by the PUTU- and SG-iteration model against Ev-values measured in the weighing lysimeter, it appears that the SEE attained with both models was acceptable (i.e. SEE < 0,5 mm/h) indicating that on an hourly basis either model may be used. Interestingly, for potato PUTU proved most accurate, with $r^2 = 0,78$ and slope = 0,96. For maize however, the SG-iteration model was more accurate with $r^2 = 0,71$ and a slope of 1,02. PUTU appeared to underestimate hourly evaporation by some 13% in maize.

Based mainly upon the favourable SEE of less than 0,15 mm/h, it was concluded that either model provides suitably accurate simulation of hourly plant evaporation.

7.3.4 Evaluation of canopy resistance r_v

Daytime E_v-values were simulated by totalling hourly simulated E_v. Unexpected bias appeared in the results with the changing r_v and an investigation of $r_v = 33$ s m^{-1} and $r_v = 70$ s m^{-1} proved enlightening.

On a daily time basis for potato the SG-iteration model is more accurate with $r_v = 70$ s m^{-1} than with $r_v = 33$ s m^{-1}. However, the $r_v = 70$ s m^{-1} version underestimated daily plant evaporation by 16%. The standard error of estimate of both alternatives was acceptable at less than 0,6 mm/d as were coefficients of determination of approximately $r^2 = 0,7$.

For maize however, it appears that $r_v = 33$ s m^{-1} is superior. The $r_v = 70$ s m^{-1} version underestimated daily E_v by 18%. The SEE is bordering on acceptability, at approximately 0,6 mm/d. Based on this evidence it was concluded that an $r_v = 33$ s m^{-1} is probably a more acceptable value for both crops.

7.3.5 Comparison of performance of SG-iteration and PUTU-model

When the performance of the two models against measured daytime E_v was compared, it appears that the SG-iteration model did in fact offer an improvement over the original PUTU-model. For the potato crop the r^2 for SG and PUTU were 0,84 and 0,74 respectively. Corresponding figures for maize were 0,81 and 0,61 . Based on this evidence it was concluded that the SG-model is an improvement on the old PUTU-model although it must be stressed that for potato the SG-iteration model underestimated daytime plant evaporation by 16% (slope = 0,84).

7.3.6 Direct comparison of SG- and PUTU-models for daytime simulation of E_v

With coefficients of determination r^2 approximating 0.9 agreement between the two models was good. Once again, agreement appeared to be better for $r_v = 33$ s m^{-1} in the SG-model. However, an extremely high scatter was obtained for daytime for the SG-model with this canopy resistance. For both crops slopes are approximately 80% indicating that for an $R_v = 70$ s m^{-1} the SG-model may be expected to underestimate E_v-values from the PUTU-model by some 20%.

Notwithstanding the high SEE obtained for comparisons of SG versus measured plant evaporation; it was concluded that the SG-iteration model with a canopy resistance value $r_v = 33$ s m^{-1} is an improvement upon the existing PUTU-model. This new submodel for estimating plant evaporation should therefore replace the existing E_v submodel in PUTU.

Table 7.1 **Validation summary: All regressions were forced through zero. Statistics quantifying the agreement between measured E_v and E_v simulated by either the SG- or the PUTU-models on an hourly or daytime basis for AWSO and MMO and for r_v = 33 s m^{-1} and r_v = 70 s m^{-1}. Comparisons of SG- versus PUTU-models are also included**

FIG Ref	E_v derivative and Axes		Time basis	Graph type	Weather data	r_v (s m^{-1})	T_v Source	N	Slope	SEE (mm h^{-1})(mm d^{-1})	r^2
Potato											
7.1	WL	SG	Hly	Scatter	MM	33	IRT	133	0,91	0,14	0,67
7.2	WL	PU	Hly	Scatter	MM			133	0,96	0,11	0,78
7.3	DOY	SG/WL	Day	Scenario	AWS	33	ITER				
	WL	SG	Day	Scatter	AWS	33	ITER	30	0,96	9,92	0,67
7.4	DOY	SG/WL	Day	Scenario	AWS	70	ITER				
	WL	SG	Day	Scatter	AWS	70	ITER	30	0,84	0,60	0,84
7.5	DOY	PU/WL	Day	Scenario	AWS						
	WL	PU	Day	Scatter	AWS			30	1,07	0,98	0,74
7.6	PU	SG	Day	Scatter	AWS	33	ITER	27	0,90	1,31	0,96
7.7	PU	SG	Day	Scatter	AWS	70	ITER	27	0,78	0,36	0,93
Maize											
7.8	WL	SG	Day	Scatter	MM	33	IRT	71	1.02	0,15	0,71
7.9	WL	PU	Hly	Scatter	MM			71	0,87	0,14	0,65
7.10	DOY	SG/WL	Hly	Scenario	AWS	33	ITER				
	WL	SG	Day	Scatter	AWS	33	ITER	28	0,97	0,57	0,81
7.11	DOY	SG/WL	Day	Scenario	AWS	70	ITER				
	WL	SG	Day	Scatter	AWS	70	ITER	28	0,82	0,54	0,73
7.12	DOY	PU/WL	Day	Scenario	AWS						
	WL	PU	Day	Scatter	AWS			28	1,00	0,67	0,68
7.13	PU	SG	Day	Scatter	AWS	33	ITER	18	0,99	0,36	0,89
7.14	PU	SG	Day	Scatter	ASW	70	ITER	18	0,82	0,38	0,79

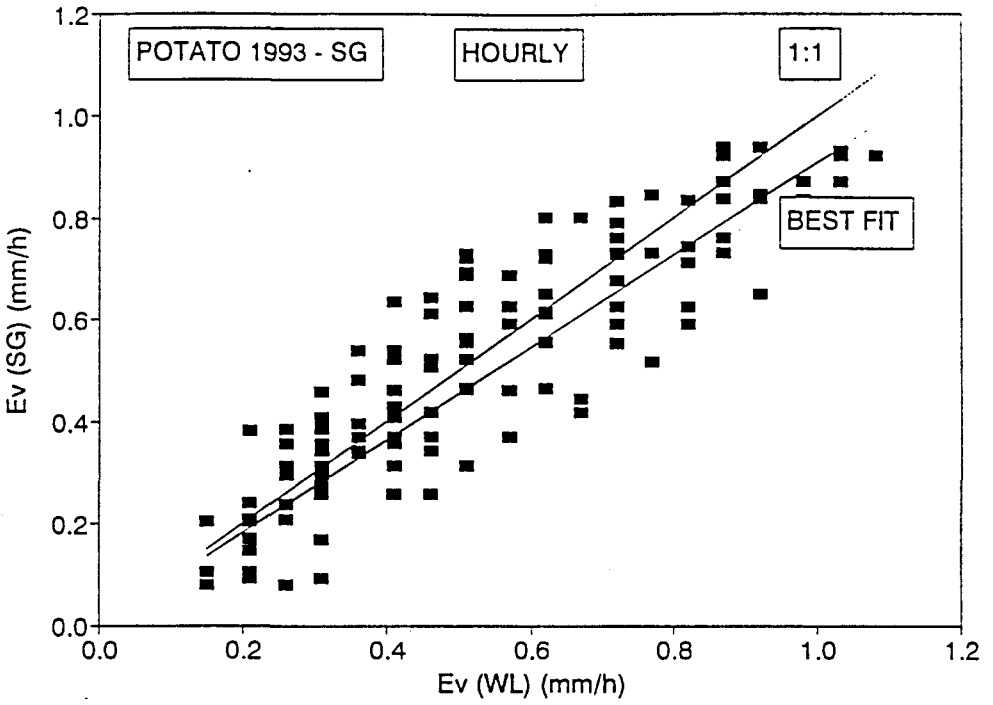

Fig. 7.1 **Scattergram of measured hourly mean E_v (WL) and simulated E_v (SG) using MMO with r_v = 33 s m^{-1} and T_v measured using the IRT for the potato crop**

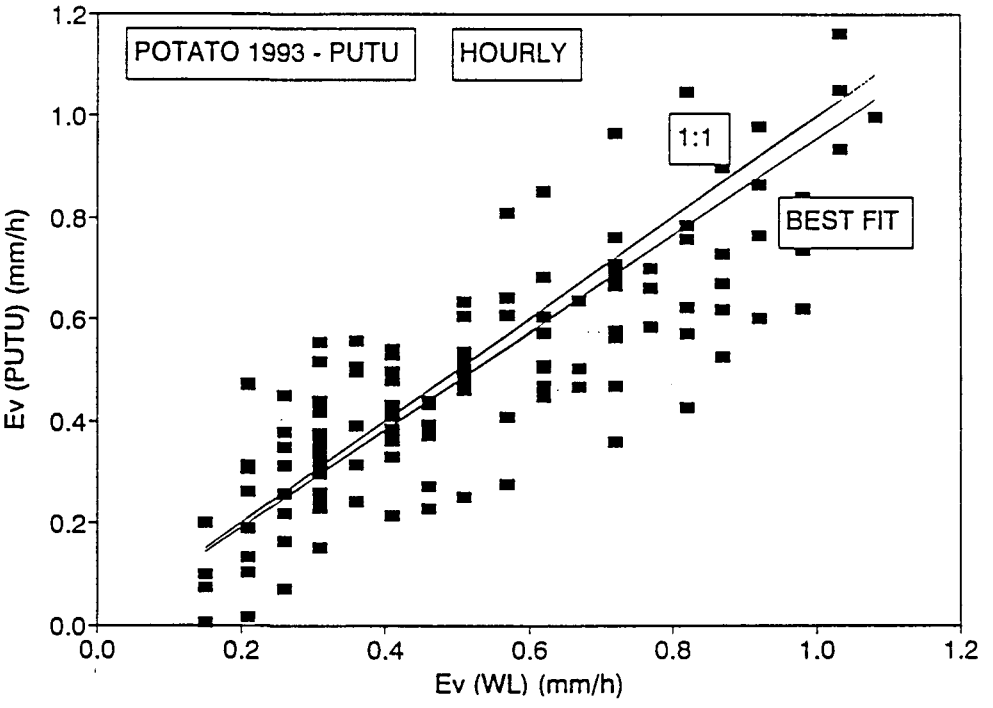

Fig. 7.2 **Scattergram of measured hourly mean E_v(WL) and simulated E_v(PUTU) using MMO with r_v = 33 s m^{-1} for the potato crop**

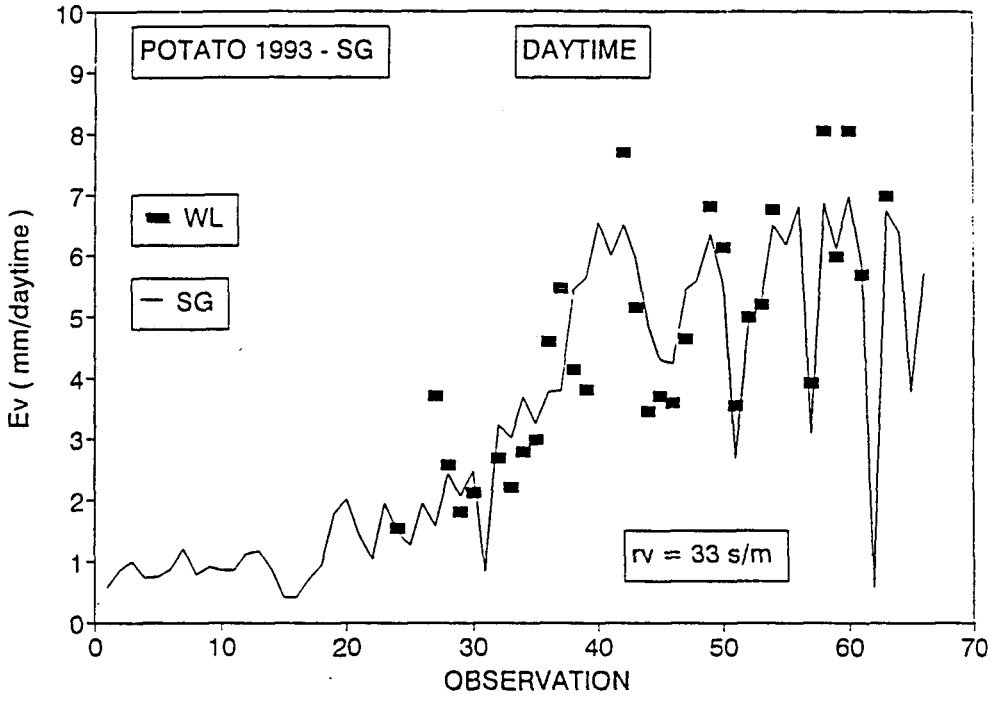

Fig. 7.3 **Seasonal variation in sunlight period E_v(WL) and E_v(SG) using AWSO with r_v = 33 s m^{-1} and iterating for Tv for the potato crop**

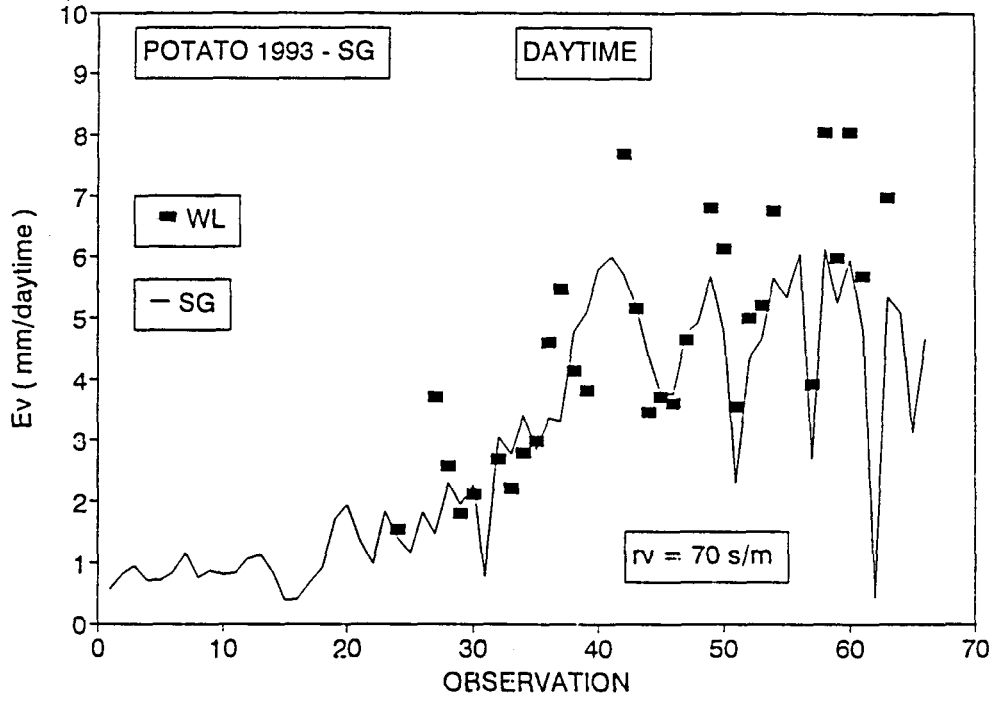

Fig. 7.4 **Seasonal variation in sunlight period E_v(WL) and E_v(SG) using AWSO with r_v = 70 s m-1 and iterating for T_v for the potato crop**

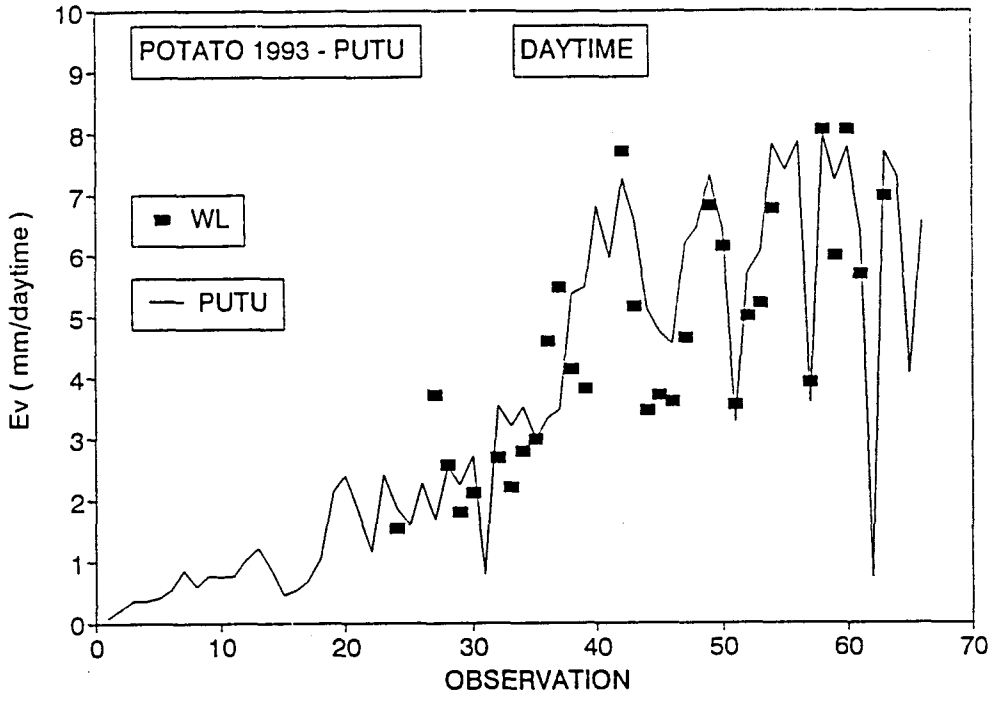

Fig. 7.5 **Seasonal variation in sunlight period E_v(WL) and E_v(PUTU) using AWSO with $r_v = 33$ s m^{-1} for the potato crop**

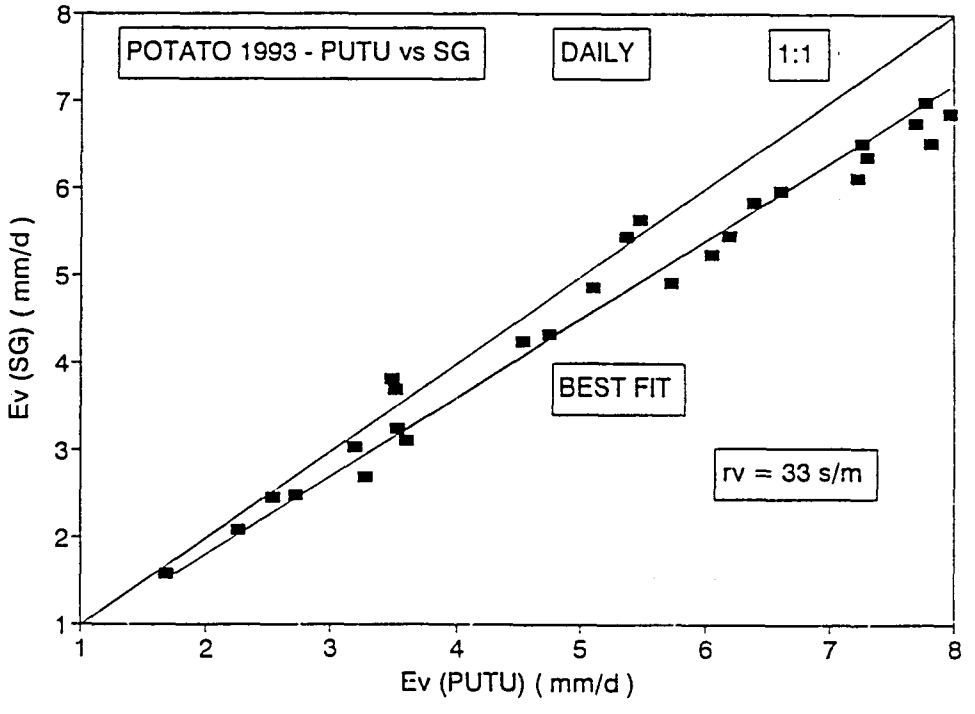

Fig. 7.6 **Scattergram for sunlight period E_v(PUTU) and E_v(SG) for $r_v = 33$ s m^{-1} using AWSO and iterating for T_v for the potato crop**

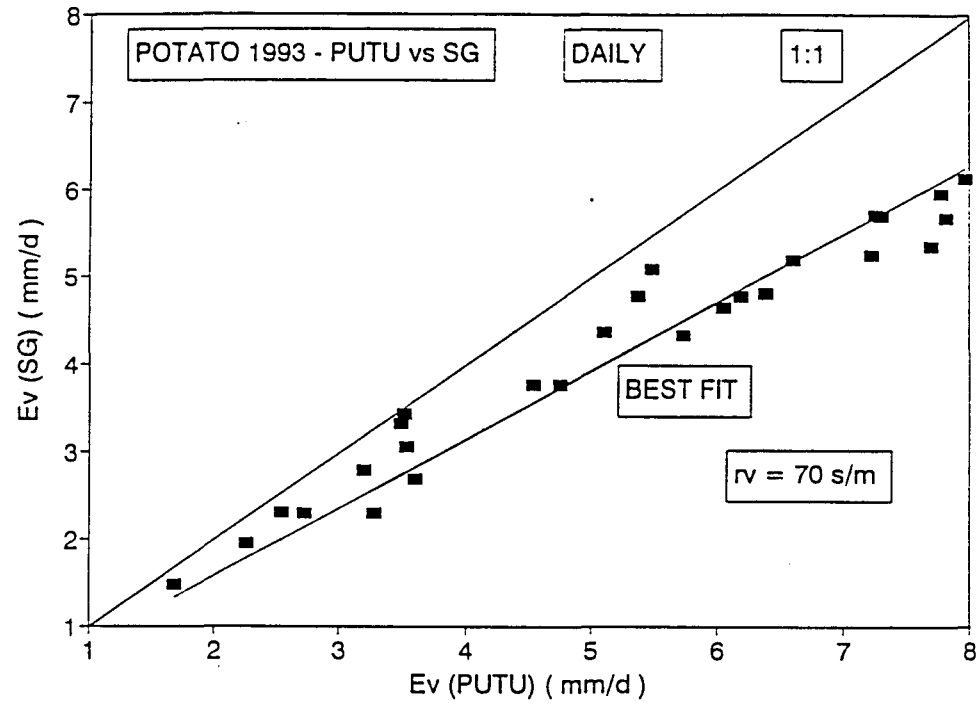

Fig. 7.7 **Scattergram for sunlight period E_v(PUTU) and E_v(SG) for r_v = 70 s m^{-1} using AWSO and iterating for T_v for the potato crop**

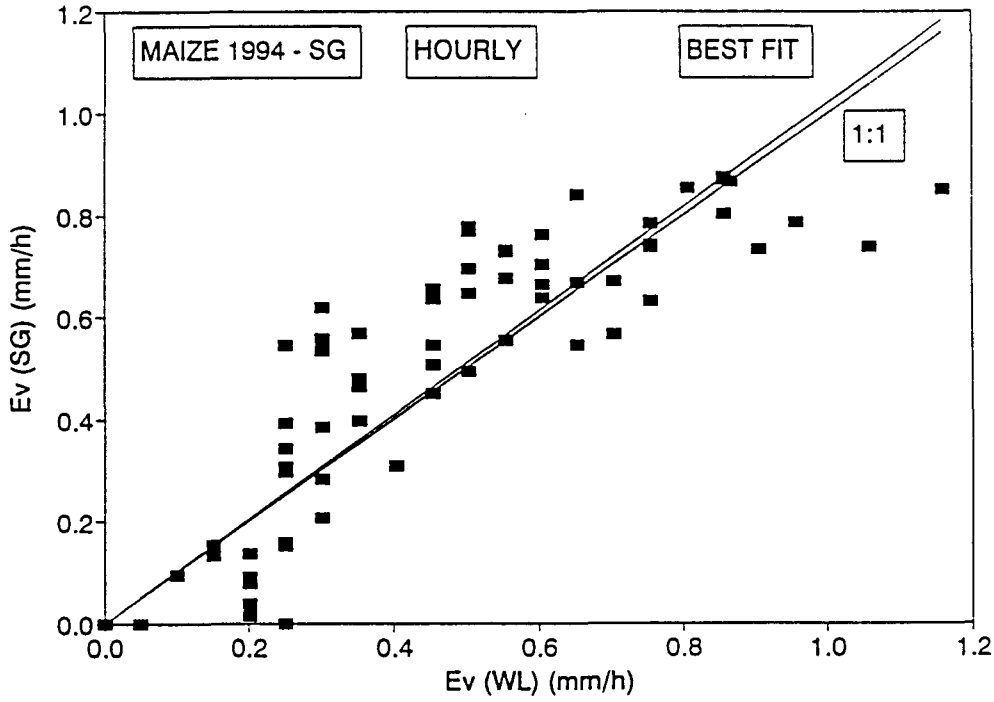

Fig. 7.8 **Scattergram for hourly mean E_v(WL) and E_v(SG) using MMO with r_v = 33 s m^{-1} and utilizing T_v measured by the IRT for the maize crop**

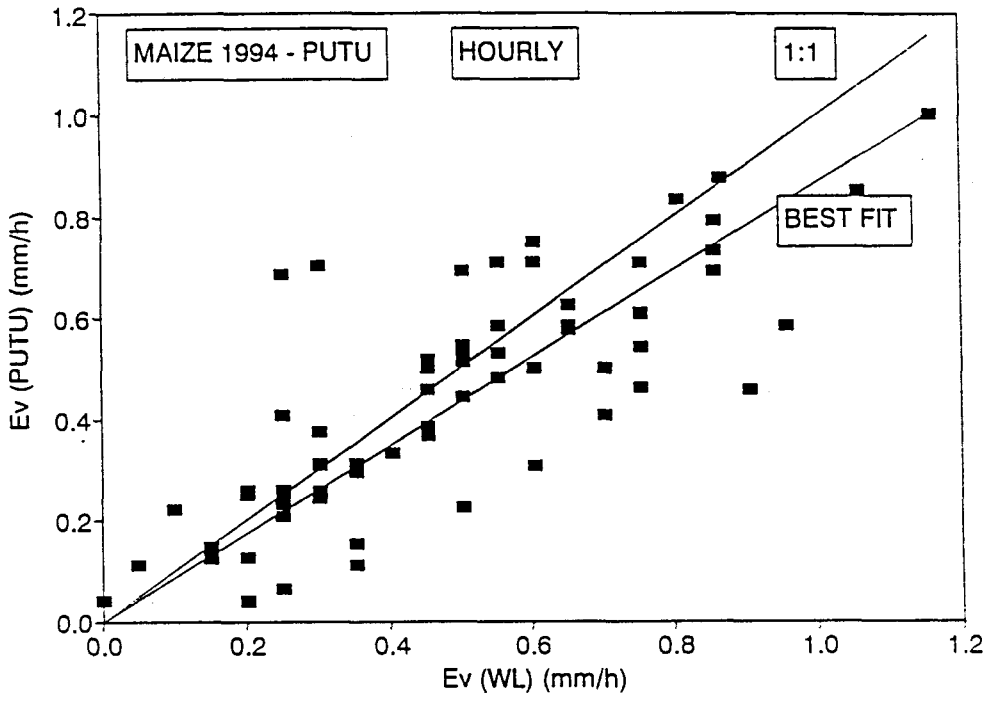

Fig. 7.9 **Scattergram for hourly mean E_v(WL) and E_v(PUTU) using MMO with $r_v = 33$ s m^{-1}**

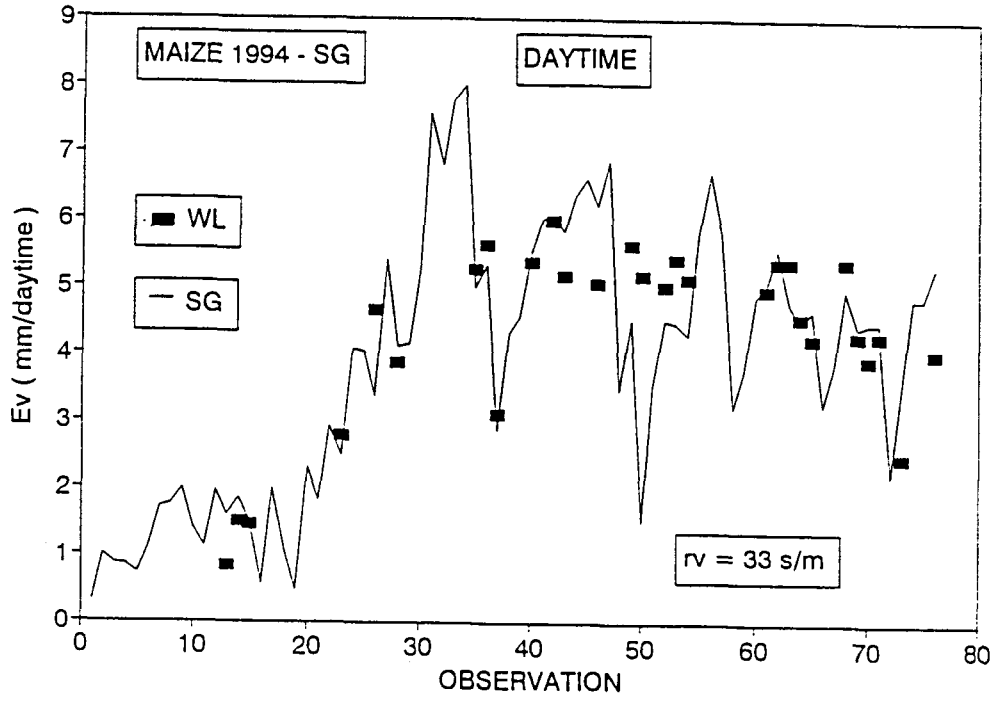

Fig. 7.10 **Seasonal variation of sunlight period E_v(WL) and E_v(SG) using AWSO with $r_v = 33$ s m^{-1} and iterating for T_v for the maize crop**

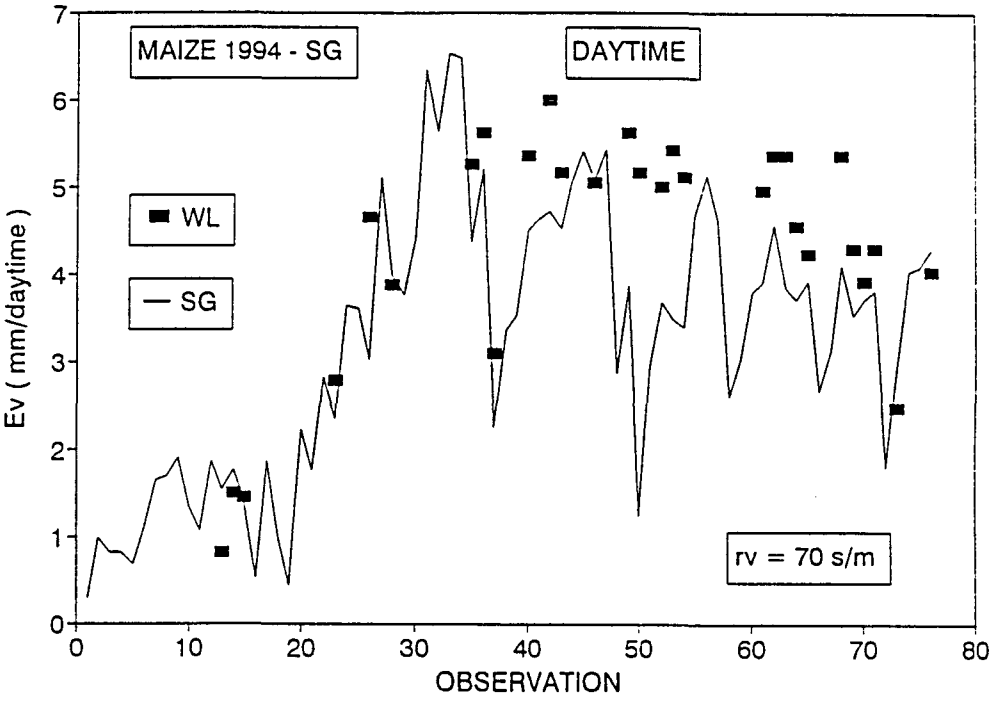

Fig. 7.11 **Seasonal variation in sunlight period E_v(WL) and E_v(SG) using AWSO with r_v = 70 s m^{-1} and iterating for T_v for the maize crop**

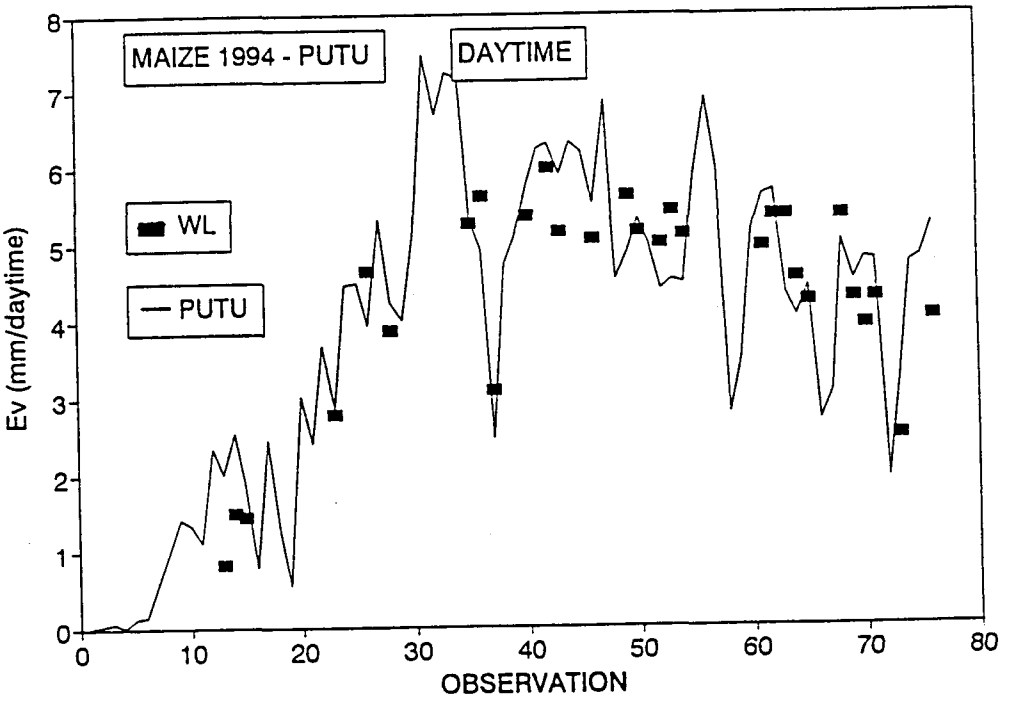

Fig. 7.12 **Seasonal variation in sunlight period E_v(WL) and E_v(PUTU) using AWSO with r_v = 33 s m^{-1} for the maize crop**

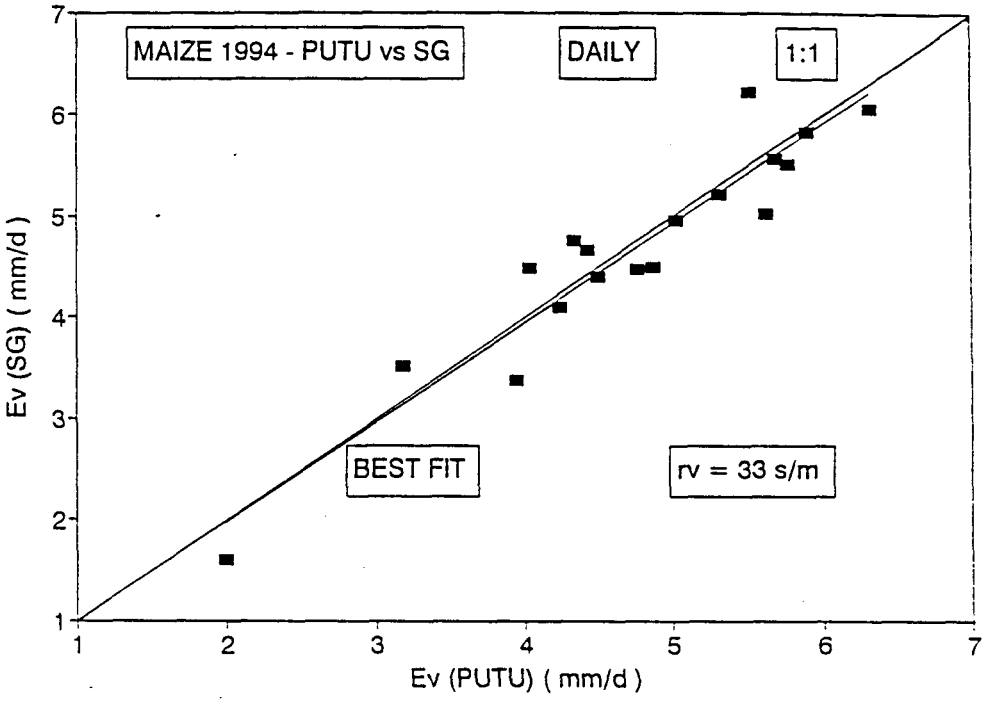

Fig. 7.13 **Scattergram for sunlight period E_v(PUTU) and E_v(SG) for r_v = 33 s m^{-1} using AWSO and iterating for T_v for the maize crop**

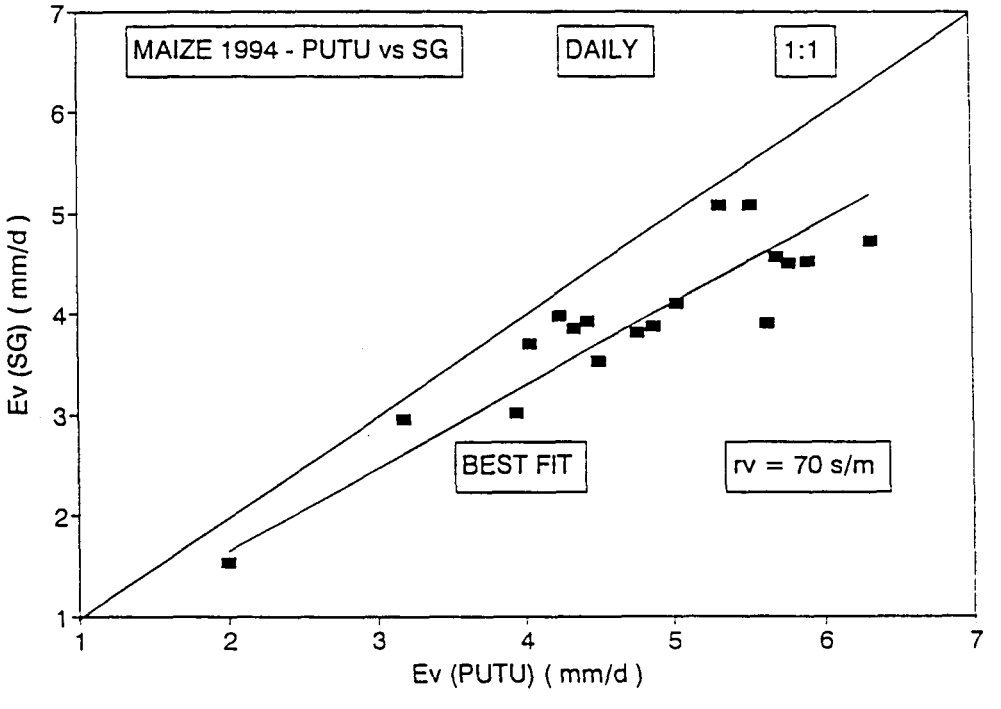

Fig. 7.14 **Scattergram for sunlight period E_v(PUTU) and E_v(SG) for r_v = 70 s m^{-1} using AWSO and iterating for T_v for the maize crop**

CHAPTER 8

SIMULATION OF EVAPORATION FROM BARE SOIL

While vegetative cover markedly influences soil surface evaporation from a cropped surface, it proved experimentally possible to measure evaporation with reasonable accuracy from only bare soil surfaces. Hence, only algorithms for simulating soil evaporation from a bare soil surface could be developed and these, unchanged, were then applied in the SG-iteration model. This situation was brought about by the poor performance of the drainage and micro-lysimeters.

8.1 OBJECTIVES

The objective of this chapter was to determine the most reliable method for simulating bare soil evaporation.

8.2 METHOD

Bare soil evaporation, E_s, was measured during two drying cycles. The two drying cycles extended through periods of 29 and 9 days respectively - Cycle 1 from DOY 256 to DOY 285 and Cycle 2 from DOY 291 to DOY 299 both in 1994. Daily measurements carried out were the following:

(i) E_s using the large weighing lysimeter, denoted E_s(WL).

(ii) E_s using 18 micro-lysimeters, denoted E_s (ML) - no measurements were made on Saturdays and Sundays.

(iii) E_s using 4 drainage lysimeters, denoted E_s(DL).

(iv) E_o using the grass lysimeter, GL, denoted E_o(GL).

The measurements of E_o(GL) were included to provide an indication of the prevailing atmospheric evaporative demand, for comparative purposes.

In addition E_s was also estimated using the energy budget - Bowen ratio technique denoted EBBR.

It was further decided to test the soil surface dry-down factor F_g suggested in Chapter 2 and Chapter 6, but also to adjust it (named FG-adj) to accommodate the second phase of evaporation explained by Jones & Kiniry, (1987). The accuracy of both the original and adjusted F_g were investigated. The adjustment for the latter was developed during the 29-day cycle and then tested on similar data from the 9-day cycle. The original F_g, Equ. 6.2, reads:

$$F_g = \exp(-0{,}4D)$$

8.3 RESULTS AND DISCUSSION

8.3.1 Measurement of soil evaporation using the different methods

Results for the two drying cycles are given in Fig. 8.1, 8.2, 8.3 and 8.4 which illustrate the discrepancy among values of E_s obtained by different methods of measurement, viz. E_s(WL), E_s(ML), E_s(EBBR) and E_o(GL). These differences are quantified in Table 8.1 and 8.2. A rapid drop in the large weighing lysimeter E_s(WL) within 3 days of a wetting event was observed during both cycles (Fig. 8.1 and 8.3), whereas only gradual decreases in E_s(ML) were discernible (Fig. 8.2 and 8.4). Standard deviations of measured values of E_s(ML) are included in these figures to demonstrate that the mean values are indeed an *artefact* of the measuring technique.

Unfortunately during Cycle 1 estimation of E_s(EBBR) (see Fig. 8.1) only commenced on DOY 266 due to initial malfunction of the Bowen ratio system. E_s(EBBR) was found to overestimate E_s(WL) (see Fig. 8.1 and 8.3 and Table 8.1 and 8.2). This is contrary to the good agreement reported in the literature.

It is clear from Table 8.2 that E_s(ML), in comparison with E_s(WL), E_s(DL), and E_s(EBBR) greatly overestimated soil evaporation from a bare soil surface.

Hence the ML-method was disregarded in any future analysis. Free water retained at the bottom of the ML would be transferred to the surface by capillary action. It is suspected that this could have caused protracted soil evaporation at a level close to reference evaporation as shown in Fig. 8.2.

A set-up procedure involving saturation and drainage on a sand bed for 48 hours should correct the problem of excessive water retention in the ML. The dry-down from the ML would then probably follow closely the E_v(WL) reported in Fig. 8.1, 8.3, 8.5 and 8.6. A test of E_s simulation could possibly be undertaken assuming a wetting event on DOY 265 (and not 256) in Fig. 8.2.

8.3.2 The expression for adjusting for second phase soil evaporation

Field observations of F_g were made using the ratio of E_s measured in the large weighing lysimeter to E_o measured in the grass lysimeter. Fig. 8.5 shows the daily trend in measured F_g, the F_g as calculated from the original exponential expression and the adjusted F_g denoted F_g-adj. The expression for F_g-adj was developed initially by trial and error. We assumed that second phase soil evaporation could be simulated by adding a second exponential decay expression to the original expression.

The resulting expression reads:

$$F_g\text{-adj} = \exp(-0{,}4\ D) + 0{,}06\ \exp(-0{,}0001\ D) \qquad 8.1$$

8.3.3 Validation of the dry-down factors

From Fig. 8.5 and 8.6 it is apparent that values of both F_g and F_g-adj (Equ. 8.1) compared excellently with measured F_g (where measured $F_g = E_s(WL)/E_o(GL)$ through the first 6 days of the first drying cycle. Thereafter the original F_g showed a tendency to underestimate measured F_g while F_g-adj compared excellently with F_g measured.

The accuracy of both F_g and F_g-adj as obtained from Equ. 8.1 were compared against the independent data set measured during Cycle 2. The good agreement is demonstrated in Fig. 8.6 and Table 8.3. A slope of 1,25 indicated that F_g-adj overestimated E_s during the drying cycle. Coefficients of $r^2 =$ 0,86 are satisfactory however. Once again deviation between theory and experiment could have been due to incorrect definition of the timing of the wetting event. This problem deserves further investigation.

8.4 CONCLUSIONS

It was concluded that inclusion of an additional exponential decay expression to accommodate second phase soil surface evaporation did slightly improve the existing exponential expression for F_g. As such it is recommended that the improved version be utilized in future.

In summary, it was found that:

- Total E_s measured using micro-lysimeters overestimated total E_s measured in the large weighing lysimeter by a factor of 3.

- Total E_s measured using drainage lysimeters overestimated total E_s measured in the large weighing lysimeter, by a factor of approximately 1,5 (see Table 8.2).

More detailed conclusions possible from the work include:

- Both soil dry-down factors, i.e. F_g and F_g-adj, (from Equ. 8.1) model the rate of evaporation from a bare soil surface satisfactorily.
- Because of the discrepancies between E_s(WL) and E_s(ML) it was decided the micro-lysimeter data could be used for neither model development nor validation.

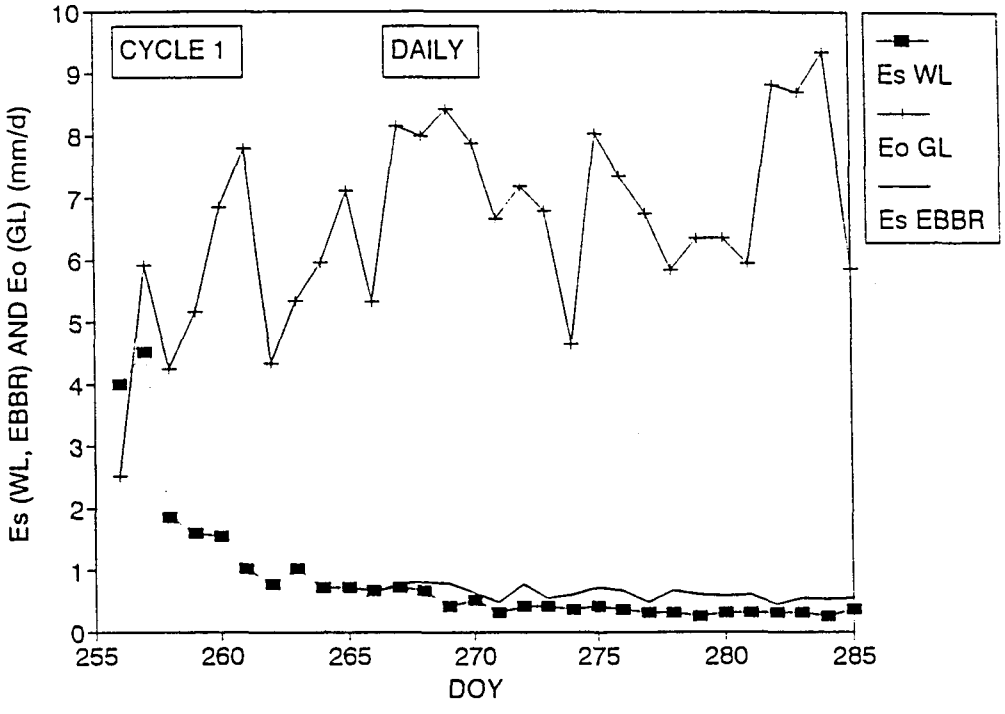

Fig. 8.1 **Daily trend in soil evaporation measured by weighing lysimeter, E_s(WL), and Bowen Ratio E_s(EBBR) and reference evaporation E_o(GL) through Cycle 1**

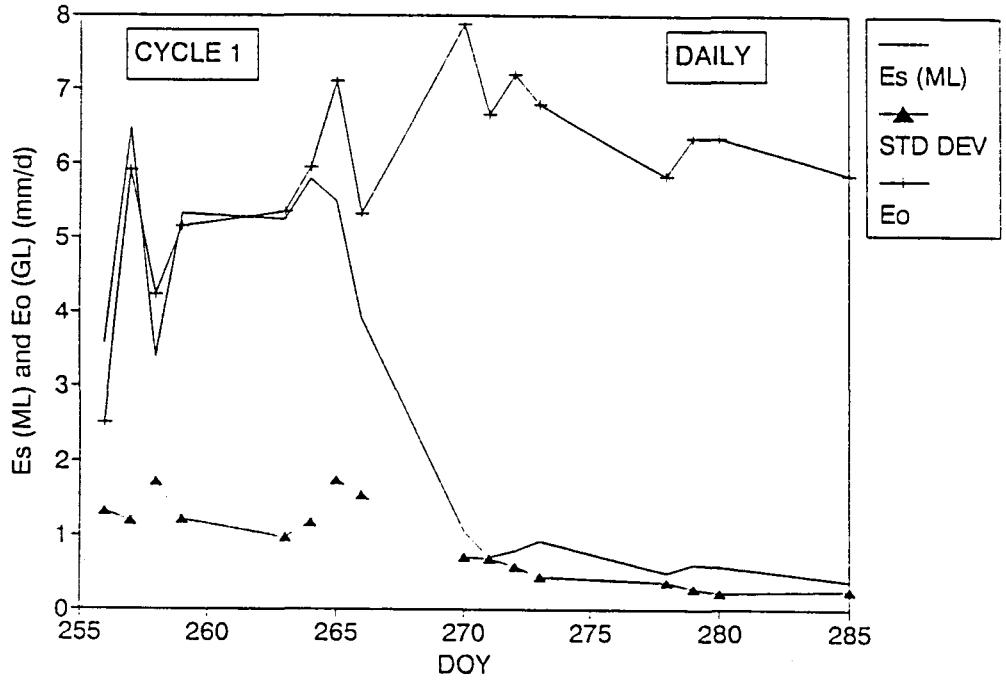

Fig. 8.2 **Daily trend in soil evaporation as measured by micro-lysimeters E_s(ML), each value's standard deviation and reference evaporation E_o through Cycle 1**

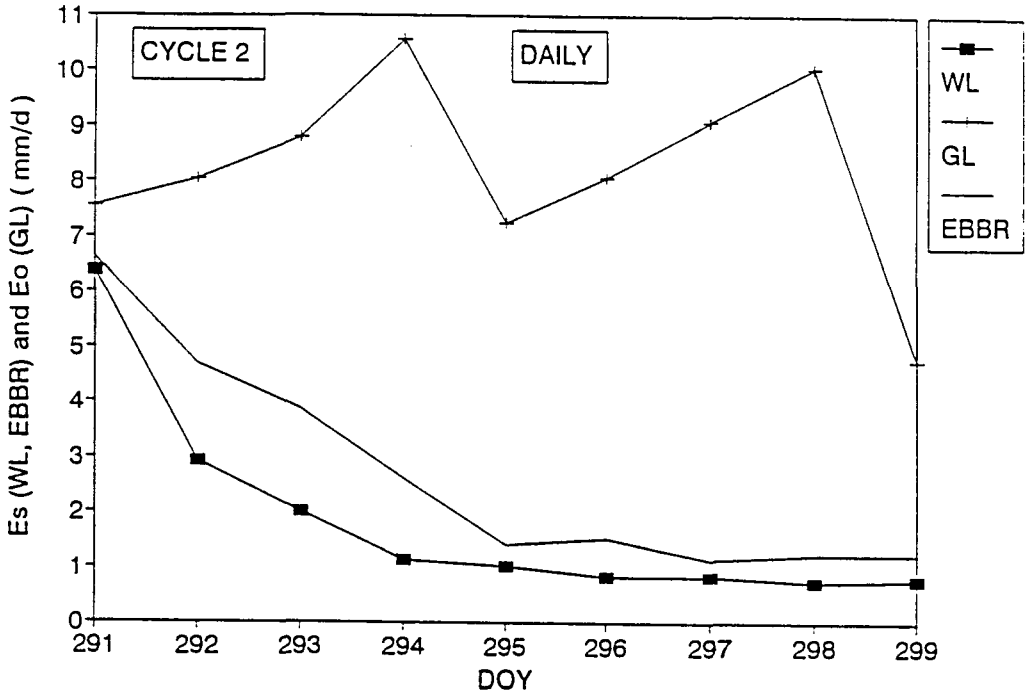

Fig. 8.3 **Daily trend in soil evaporation measured by weighing lysimeter, E_s(WL), and Bowen Ratio E_s(EBBR) and reference evaporation E_o(GL) through Cycle 2**

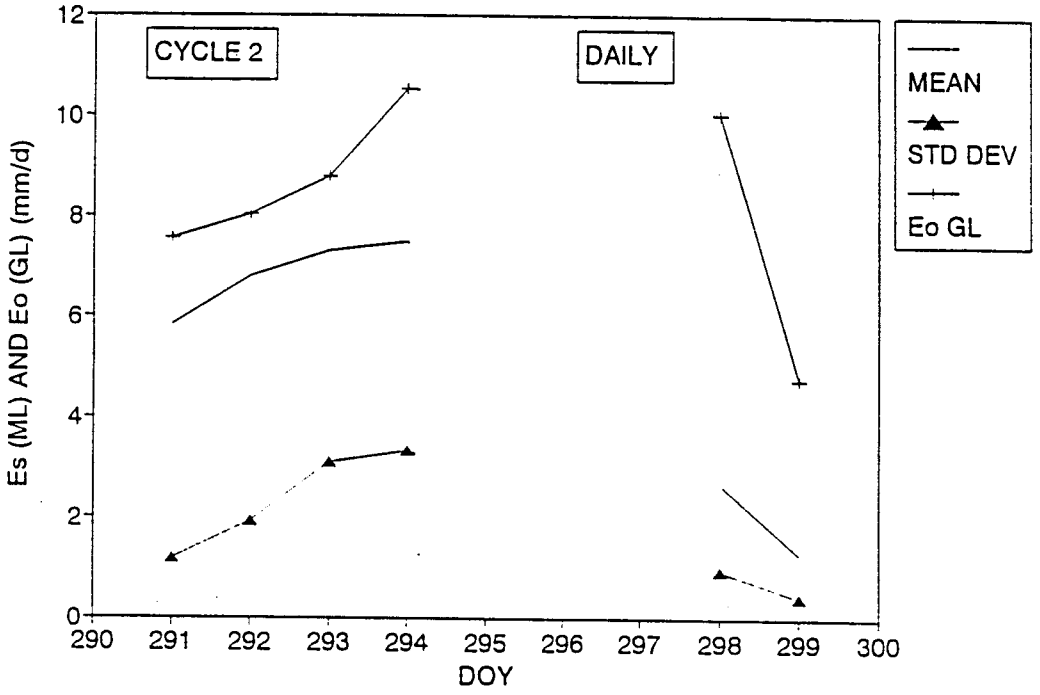

Fig. 8.4 **Daily trend in soil evaporation as measured by micro-lysimeters E_s(ML) each value's standard deviation and reference evaporation E_o through Cycle 2**

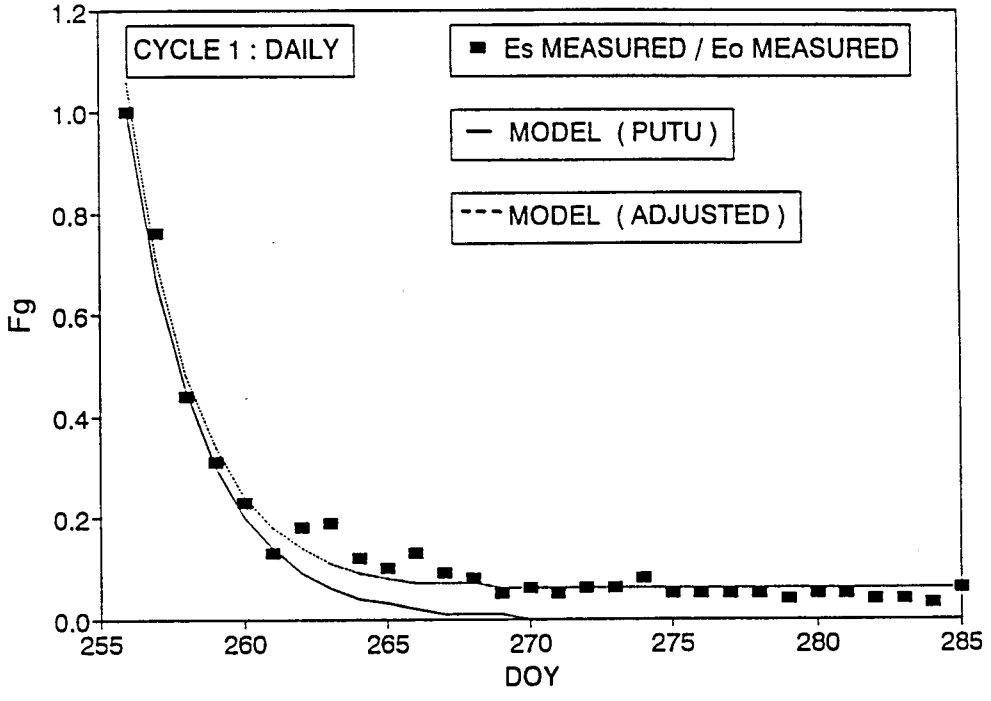

Fig. 8.5 **Daily variation in F_g measured and modelled by the original PUTU and Equ. 8.1 (adjusted) through Cycle 1**

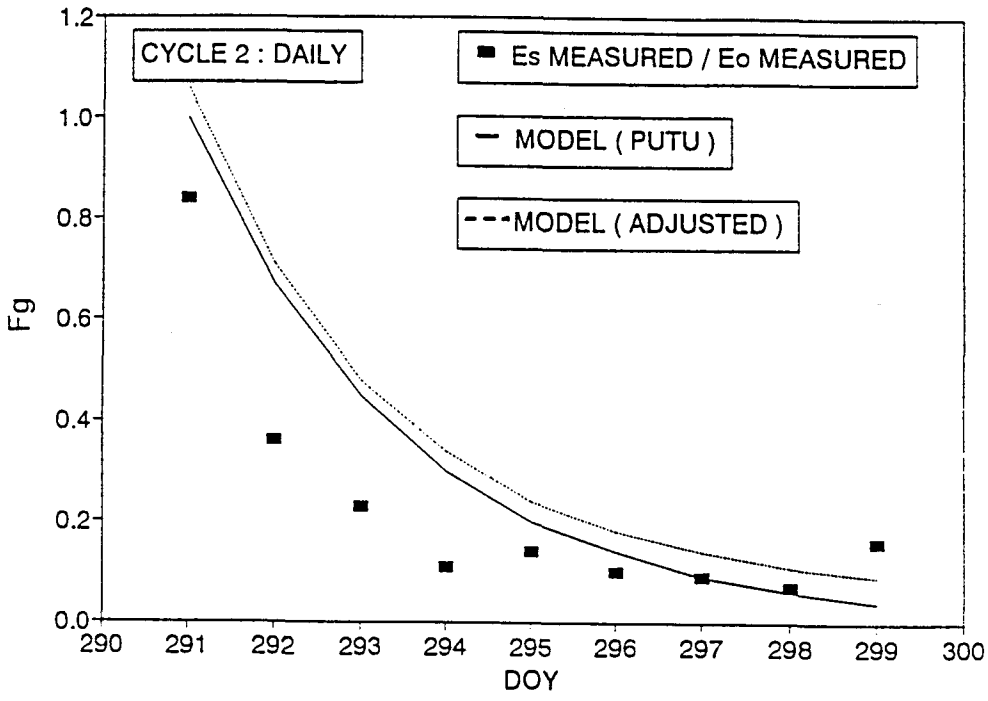

Fig. 8.6 **Daily variation in F_g measured and modelled by the original PUTU and Equ. 8.1 (adjusted) through Cycle 2**

Table 8.1 **Statistics quantifying the agreement between E_s(EBBR) and E_s(WL) for Cycle 2**

Statistical parameter	Parameter value
Intercept (mm)	0
SEE (mm)	0,86
r^2	0,82
n	9
Slope	1,24

Table 8.2 **Total E_s measured in the weighing lysimeter, WL, micro-lysimeters, ML, drainage lysimeter, DL, and Bowen ration EBBR during Cycle 1 and 2**

Cycle 1 (29-day)				Cycle 2 (9-day)			
E_s(WL)	E_s(ML)	E_s(DL)	E_s(EBBR)	E_s(WL)	E_s(ML)	E_s(DL)	E_s(EBBR)
	mm				mm		
25,7	75,9	36,9	NA	16,6	47,3	NA	24,3
Ratio(%)	295	143	NA	285	NA	146	

Table 8.3 **Statistics quantifying the agreement between measured F_g, F_g as calculated from the original F_g function and F_g-adj calculated using Equ. 8.1 during Cycle 2**

Statistical parameter	Parameter value	
	F_g	F_g-adj
Intercept	0,04	0,08
SEE	0,13	0,12
r^2	0,86	0,86
n	9	9
Slope	1,23	1,25

CHAPTER 9

VALIDATION OF THE SOIL SURFACE EVAPORATION MODEL FOR POTATO AND MAIZE CROPS

9.1 OBJECTIVE

In this chapter, the reliability of simulating E_s for potato and maize crops using the SG-iteration and PUTU models was investigated.

9.2 MATERIALS AND METHOD

Investigations proceeded mainly on data from the weighing lysimeter and micro-lysimeters. Both MMO and AWSO were used.

9.2.1 Simulation of soil evaporation for potato and maize crops using micro-meteorological observations

Exactly the same equations (with appropriately substituted subscripts) and iteration methods as used when simulating E_v were applied here. Once again MMO were used. Seed temperatures for the iterations were taken to be the mean of T_{ss} and T_{sd}. As first approximation soil surface resistance to gaseous water exchange, r_{ss}, was taken to increase as the soil surface water content decreases. Thus, r_{ss} was assumed to be equal to r_{so}/F_g, where r_{so} equals the corresponding value for short grass surface, viz 33 s m^{-1}. No comparison between simulated and measured soil evaporation could be made because hourly measurements of E_s were not possible, so scenarios of simulated E_s are merely reported.

9.2.2 Simulation of soil evaporation for potato and maize crops using the automatic weather station

Daytime values of E_s were obtained by totalling hourly E_s simulated by the SG-iteration and PUTU models from AWSO input. In case of E_s(SG), T_{sm} was obtained by iteration and r_{ss} calculated from r_{so}/F_g where r_{so} equaled r_v for short grass. Once again the relevant equations from Chapter 2 with appropriate subscripts were used.

In the case of E_s(PUTU) the new F_g-adj was used together with the equation for R_n obtained in Chapter 4, viz

$R_n = 0{,}6\ R_s - 57\ W\ m^{-2}$.

Both E_s(PUTU) and E_s(SG) for potato and maize were compared against the weighing lysimeter and the micro-lysimeters in early crop growth stages (i.e. bare soil). In the weighing lysimeter the emergence of potato plants commenced on DOY 284 and of maize on DOY 31.

9.3 RESULTS AND DISCUSSIONS

Fig. 9.1 and 9.4 are scenarios of hourly mean E_s(SG) using MMO for the potato and maize crops respectively. No field measurements were available against which to test E_s(SG) on an hourly basis.

Fig. 9.2 and 9.5 graphically depict the daytime soil surface evaporation measured using the weighing lysimeter up to day of emergence - DOY 284 for potato and DOY 31 for maize and E_s(PUTU) estimated using the PUTU-model with $r_v = 33\ s\ m^{-1}$ and AWSO on a daily basis for the two crops.

The agreement for both E_s(PUTU) and E_s(SG) with E_s(WL) is summarized in Table 9.1. Fig. 9.2 and Fig. 9.5 compare E_s(WL) (solid blocks) and E_s(PUTU) for potato and maize respectively. The solid blocks in Fig. 9.2 and Fig. 9.5 reflect bare soil evaporation.

Fig. 9.3 and 9.6 show the large discrepancies between E_s(PUTU) and each of the mean value of sixteen micro-lysimeters used to measure E_s(ML) over virtually the entire growing period. The extremely poor agreement between E_s(ML) and E_s(PUTU) and E_s(SG) respectively is demonstrated by the poor results of statistical tests shown in Table 9.2.

Table 9.1 Comparison of E_s(WL) against E_s(PUTU) and E_s(SG) on daytime basis for bare soil conditions using r_v = 33 m s^{-1} and AWSO for both maize and potato

Statistical parameter	Parameter value			
	Potato		Maize	
	E_s(PUTU)	E_s(SG)	E_s(PUTU)	E_s(SG)
Intercept (mm d-1)	-0,86	-0,78	1,87	1,53
SEE (mm d-1)	0,53	0,67	1,57	1,63
r^2	0,96	0,83	0,26	0,10
n	12	12	10	10
Slope	1,86	1,69	0,35	0,46

The decrease in simulated E_s(PUTU) as the growing season lengthens is expected.

Table 9.2 Statistical comparison E_s(ML) and E_s(PUTU) and E_s(SG) on a daytime basis respectively, using r_v = 33 s m^{-1} and AWSO for both potato and maize crops

Statistical parameter	Parameter value			
	Potato		Maize	
	E_s(PUTU)	E_s(SG)	E_s(PUTU)	E_s(SG)
Intercept (mm d-1)	1,37	1,90	0,35	0,01
SEE (mm d-1)	0,94	1,11	0,54	0,64
r^2	-0,26	0,13	0,06	0,11
n	17	17	29	29
Slope	-0,11	-0,05	0,02	0,08

According to the results of statistical tests reported in Table 9.1 and 9.2, both models, E_s(PUTU) and E_s(SG), poorly simulate both E_s(WL) and E_s(ML).

9.4 CONCLUSION

Because hourly measurement of soil evaporation was not possible, no comparisons of E_s obtained from the SG-model using MMO against measured values were possible.

Both E_s measured with the large weighing lysimeter, under bare soil conditions, as well as E_s measured by the micro-lysimeters, compared most unsatisfactorily with results from both models.

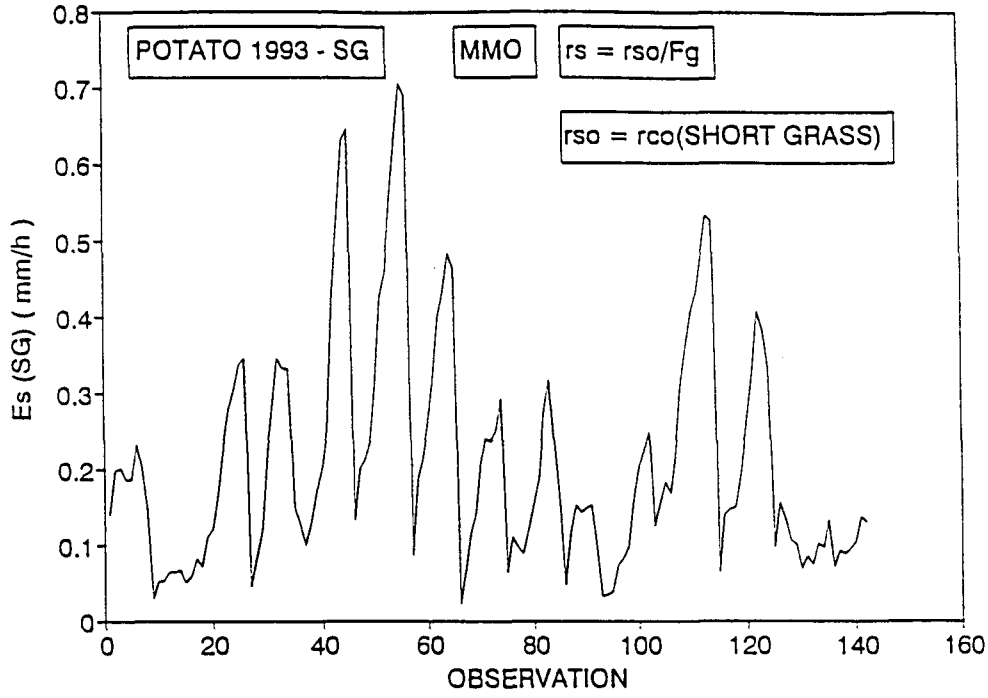

Fig. 9.1 **A sequence of hourly soil surface evaporation values simulated using the modified SG-model and MMO for the potato crop**

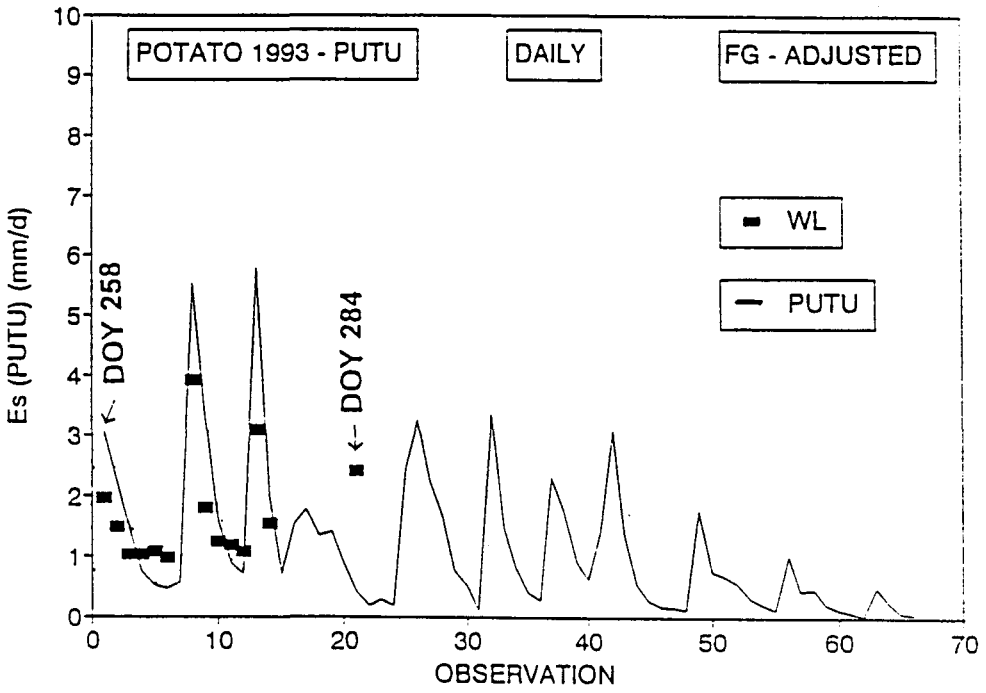

Fig. 9.2 **A sequence of daytime soil surface evaporation values measured in the weighing lysimeter, WL, and simulated by the PUTU-model with F_g-adj on AWSO for the potato crop which emerged on DOY 284 corresponding to observation 22**

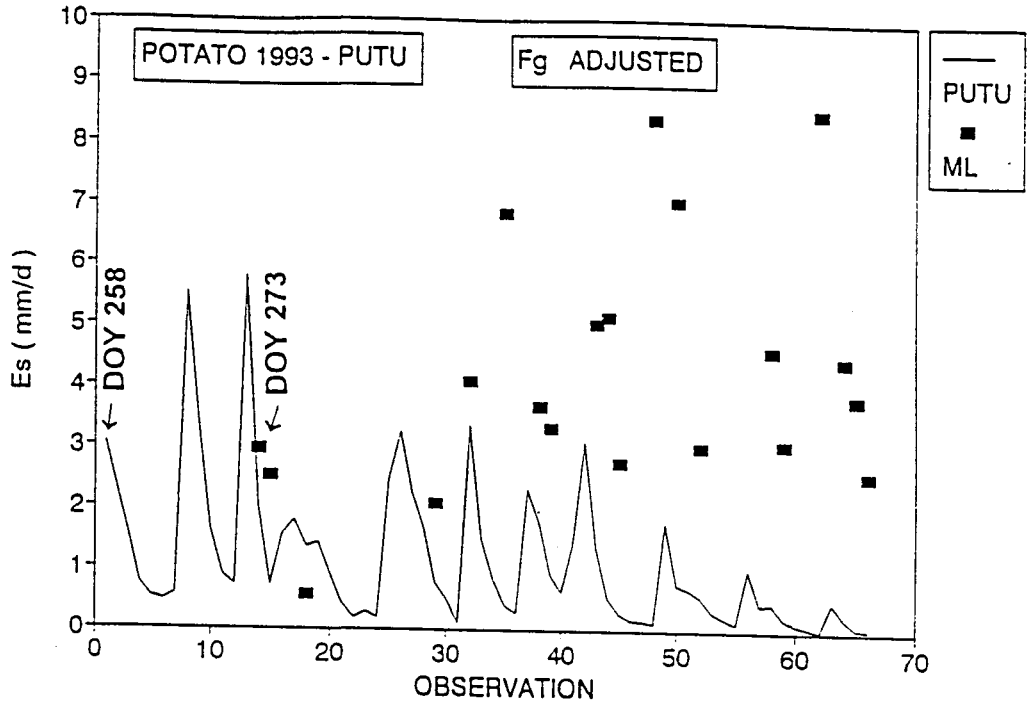

Fig. 9.3 **A sequence of daytime soil surface evaporation values measured by micro-lysimeters, ML, and simulated by the PUTU-model with F_g-adj on AWSO for the potato crop which emerged on DOY 284 corresponding to observation 22**

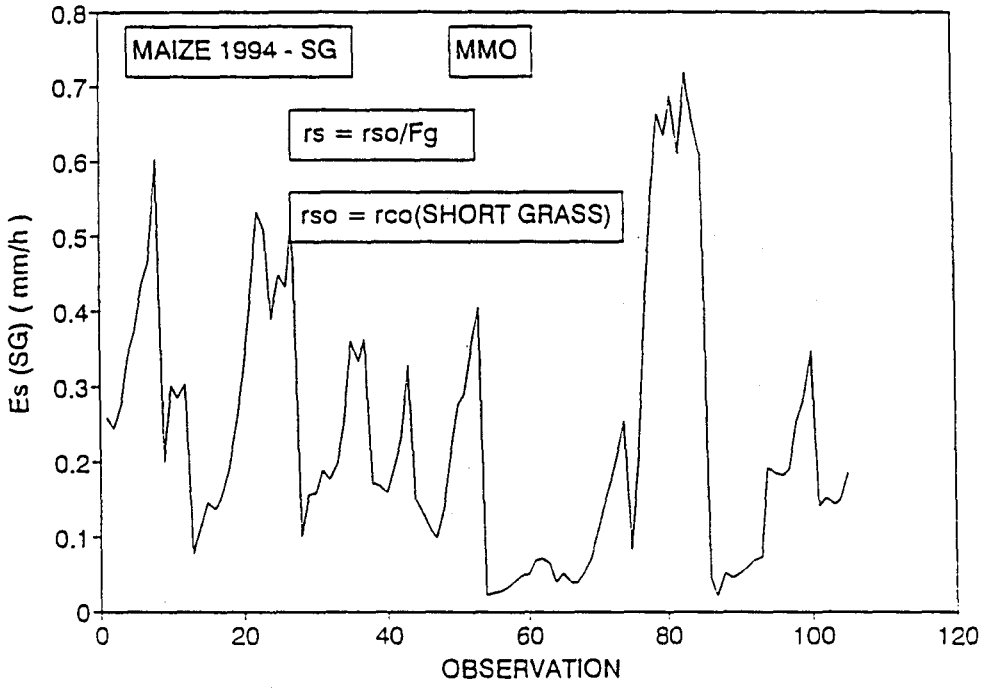

Fig. 9.4 **A scenario of hourly values of E_s simulated using the modified SG-model with MMO for the maize crop**

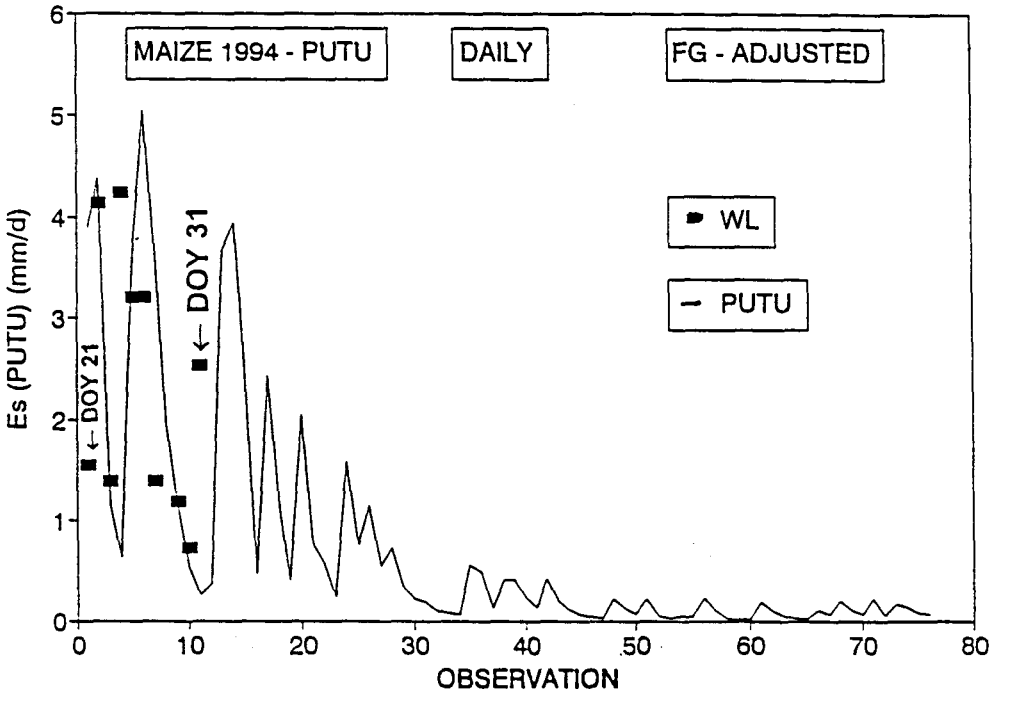

Fig. 9.5 **A sequence of daytime soil surface evaporation values measured in the weighing lysimeter, WL, and simulated by the PUTU-model with F_g-adj on AWSO for the maize crop which emerged on DOY 31 corresponding to observation 11**

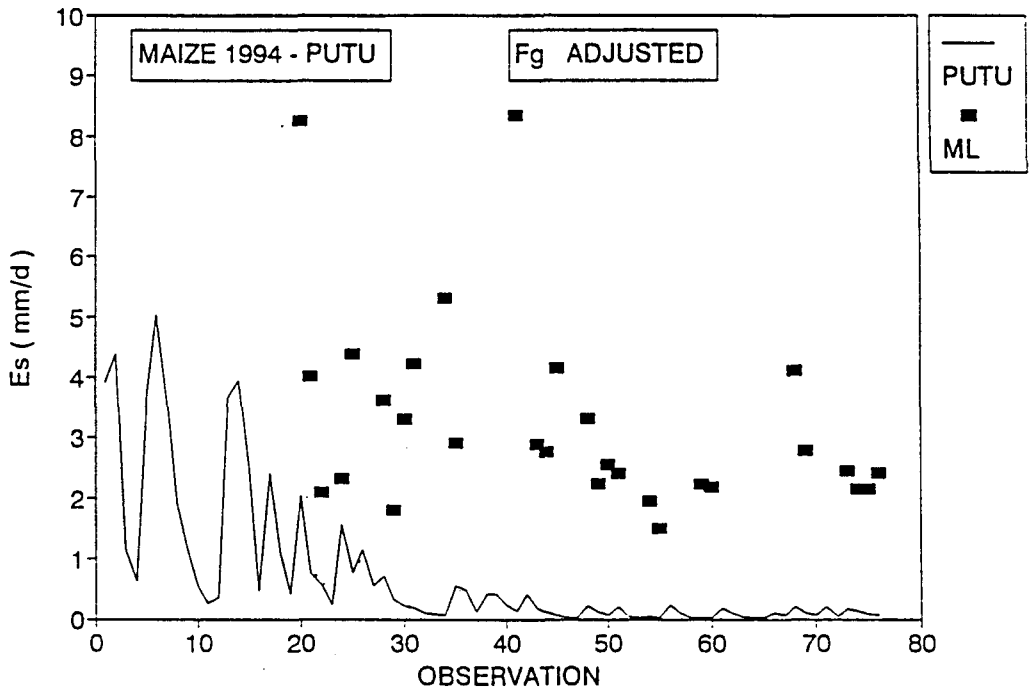

Fig. 9.6 **A sequence of daytime soil surface evaporation values measured by micro-lysimeters, ML, and simulated by the PUTU-model with F_g-adj on AWSO for the maize crop which emerged on DOY 31 corresponding to observation 11**

ACKNOWLEDGEMENTS

The authors wish to record their sincere gratitude to:

1. Water Research Commission for the financial support which made this entire project possible.

2. The UOFS for providing facilities and personnel time.

3. Mr. E. Engelbrecht, Bainsvlei, Bloemfontein, for cultivating the potatoes.

4. Professor A.T.P. Bennie, Department of Soil Science, UOFS, for providing the three phase vacuum pump.

5 Particularly Dr. Peter MacR Reid, and Dr. George Green of the Water Research Commission for encouragement and valuable advice.

6. The entire project steering committee as listed below for extremely useful advice and guidance throughout the duration of the project.

Members of the Steering Committee were:

Dr. G.C. Green

Dr. C. Everson

Mr. D.S. van der Merwe

Dr. M. Hensley

Prof. M.J. Savage

Prof. A.T.P. Bennie

REFERENCES

Bennie, A.T.P., Hoffman, J.E., Coetzee, M.J. & Vrey, H.S., 1994. Opgaring en Benutting van reënwater in grond vir die stabilisering van plantproduksie in halfdroë gebiede. WNK-verslag nr. 227/1/94, Pretoria.

Berliner, P., Oosterhuis, D.M. & Green, G.C., 1984. Evaluation of the infrared thermometer as a crop stress detector. *Agric. and For. Meteor.* 31. 219 - 230.

Boast, C.W. & Robertson, J.M., 1982. A "Micro-Lysimeter" method for determining evaporation from bare soil: Description and laboratory evaluation. *Soil Sci. Soc. Am. J.* 46. 689 - 696.

Campbell, G.S., 1977. An introduction to environmental biophysics. Springer-Verlag. New York Inc. pp. 159.

De Jager, J.M., Van Zyl, W.H., Bristow, K.L. and Van Rooyen, A., 1982. Besproeiingskeduleringvan koring in die besproeiingsgebied van die Vrystaatstreek. Verslag aan die Waternavorsingskommissie. pp. 300.

De Jager, J.M., van Zyl, W.H., Kelbe, B.E. and Singels, A., 1987. Research on a weather service for scheduling the irrigation of winter wheat in the OFS region. Final Report submitted to the Water Research Commission by Department Agrometeorology, UOFS. WRC Report No. 117/1/87. pp 281.

De Jager, J.M. & Van Zyl, W.H., 1989. Atmospheric evaporative demand and evaporation coefficient concepts. *Water S.A.* 15: 103-110

De Jager, J.M., 1992. The PUTU decision support system using weather data and mathematical simulation of crop growth. Monograph, Dept. of Agrometeorology, UOFS.

Evett, S.R., Warrick, A.W. & Matthias, A.D., 1995. Wall material and cropping effects on micro-lysimeter temperatures and evaporation. *Soil Soc. Am. J.*, 59 : 329 - 336.

Fouché, H.J., 1992. Simulering van die produksiepotensiaal van veld en die kwantifisering van droogtes in die Sentrale Oranje Vrystaat. Ph.D. Proefskrif U.O.V.S. pp.95

Hattingh, H.W., 1991. Private communication. Glen.

Jensen, M.E., Burman, R.D. & Allen, R.G., 1990. Evapotranspiration and irrigation water requirements. ASCE - Manuals and Reports on Engineering Practice. No. 70. pp 332.

Jones, C.A. & Kiniry, J.R., 1987. Ceres-Maize : A simulation model of maize growth and development. ISBN 0-89096-269-3.

Lang, A.R.G., 1973. Measurement of evapotranspiration in the presence of advection, by means of a modified energy balance procedure. *Agric. Meteor.* 12, 75 - 81.

Matthias, A.D., Salehi, R. & Warrick, A.N., 1986. Bare soil evaporation near a surface point-source emitter. *Agric. Water Manage.*, 11: 257-277

Nichols, W.D., 1992. Energy budgets and resistances to energy transport in sparsely vegetated rangeland. *Agric. and For. Meteorol.* 60, 221-247.

Ritchie, J.T., 1983. Efficient water use in crop production: Discussions in the generality of relations between biomass production and evapotranspiration. In: Taylor, H.M., Jordan, W.R. and Sinclair, T.R. (Editors). Limitations to efficient water use in crop production. *Amer. Soc. Agron.* 29 - 44.

Russel, 1980. Crop evaporation, surface resistance and soil water status. *Agric. Meteorol.* 21 : 213 - 226.

Schulze, R.E., 1984. Hydrological simulation as a tool for agricultural drought assessment. *Water S.A.* 10(1), 55 - 65.

Shaw, R.H. & Pereira, A.R., 1982. Aerodynamic roughness of a plant canopy. A numerical experiment. *Agric. Meteorol.* 26: 51-65.

Sharatt, B.S., Campbell, G.S. & Glen, D.M., 1992. Soil heat flux estimation based on the finite-difference form of the transient heat flow equation. *Agric. and For. Meteor.* 61. 95 - 111.

Shuttleworth, W.J. & Gurney, R.J., 1990. The theoretical relationship between foliage temperature and canopy resistance in sparse crops. *Q. J. R. Meteorol. Soc.* 116, 497-519.

Shuttleworth, W.J., 1991. Evaporation models in hydrology. In: Schmugge, J.J. and André J. (Editors), Land surface evaporation. Springer, New York, pp 93-120.

Singels, A. & De Jager, J.M., 1991. Evaluating different wheat production strategies for the Orange Free State using stochastic dominance and a crop growth model. *S.Afr. J. Plant Soil* 8(3), 113-118.

Smith, M., 1992. Report on the expert consultation on revision of FAO methodologies for water requirements. FAO, Rome, Italy. 28 - 31 May, 1990. Land and Water Development Division, Food and Agriculture Organization of the United Nation. BP 1960.

Steiner, J.L., 1989. Tillage and surface residue effects on evaporation from soils. *Soil Sci. Soc. Am. J.* 53:911-916.

Unger, P.W. & Phillips, R.E., 1973. Soil water evaporation and storage. Proceedings of the national convention, Tillage Conference. *Soil Cons. Soc. Am.* 42 - 54.

Van Zyl, W.H. & De Jager, J.M., 1987. Accuracy of the Penman-Monteith equation adjusted for atmospheric stability. *Agric. For. Meteor.*, 41, 57 - 64.

Van Zyl, W.H., De Jager, J.M. & Maree, C.J. & Singels, A., 1988. A simple, accurate method of estimating maximum total evaporation from a wheat crop during the daylight period. *S. Afr. J. Plant Soil* 5(2), 114-116.

Van Zyl, W.H. & De Jager, J.M. 1992. Effect of climate on plant evaporation coefficients for the potato crop. *Agric. & For. Met.*, 60: 167 - 179.

Van Zyl, W.H. & De Jager, J.M., 1994. Research on the climatic dependence of evaporation coefficients. Report to the WRC. 260/1/94. pp. 1 - 166.

APPENDIX I

CALIBRATION OF VARIOUS SENSORS

Table I.1 Comparison against the standard net radiometer of the two net radiometers used in the field in the investigation

Statistical parameter	Parameter value	
	Net radiometer 1	Net radiometer 2
Slope	0,96	0,94
Intercept	2,29	0,04 W m^{-2}
n	143	143
r^2	1,00	1,00
SEE	4,56	3,50 W m^{-2}

Table I.2 Comparison of the different soil heat-flux sensors (SHF) used in the investigation

Statistical parameter	Parameter value		
	SHF1 and SHF2	SHF2 and SHF3	SHF3 and SHF4
Slope	1,00	1,03	1,00
Intercept	-0,34	-0,37	0,20 W m^{-2}
n	197	197	197
r^2	1,00	1,00	1,00
SEE	0,74	1,47	0,94 W m^{-2}

Table I.3 **Comparison between the infra-red thermometer (IRT) used in the study and the black body supplied by the manufacturer as measured by a mercury-in-glass thermometer**

Statistical parameter	Parameter value
Slope	0,97
Intercept	0,90 °C
n	28
r^2	0,99
SEE	0,45 °C

Table I.4 **Comparison between soil and leaf surface temperatures (Tss, Tsd, Tvs and Tvd) measured by an infra-red thermometer and thermocouples**

Statistical parameter	Parameter value			
	T_{ss}	T_{sd}	T_{vs}	T_{vd}
Slope	0,89	0,48	0,40	0,78
Intercept	2,45	11,53	14,01	2,31°C
n	12	12	12	12
r^2	0,87	0,63	0,40	0,92
SEE	3,07	1,24	2,25	0,77°C

Table I.5 Comparison between three three-cup anemometers against a wind-run meter

Statistical parameter	Parameter value Sensor 1	Sensor 2	Sensor 3
Slope	1,02	1,00	1,08
Intercept	0,14	0,20	0,17 m s^{-1}
n	12	12	12
r^2	0,95	0,96	0,95
SEE	0,15	0,14	0,16 m s^{-1}

Table I.6 Comparison between known weights applied to the large weighing lysimeter and the values registered by the lysimeter

Statistical parameter	Parameter value
Slope	0,99
Incercept	0,00 kg
n	9
r^2	1,00
SEE	0,38 kg

Table I.7 Comparison between two eddy correlation systems used to determine sensible heat flux density, C

Statistical parameter	Parameter value
Slope	0,91
Intercept	5,92 W m^{-2}
n*	23
r^2	0,97
Standard error	10,00 W m^{-2}

Table I.8 Comparison between eddy correlation systems used to measure latent heat flux density, LE

Statistical parameter	Parameter value
Slope	1,03
Incercept	-2,42 W m^{-2}
n	27
r^2	0,89
Standard error	5,64 W m^{-2}

Table I.9 Comparison between soil heat flux, G, calculated using the method of finite temperature differences and G measured using heat flux plates

Statistical parameter	Parameter value
Intercept	0,36 W m^{-2}
Standard error of estimate	50 W m^{-2}
r^2	0,76
n	509
Slope	0,97

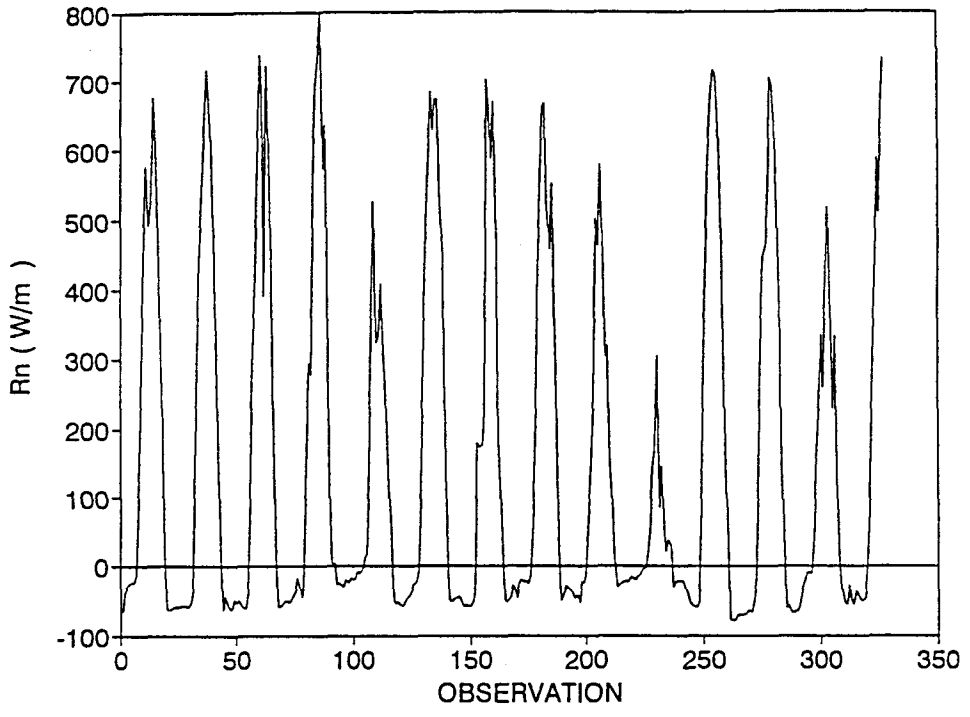

Fig. I Variation of net radiation measured above a potato canopy over a fourteen day period

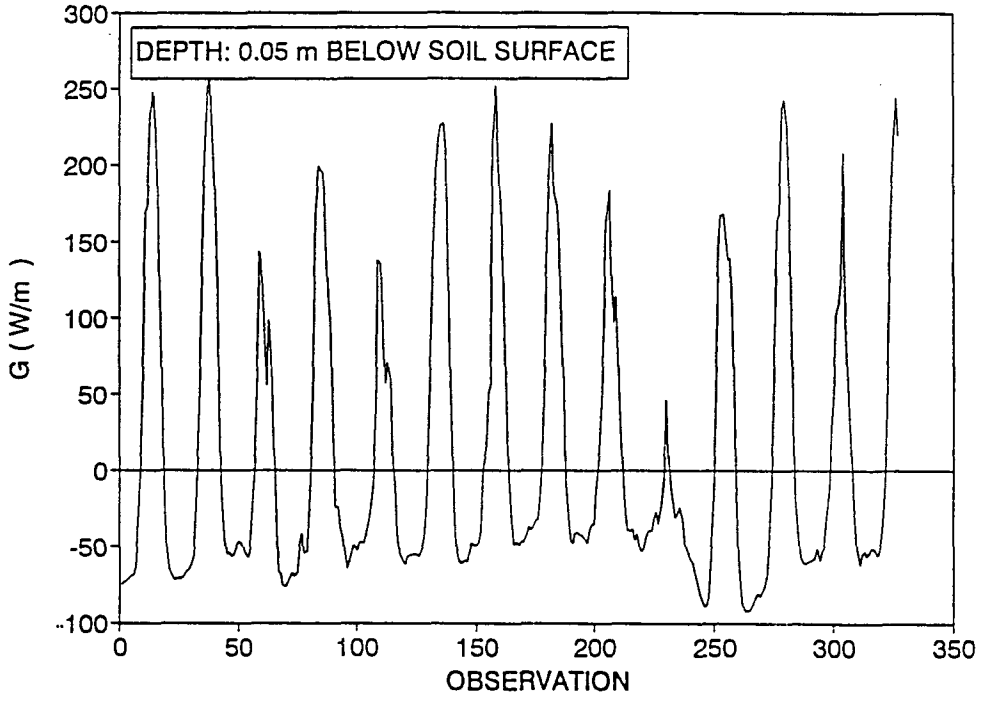

Fig. II Variation of soil heat flux density measured within a potato canopy over a fourteen day period

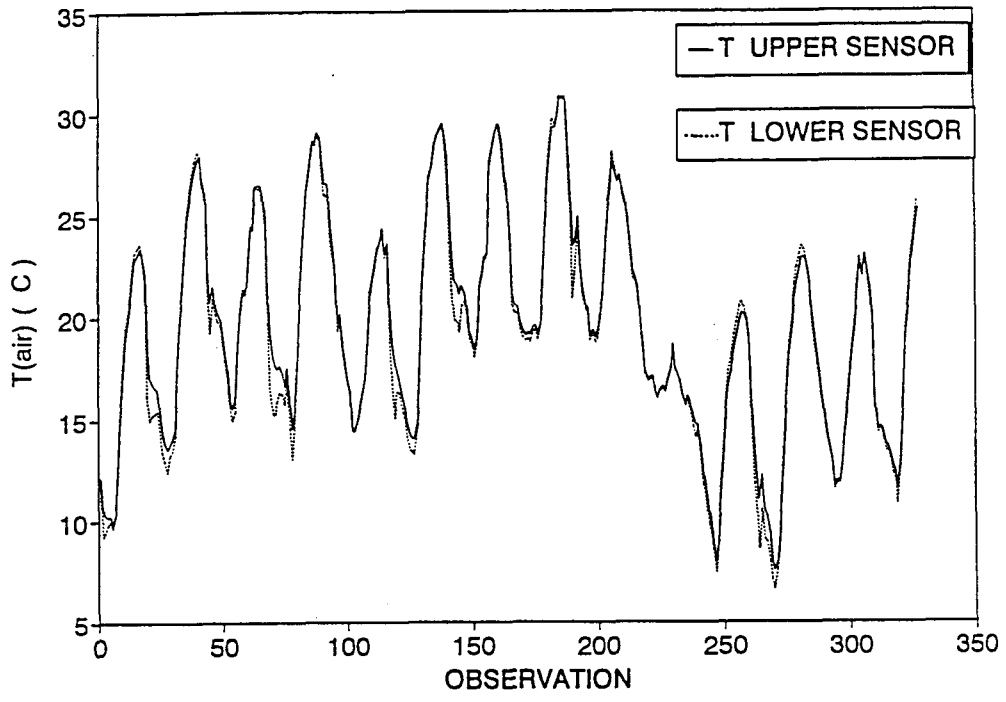

Fig. III **Variation of measured upper and lower air temperature above a potato canopy over a fourteen day period using the Bowen ratio system**

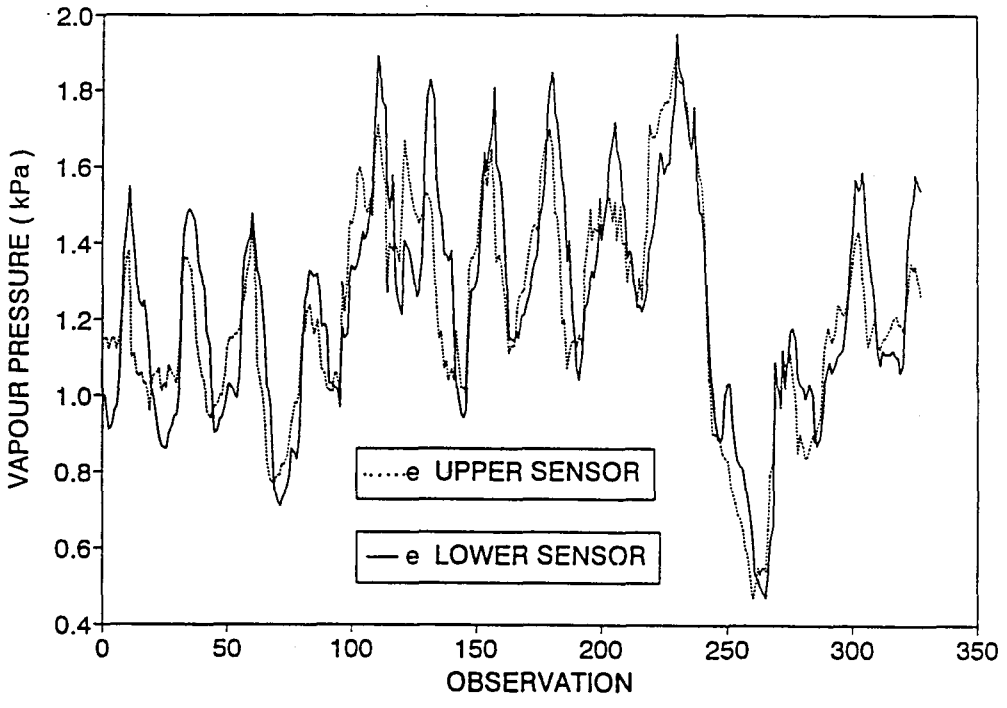

Fig. IV **Variation of measured upper and lower vapour pressure above a potato canopy over a fourteen day period using the Bowen ratio system**

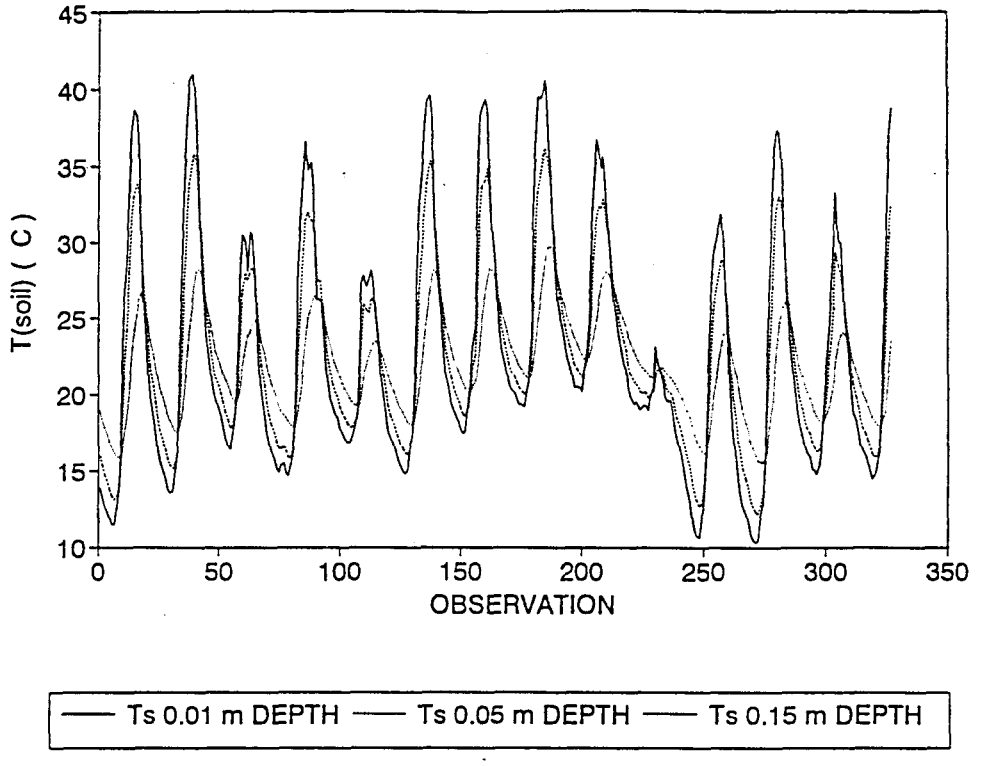

Fig. V Variation of soil temperatures at indicated depths (see below figure) as measured with a copper-constantan thermocouples over a fourteen day period

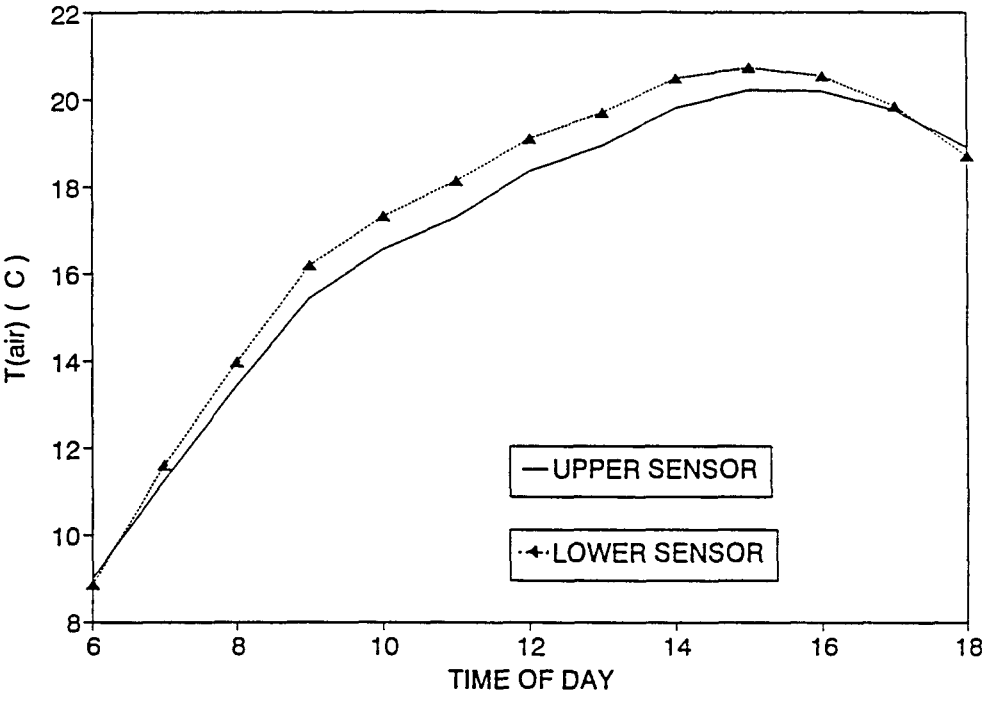

Fig. VI **Typical variation of upper and lower air temperature measured using the Bowen ratio unit during daytime i.e. between 6:00 and 18:00 above canopy**

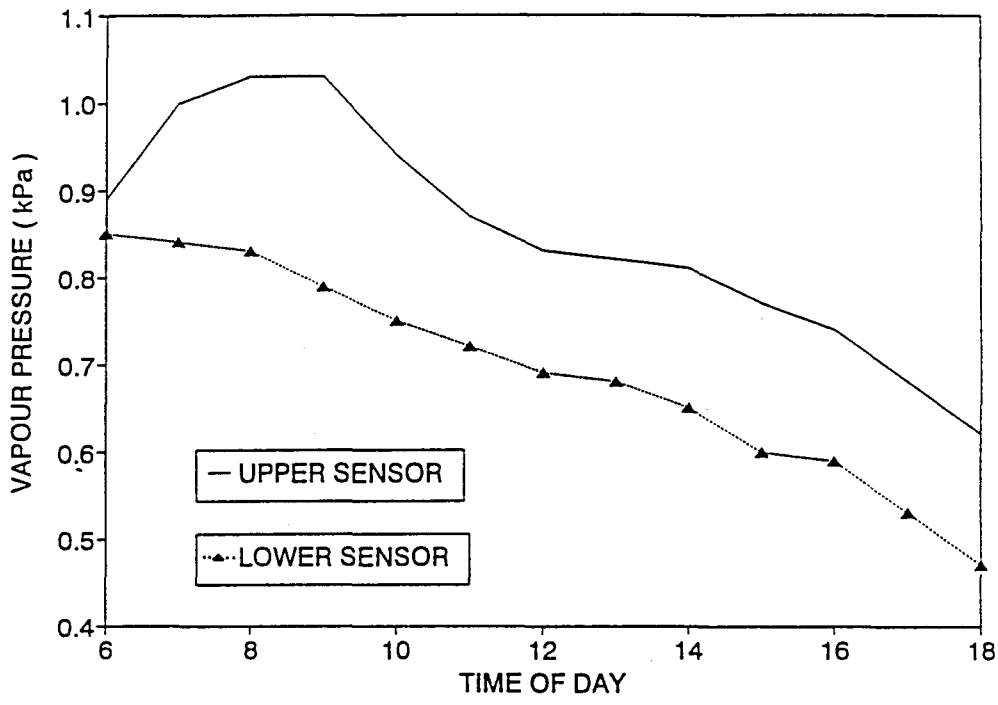

Fig. VII **Typical variation of upper and lower vapour pressure measured using the Bowen ratio unit during daytime i.e. between 6:00 and 18:00 above canopy**

APPENDIX II

MEASUREMENT OF SOIL HEAT FLUX DENSITY

Measurement of soil heat flux density using soil heat flux sensors are subject to inaccuracies stemming from non-horizontal installation, or the effects of heat storage in the soil layer immediately above the flux plate. It was therefore deemed wise to test the agreement between soil heat flux density measured by heat flux plate against that derived from measured soil temperature profiles. The method of Campbell (1977), also fully described by Sharatt, Campbell & Glen (1992), was used. This method utilizes soil physical parameters and measurements of soil temperatures at two different depths. Thus, four copper-constantan thermocouples were installed 40 mm below soil surface immediately above the soil heat flux sensor. A further four were installed below the soil heat flux sensor at a depth of 150 mm below the soil surface. In each case the average temperature from the four thermocouples at each depth was used in the calculations. Hourly mean values of all observations, i.e. the sensors and soil temperatures were recorded on a 21X data logger from Campbell Scientific, Logan, USA. From these data, the hourly mean soil heat flux density measured by plate sensors, SHF_p, were compared to values calculated by the temperature profile method, SHF_t.

Fig. VIII shows the variation in SHF_p and SHF_t over a period of 13 days as determined by both methods. Good agreement is evident and a linear regression relationship with a virtual 1:1 slope was found. It reads:

$$SHF_t = 0{,}98\ SHF_p - 0{,}36\ W\ m^{-2} \qquad I\ 4.1$$

For 509 hourly observations the coefficient of determination was $r^2 = 0{,}81$. It was concluded that the soil heat flux plates had been correctly installed and the results obtained may be deemed to be accurate.